Modelling the performance of a batch jig processing a typical South African coal

Grerley Mutibura

A dissertation submitted to the faculty of Engineering and the Built Environment, University of the Witwatersrand, in fulfillment of the requirements for the degree of Master of Science in Engineering

Johannesburg, 4 June 2015

Declaration

I declare that this dissertation is my own work aided only by the guidance of my supervisor. It is being submitted for the Degree of Master of Science in Engineering to the University of the Witwatersrand, Johannesburg. It has not been submitted before for any degree or examination to any other University.

Grerley Mutibura

4th day of June 2015

Abstract

Jigs have been used in mineral beneficiation for many years. They have a number of desirable qualities some of which include simplicity of operation and cost effectiveness. Jigs have been successfully applied for the beneficiation of a number of minerals and are extensively used in the processing of iron ore and coal.

The concept of process optimization is one that is fundamental in the processing of minerals. Likewise it applies to the jigging processes as performance has been found to be a function of the feed characteristics e.g. feed composition and density distribution. The effect of the size range and the particle size has largely been untested on jig performance. Hence, this investigation aims to shed more light on the influence of these two factors on jig performance.

Mathematical models of mineral processes have been increasingly used as a cost effective way to investigate different processing options. In the case of the modeling of jigs, King`s stratification model has been found to be particularly useful. Although its efficiency as a simulator has been proven for synthetic systems in which particles have essentially the same size and shape, its applicability has not been investigated for practical contexts where size and size range vary significantly. This context is the focus of the investigation reported in this thesis.

Using a batch jig, tests were conducted on a typical South African coal. The choice of coal as a test material was motivated by the ease with which density distributions can be measured for coal systems. The coal samples were screened into different size fractions and 15 different combinations of particle were prepared for testing in a laboratory batch jig.

The results show that for the samples tested the quality of separation increased as particle size increased i.e. improvements in jig performance of between 10% and 20% were achieved in some samples as the particle size was increased. On the other hand the quality of separation decreased as the size range increased. It was also found that the jig performance is more sensitive to particle size than it to the particle size range. The study revealed that the King model is a good simulator of stratification behaviour of jigs as it was able to produce reasonably good levels of agreement between modeled and experimental data for most samples that were tested.

No apparent trend could be observed with regard to the effect of variations in size and size range on the stratification parameter in the King model. It appears that in the context investigated in the study, this parameter is relatively independent of size and size range and was fairly similar for all tests conducted in this study. In several of the tests, particularly those with a large range of sizes, the model did not fit the data very well. However, in general, it appears that the King model can be used with the same degree of confidence as a simulator for systems where the ratio of the top to the bottom sizes of the jig is 2.4 or less.

Dedication

To God Almighty

And to my family;

My parents Justin Mutibura and Kudzai Manyinyire

My sisters Amarylis Mutibura and Belinda Mutibura

My brothers Ivor and Lesley Mutibura

My friend Yamurai Mafukidze

Grerley Mutibura

Acknowledgements

Above all I would like give thanks and praise to the Lord almighty for granting me the strength and the opportunity to do a masters project. It is by His grace that I was able to endure through every step of this project.

Secondly, I would like to thank my supervisor for this Master of Science Dissertation, Professor Lorenzo Charles Woollacott. His guidance, mentorship, supervision of this work and encouragement in times of difficulty is deeply appreciated.

Thirdly I would like to thank the lab and technical stuff at the school of Chemical and Metallurgical Engineering for their assistance in setting up the jig lab and making all required apparatus available. I am indebted to them and hope to see them continue assisting many generations of students in this way.

Finally, I would like to thank Mintek for allowing me to use their jig facilities.

Grerley Mutibura

Table of Contents

List of figures

List of tables

Chapter 1: Introduction

1.1. Background

Mineral jigging is a process of separating particles of different densities by allowing them to settle in a fluid under a pulsating motion. It is particularly efficient for processing ores in which significant differences in particles densities exist. In mineral processing, jigs are used for the pre-concentration of ferrous ores and washing of coal amongst other applications.

South Africa relies heavily on coal as a primary fuel source. It is predicted that up until about 2030, 88% of all power will continue to be generated from coal (**Dempers, 2006**). This makes it a very important commodity and performance measurement criteria for coal processing have been developed over a long period of time and are easy to implement and understand. South African coal is difficult to jig because it contains significant proportions of near density i.e. material with densities close to the cut density. Although not the main focus of this thesis, any work that might contribute to improving the processing efficiency of coal is highly relevant to the country.

Although jigging is one of the oldest mineral processing technologies in use today and has been the subject of considerable research for many years, the dynamics which affect its performance still remain inadequately understood. Consequently, the mathematical models of these dynamics that have been formulated are inadequate in several respects. One of these is that they do not account very well for the effects which particle size exert on jig performance. This means that the current capability to reliably simulate the performance of jigs in mineral processing circuits is somewhat limited and the potential benefits for process design and process troubleshooting which simulation offers is constrained. The objective of the study reported in this thesis is to investigate some of these influences and the extent to which one of the most promising models available is able to account for the influences investigated.

The model in question was formulated by Professor King (**King, 1987, 2001**). It has been formulated on the assumption that all particles in a jig bed are mono-sized spheres. However, there are indications in the literature that it is able to simulate stratification patterns in more practical systems where the size and shape of particles violate this assumption but no validation

work of this kind has been reported. The study reported in this thesis aims to make a contribution in this area.

1.2. Problem Statement

Any attempt to improve the efficiency of a mineral processing unit operation or to improve the capability of models to simulate their performance must be based on a good understanding of the dynamics that influence separation performance. The understanding of the influence of particle size and particle size range on this performance is currently inadequate in general and more specifically, is inadequately accounted for in the mathematical models that are currently available. This is particularly true for complex systems such as with South African Coals which contain considerable proportions of near density materials, i.e. material that has density close to the cut density of the separator. The study reported in this thesis aims to test the effect of particle size and size range on jig performance and to investigate how well the King stratification model describes the stratification behavior of a typical South African coal.

1.3. Research objectives

The questions which this study aims to address are as follows:

- How does particle size and size range affect jig performance?
- How well does the King model describe stratification behaviour in the jig for different particle sizes and sizes ranges?
- How does the stratification parameter (α) in the King model vary with particle size and with particle size range?

1.4. Structure of this thesis

The first chapter is the introduction which gives a background to the problem to be tackled. In the second chapter a review of jigging technology, relevant theories and models are presented. Emphasis is placed on theories and models that describe the mechanism by which a bed of particles is stratified in the jig. The capability of the jig to handle a wide feed size ranges and resulting efficiencies are also discussed.

Chapter three provides a detailed description of the experimental work and equipment used to achieve the set objectives. Presented here are the experimental design, procedures followed, the laboratory work performed and how the data was analyzed.

The fourth chapter aims to characterize how the size and size ratio of particles in the jig bed i.e. the ratio of the largest and the smallest particles, affects stratification behavior and performance indicators that are commonly used to quantify separation performance. This information is critical for jig plant design as this allows the design engineer to optimize the design of a plant.

The fifth chapter investigates the ability of the King stratification model in reliably predicting the stratification behaviour of a typical South African coal. The effect of size and size range is investigated and results on the reproducibility of jigging experiments are presented.

The final chapter summaries all the major findings, their relevance and provides some recommendations for future work.

Chapter 2: Literature Review

2.1. Mineral Jigging

Jigging is one of the oldest gravity separation methods used in mineral processing (**Burt, 1984**). It has a significant number of favorable properties, which include cost effectiveness, high separation precision, high throughput and easy maintenance (**Mehrotra, *et al* 1997**). A wide range of minerals can be processed ranging from coal to diamonds, andalusite to zirconia, mineral sands to metal oxides and from industrial minerals to precious metals (**Lin, *et al* 1997**). In the U.S 37% of the coal beneficiation plants make use of jigs for coal washing and on a broader scale half of the world's coal is washed in this way (**Mehrotra, *et al* 1997**). Due to the complexity of South Africa coals jigging is not widely used in this country because coals in this country contain significant proportions of near density material which negatively affects separation efficiencies. When material cannot be processed efficiently using jigs, the most common alternative is dense medium separation.

2.2. Dense Medium Separation (DMS)

DMS is a process widely used in South Africa and globally for the processing of coal. This process uses a slurry of magnetite suspended in water as the medium of separation. The effective density of the slurry can be controlled by adjusting the concentration of the solids in the slurry. Float-sink separation is achieved when the coal is placed in the media; coal with densities less than the density of the media will float and that which has densities greater than that of the medium sinks. DMS achieves very precise density separations, but efficiency decreases as the percentage of near density material increases. However it has relatively high operating costs because it consumes large volumes of water, requires extensive media recovery and is associated with high media replacement cost due to the inevitable loss of media during processing (**King, 2001**). In addition it becomes difficult to achieve separations above an S.G of 3.6 with current ferrosilicon media in iron ore beneficiation. Kumba Iron Ore`s Sishen mine has managed to utilize atomized silicon as the media to achieve separations S.G's of up to4.2; (**Myburgh, *et al* 2014**). However, the high cost of the atomized silicon leads to a significant increase in operating costs.

2.3. The jigging process

Jigging is a process of sorting a bed of particles in a fluid environment according to density. This is achieved by stratification which is brought about by the movement of particles which are intermittently fluidized by vertical pulsation of a fluid or air (**Burt, 1984**). **Mehrotra *et al.*, 1997,** describes jigging as a cyclic process with four distinct stages. These stages are lift, expansion, exhaust and compression respectively. The jig mechanism sustains fluid pulsation such that each jig cycle has an up stroke (pulsation) and down stroke (suction). The lift stage occurs at the beginning of the up-stroke and at this stage the bed is lifted. In the expansion stage the base of the bed starts resettling resulting in relaxing or loosening of the bed causing an increase in the volume of the bed, which occurs at the end of the up-stroke. The last two stages occur during down-stroke or suction whereby the particles are resettling and the bed volume compressed to its initial volume. Repetition of the pulsation and compaction results in stratification of the bed according to density. This stratification process results in the formation of layers of varying density, the density profile of this resulting bed is such that less dense particles are near the top of the bed and higher density particles are near the base. The development of this bed is a function of the density and size of particles in the feed and of operating variables such as residence time in the jig, bed thickness and the nature of the jig cycle (**Myburgh, 2010 and Myburgh *et al.*, 2014**).

2.4. Types of jigging devices

Various jig designs have been developed over the years for a number of applications in the mineral processing industry. Table 1 below gives a brief over view of different types of jigs, their applications and some examples **(Burt, 1984 & Wills, 1992).**

Table 1 : Types of Jigs with examples (Burt, R.O., 1984)

Type	Method of Pulsation	Mineral Jigs		Coal Jigs	
		Over the screen	Through the screen	Over the screen	Through the screen
Movable screen	Plunger	Halkyn James	Hancock	Wilmot Pan	-
Fixed Screen Plunger	Plunger	Harz, McLanahan, stone	Cooley, Collom, May	ORC, Elmore, Reading	Faust
Mechanical	Diaphragm	Bendelari, Ruoss	Denver, Wemco/Remer, Yuba Richard, Pan Am.Placer, Panam-Kraut, IHC	Jeffrey	-
Pulsator	Air	OPM Series	-	Baum, Batac, Tacub	Feldspar , Cortex
	Water Vane	Richard	Pan America Neil		Vissac

2.5. Jigging theories and models

2.5.1. Introduction

Though jigging has been in use for many years there is no single clear cut theory that entirely and accurately describes the performance of a jig **(Wills, 1992).** As a result a number of theories have been developed. These theories range from simplistic single particle descriptions to some more complex ones which make use of stochastic theory. **Mehrotra*, et al* (1997),** reviewed the most notable theories on the subject and classified them as follows:

- Classic theory based on single particle behaviour
- Potential theory
- Dispersion models of particle suspension
- Energy dispersion theories
- Stochastic analysis
- Empirical models
- DEM and CFD

2.5.2. Classic theory based on single particle behaviour.

The theory proposes that jigging occurs according to three mechanisms: differential acceleration, interstitial trickling and hindered settling. It is believed that a combination of all three mechanisms occurs in the jig depending on the jig cycle that is used **(Burt, 1964).**

Differential acceleration

The acceleration of a given particle in a fluid is a function of the relative density of the particle and fluid only i.e. it is independent of the particle size and shape. This suggests that if particles are allowed to fall through the medium a sufficient number of times and with a sufficiently short time of fall the respective distances travelled by different particles should show more likeness to the initial acceleration of particles. In this case stratification would occur on the grounds of specific gravity only **(Burt, 1964)**.

Hindered settling

If particles are permitted a sufficiently long time to settle in a fluid, they will eventually reach their terminal velocity. The settling velocity of such particles follows either Stokes law or Newton`s depending on whether it's a small or a large particle respectively. Intermediately sized particles follow a combination of the two. However such ideal behavior does not occur as the number of particles becomes large and particle crowding occurs. Under these conditions settling is referred to as 'hindered' because particles prevent each other from settling freely. The system will behave as a single entity i.e. the entire bed behaves as if it had a single density of a slurry, as a result the terminal velocity becomes a function of the particle weight instead of the particle density **(Burt, 1964)**.

Interstitial trickling

As the bed of particles settles down at the end of a given jig cycle, the bed consolidates and the larger particles are forced to interlock under the influence of the suction force. The interlocking results in the formation of channels to the base of the jig bed and heavier particles of sufficiently small size are capable of trickling through these channels to the base. This has a significant effect on the recovery of smaller heavy minerals **(Burt, 1964)**.

The dominant mechanism with which stratification occurs depends on the nature of the feed to the jig and jig cycle used. For instance if there are significant size differences between the smallest and largest particles in the feed and the duration of down stroke is sufficiently long then significant interstitial trickling may occur. This in turn affects the overall jig performance as particles penetrate further down into the bed than they otherwise would.

These theories reduce the analysis of particle behaviour in the jig to focus on single particles, and, in particular their settling velocities. Some short comings of this model are that it uses an idealized model to describe the behaviour of water in the jig. **Lin *et al.*, 1997, de Jong *et al.*, 1996** and **Viduka *et al.*, 2013** all show that water displays more complex behaviour in the jig than the simplified model that is proposed by the classic theory. This simulation model ignores the significant damping of the water motion due to the bed of particles i.e. the physics behind the interaction of particles and water is ignored. The second problem with this theory is that it only looks at the process from a 2 dimensional perspective which makes it difficult to model mechanisms such as interstitial trickling (**Mehrotra *et al.*, 1997**).

More recent work by **Kuang Ya-li *et al.*, 2008** investigated the laws governing the motion of groups of particles relative to the analysis of single particles proposed by the classic theory. They found that looking at groups of particles instead of single particles gives a more accurate insight into the behaviour of particles in a jig.

2.5.3. Potential energy theory

This theory was first developed by **Mayer, 1964**, who postulated that the driving force of bed stratification in jigging is the difference in potential energy of the system before and after stratification i.e. a stratified bed has a lower potential energy than a stratified bed. Accordingly, the unstratified bed of particles is viewed as unstable under gravity potential. As all systems strive to attain stability or reach equilibrium (equilibrium is state in which opposing forces acting on the particles are equal) by minimizing the Gibbs free energy, an unstratified bed of particles will attain stability by minimizing the difference between the stratified and unstratified states of the bed. This is achieved by redistribution of particles within the bed. Mayer argued that the energy supplied by the jig strokes was not responsible for stratification of the bed but rather just

unlocked the potential in the bed to stratify. His theory suggests that stratification can be described by the following equation;

$$S = J\exp(-kt)$$

where S is the stratification rate, J is the jiggability and K a constant. In this instance, jiggability means the ease with which a bed of particles can be stratified in a jig. The flaw of this approach is that it fails to take into account the dispersive processes that occur in the bed during jigging.

2.5.4. Energy Dissipation Theories

The main proponents of this theory are **Rong, 1990** and **Rong *et al.*, 1993**. They did work on air pulsated jigs and their main aim was to try and identify a single parameter that has the key influence on bed stratification which in turn depends on jig operating parameters, feed characteristics and jig size. This parameter was found to be the total energy dissipated during a single jig cycle. The main proposition of this theory is that any combination of the jigging parameters that results in the same dissipation of energy in the bed of the jig will result in similar stratification results. They also found that the frequency of pulsation and operating air pressure have the greatest effect on the energy dissipated. This approach neatly ties together the bed stratification mechanism to the operating parameters as well as the air-water behavior in the jig. The short coming of this theory is that it does not predict the concentration profiles in the jig bed.

2.5.5. Stochastic analysis

This theory argues that analyzing jig behaviour by focusing on single particles is not realistic. The theory also argues that since the particles in the jig behave as a single body, critical processes that occur in the bed are over looked if single particle analysis is used. As such the theory uses the laws of statistical mechanics to describe particle behaviour in the bed (**Mehrotra *et al.*, 1997**). It concludes that stratification of the bed by density is effective if the bed is statistically unstable for the complete jig cycle. Statistical stability is defined as a state in which the volume of the bed in the loosened state remains unchanged relative to some mean value. This theory explains well the interconnections between regimes of liquid movement and degree of stratification. However, it fails to shed light on the relation between operating parameters and stratification performance (**Lin *et al.*, 1997)**.

2.5.6. Empirical Models

This approach attempts to describe jigging process kinetics by the use of empirical models. Based on the assumption that the jigging time strongly affects bed stratification, an attempt is made to express stratification as a function of jigging time. The following two parameter Weibull distribution has been proposed to relate jig performance, to a number of jigging parameters.

$$Y(t) = 1 - \exp\left(-\frac{t}{\theta}\right)^{\beta}$$

Y(t) is the yield at time t, θ and β are empirical parameters which must be determined experimentally. β is a measure of the relative delay in the separation process, θ is the jiggability , which represents the ease with which stratification of a bed of particles in the jig occurs. **Lin *et al.*, 1997**, **Mehrotra *et al.*, 1997** and **Rong *et al.*, 1993**, proposed a power function equation to relate stratification indices to the jigging time because they argued that stratification is strongly affected by the parameters that affect water behaviour in a jig. They conducted a number of experiments to determine how stratification parameters such as yield were affected by jigging time and they modeled this into an equation in the form of a power function.

2.5.7. Discrete Element Method (DEM) and Computational Fluid Dynamics (CFD)

DEM is a numerical mode for computing the motion and effect of a large number of particles interacting in a given bound environment, while CFD is a detailed model that describes the behavior of fluid in a given and how it affects solid objects as it flows past them. This approach has been applied to the context of jigging. The DEM method coupled with simplified fluid models have been used to simulate the motion of individual particles discretely to give an insight into the micro-mechanical processes that occur at particle level **(Viduka *et al.*, 2013)**. These modeling techniques assume a uniform fluid field and do not account for the effect of non-uniform fluid velocity on particle drag forces. A number of these models exist i.e. the Euler-Lagrange (DEM-CFD) model, Direct Numerical Simulation-DEM and the lattice Boltzmann-DEM. **Viduka *et al.*, (2013)** claims that the Euler-Lagrange DEM model is superior to other DEM models because it offers superior computational convenience. It solves the liquid flow using Navier-Stokes and continuity equations. On the other hand the motion of individual particles is obtained by solving newton's second law of motion and the liquid-particle coupling is

obtained from solving Newton`s third law. This approach generates detailed information on particle trajectories and transient forces between particle and the fluid and particle respectively **(Xia *et al.*, 2007)**.

2.5.8. Dispersion models of particle suspension: The King Model

The potential energy theory was extended by a number of investigators to include dispersive forces due to factors like inter-particle collisions **(Mehrotra and Mishra, 1997)**. Probably the most significant contribution to the quantitative analysis to the stratification phenomenon was by **King, 1987** initially and then by **Tavares and King (1995)**. Like **Mayer, 1964**, they propose that density stratification of particles in a bed is a result of the need to minimize the potential energy of the bed of particles as particles of different densities interchange positions in the bed. This model has received strong empirical endorsement (**Tavares *et al.*, 1995; Venkoba Rao *et al.*, 2003; Venkoba Rao, 2007; Woollacott *et al.*, 2014**). However, no work has been done to establish the limits of its applicability i.e. the extent to which it is not able to describe stratification patterns when there are significant variations in particle size. Accordingly, this model is reviewed in detail.

2.5.9. The King stratification model

The theory **(King, 1987, Tavares and King 1995, King, R.P. 2001),** considers a bed of particles of equal sizes, with a variety of densities. For such a system the reduction in potential energy of the bed that results from a particle switching positions with a particle at a distance dH below it is

$$\frac{dE}{dH} = -gV_p\,(\rho - \bar{\rho}).$$

V_p is the particle volume, E is the potential energy of the system, H is the height of the particle bed.

According to **King, 1987** the stratification that occurs in the jig bed can be described by the volumetric concentration of the particles,(C_ρ). The variation of concentration with height is called the concentration profile.

Due to the effect of the stratification potential, particles move upwards or downwards depending on whether the difference between the density of the particle and the average density of particles in the layer in which it is located is positive or negative. If the difference is positive then the particles migrates downwards otherwise they move upwards. The flux of particles of density ρ as a result of the potential gradient setup in the bed is given by

$$\emptyset_{st}^{v} = -C_{\rho}\ u\ \frac{dE}{dH}.$$

Where $\emptyset_{st}^{v}$ is the stratification flux (the superscript v denotes that this quantity is perceived on a volumetric basis), u is the migration or penetration velocity and dE/dH is termed the stratification potential. The penetration velocity, u is achieved by a given particle in a system in which there are no dispersive forces or they are very small and the stratification potential is one. By substituting the stratification potential dE/dH we obtain

$$\emptyset_{st}^{v} = -C_{\rho}\ ugV_{p}\ (\rho - \bar{\rho}).$$

The feature of the King model that differentiates it from the Mayer`s Potential energy minimization approach is that **King, 1987** noted that in reality it would be impossible to achieve the perfect stratification as postulated by Mayer. This is because dispersive forces which he deemed to be Fickian in nature, constantly work to de-stratify the bed. This de-stratifying or dispersive flux, $\emptyset_{disp}^{v}$ is described by

$$\emptyset_{disp}^{v} = -D\ \frac{dC_{\rho}}{dH}.$$

The Diffusion coefficient D is a function of particle size, and shape and the bed expansion mechanism **(Tavares and King, 1995).** After a sufficiently long period of time the bed of particles reaches a state of dynamic equilibrium, whereby the de-stratifying flux is equal but opposite to the stratifying flux;

$$\emptyset_{disp}^{v} = -\emptyset_{disp}^{v}.$$

Hence,

$$-D\ \frac{dC_\rho}{dH} = -(\ -C_\rho\ ugV_p\ \ (\rho -\ \bar{\rho}).$$

This further reduces to;

$$\frac{dC_\rho}{dH} =\ -\frac{C_\rho\ ugV_p}{D}\ (\rho -\ \bar{\rho}).$$

The relative height h of the bed can be defined as $h=H/H_{bed}$ where, H_{bed} represents the height of the bed. In the equation above the penetration velocity, acceleration due to gravity, volume of particles and the diffusion constant are all constant and can be combined into a single parameter called the stratification coefficient (α).

$$\alpha = \frac{ug\ V_\rho H_{bed}}{D}.$$

This constant describes the jigging action and is independent of particle density. **Woollacott *et al.*, (2014),** showed that monosize particle with similar shapes will result in similar values of α. The King model is given by

$$\boldsymbol{\frac{dC_\rho}{dh} =\ -\alpha\, C_\rho\,(\rho -\ \bar{\rho}(h))}.$$

This equation can be integrated to give the concentration profile in the jig bed. The integrated form is as follows;

$$\boldsymbol{C_\rho\ =\ C_\rho^0\, exp\,(-\alpha\,\rho_\rho\, h +\ \alpha \int_0^h \bar{\rho}\ (k)dk\ )}$$

In this case k is used to represent the relative height instead of h within the integral and $\boldsymbol{C_\rho}$ is the volumetric concentration of particles within a density class j. $\boldsymbol{C_\rho^0}$ is the concentration of the component that has a density ρ at the bottom of the jig bed where the relative height (h) is equal to zero.

The concentration of a component at the bottom of the jig bed is related to the concentration of that same component in the feed by equation below.

$$C_\rho^0 = \frac{C_\rho^f}{\left[\int_0^1 \left\{\exp\left(-\alpha\, \rho_p\, h + \alpha \int_0^h \bar{\rho}\, du\right)\right\}\, dh\right]}$$

To solve this equation numerically, an iterative procedure is suggested with starts by assuming the initial density profile, then integrating numerically , and normalizing successive estimates of C_ρ^0 to satisfy the constraint that $\sum_{all\ \rho} C_\rho^0 = 1$ **(King, 1987 and King, 2001).**

2.6. Stratification by particle size in a batch jig

The literature review showed that particle size and density both have an effect on the performance of gravity separators in separating particles (**Xia *et al.*, 2007; Venkoba Rao *et al*., 2003; Venkoba Rao, 2007**). **Xia *et al.*, 2007** also found that mono sized particles stratify better in jigs than particles with a distribution of both sizes and densities. This justifies the assumption made by **King, 1987** that his model predicts well the behaviour of particles with similar shapes and sizes in a jig. If the feed size distribution is narrow then particle separation is mainly due to density differences, i.e. the system approaches the behavior of a system of mono sized particles. However, in practice a wide range of particle sizes are fed into a jig and size segregation plays an important role in the stratification of the bed **(Caulkin *et al.*, 2010)**. **Myburgh *et al.*, 2014** and **Myburgh, 2010** found that using jig feeds with narrower size ranges i.e. splitting a -8mm + 1mm class into -8mm + 3mm and -3mm + 1mm respectively, significantly improves product yield. However no model could be found in literature that has a proven ability to describe the full effect of particle size and particle size distribution on jig performance.

An empirical model by **Venkoba Rao *et al.*, 2007** attempts such a description by extending the King model to incorporate size effects. To achieve this they proposed that the stratification parameter has a power function relationship to the particle size. This enabled him to predict the partition surfaces at various cut heights of the particle bed for both size and density. One of the key findings of their study was that separation efficiency of coarse particles is markedly better than that of finer particles. However, the model is entirely empirical in nature and has not yet been supported by any experimental data.

2.8. Summary

This review of the literature has shown that jig performance is a function of both the density and the size of the particles being processed. There are also clear indications that it is influenced by both the size and the size distribution of the particles in the bed. The full extent to which these size effects influence the performance is however still not completely known. Various mechanisms by which jigging is thought to occur have been reviewed and these support the conclusion that size effects are significant in jigging and that these need to be understood better. The King stratification model stands out not only as an elegant model but as one that is able to describe stratification in a number of different contexts using only one empirical parameter. The validation of this model has largely been limited to mono size particles but no work has been done to investigate the extent to which it is able or not to model systems where particle size varies significantly.

In conclusion, it is apparent from the review of the literature that the influence of the particle size and particle size distribution on stratification is an under-researched area from two perspectives i.e. their influence on the performance of jigs and the extent to which current models, particularly the King model is able to describe stratification when there is significant variation in size and the range of particle sizes in the bed.

Chapter 3: Experimental Design, Equipment and Procedures

This chapter presents the methodology, experimental equipment and procedures used to perform the laboratory work needed to address the research objectives of this study.

3.1. Experimental design

The design of the experimental investigation was quite straight forward. It required stratification patterns in a jig to be measured for the particle systems in which the particle size and size range varied. Batch jigging was selected as the most convenient way to establish and measure these patterns. The particle systems selected were coal samples. There were several reasons for this. First, the jigging of coal is a very relevant context for investigating jig performance. Even though it is used little in South Africa, it is widely used elsewhere in the processing of coal. Second, simple and well known techniques are available for measuring the density distributions of coal. This meant that the measurement of density stratification patterns in the jig could be accomplished relatively accurately and easily. The equipment and procedures used are described shortly. With regard to the evaluation of jig performance standard measures were used as explained shortly. With regard to investigating the ability of the King model to fit the data generated, a parameter estimation routine developed previously by Prof Woollacott was used. Each aspect of the equipment, procedures and associated data are detailed in this chapter.

3.2. Jig Equipment

The Mintek batch jig (Figure 1) was made available for this project. The Jig was an air pulsed batac-type jig. The jig chamber was made up of 25mm thick rings stacked together to form a cylindrical chamber (Figures 2 and 3). These rings were firmly clamped down to prevent water leaks. The standard testing conditions used at Mintek were followed. The Hutch water flowrate was set to flow at a rate of 500ml/min. The height of the water overflow point above the top of the bed was set at 210mm and the residence time in the jig was set to 1200 seconds (20 minutes). The Jig cycle was set as shown in the Figure 4 below.

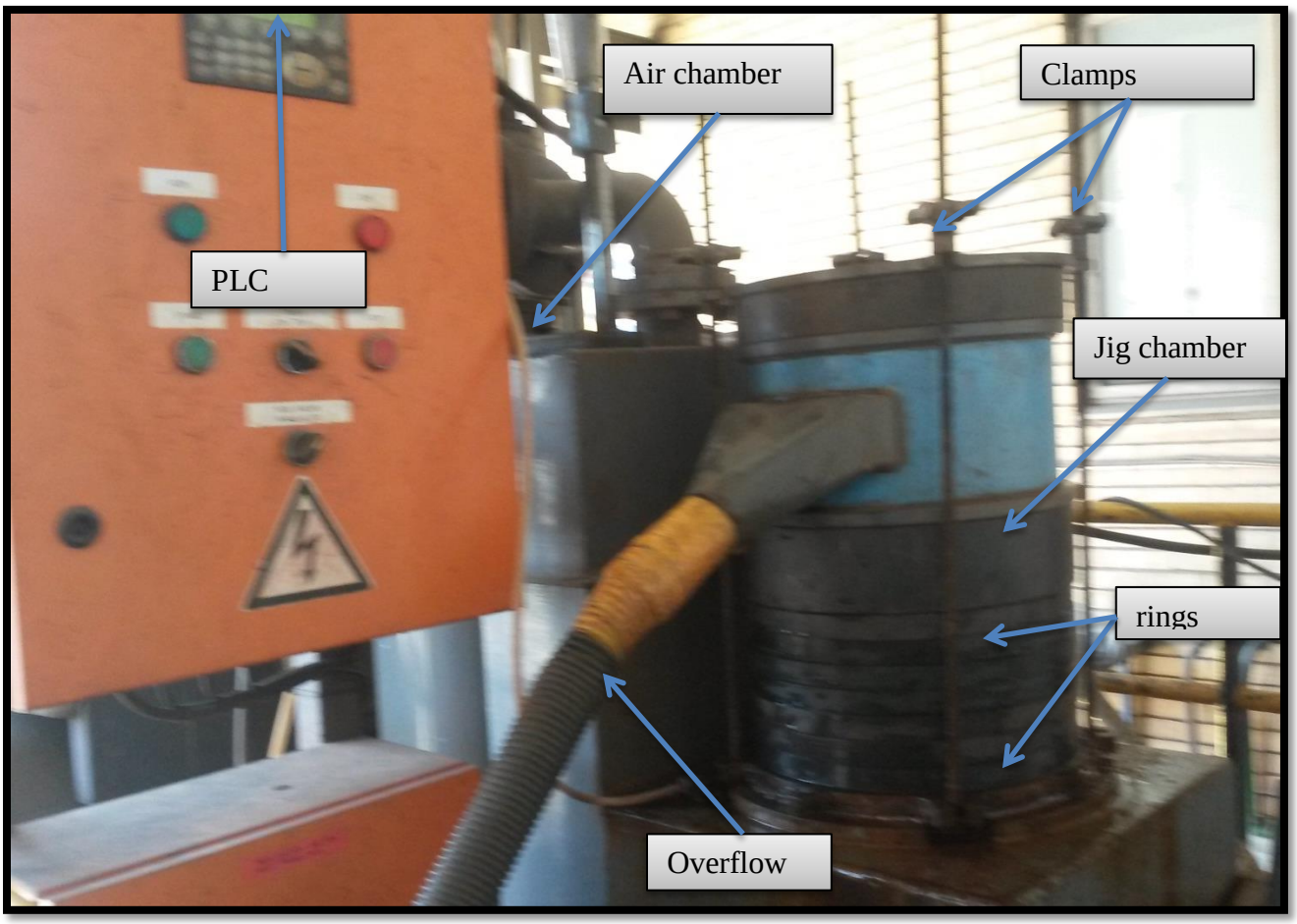

Figure 1: The Mintek batch Jig

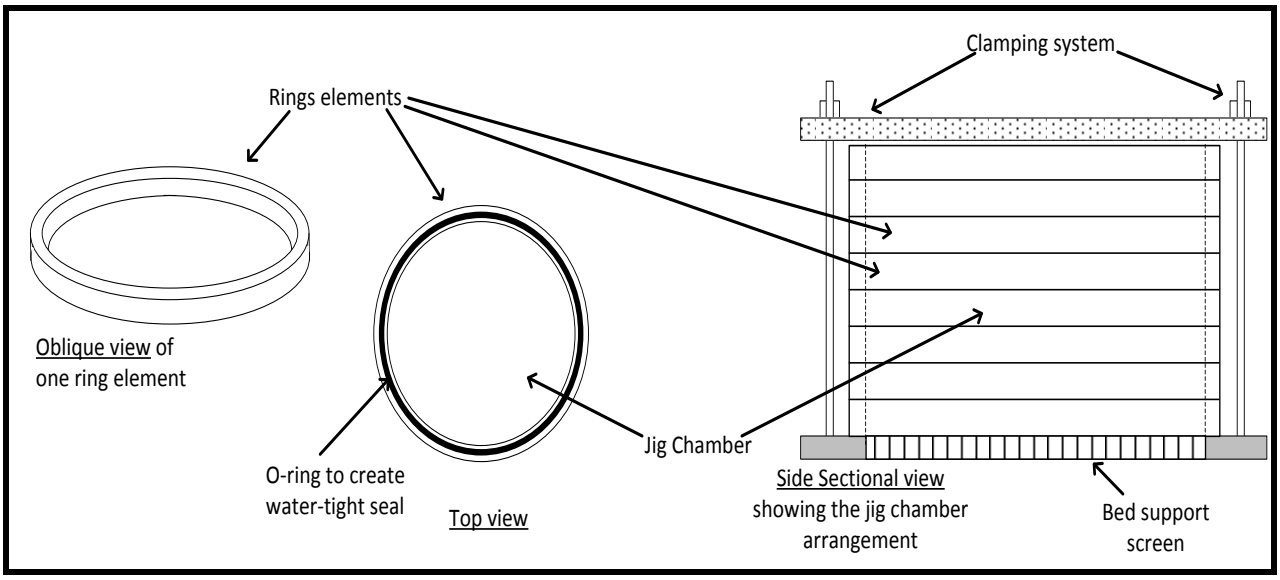

Figure 2: Jig chamber setup

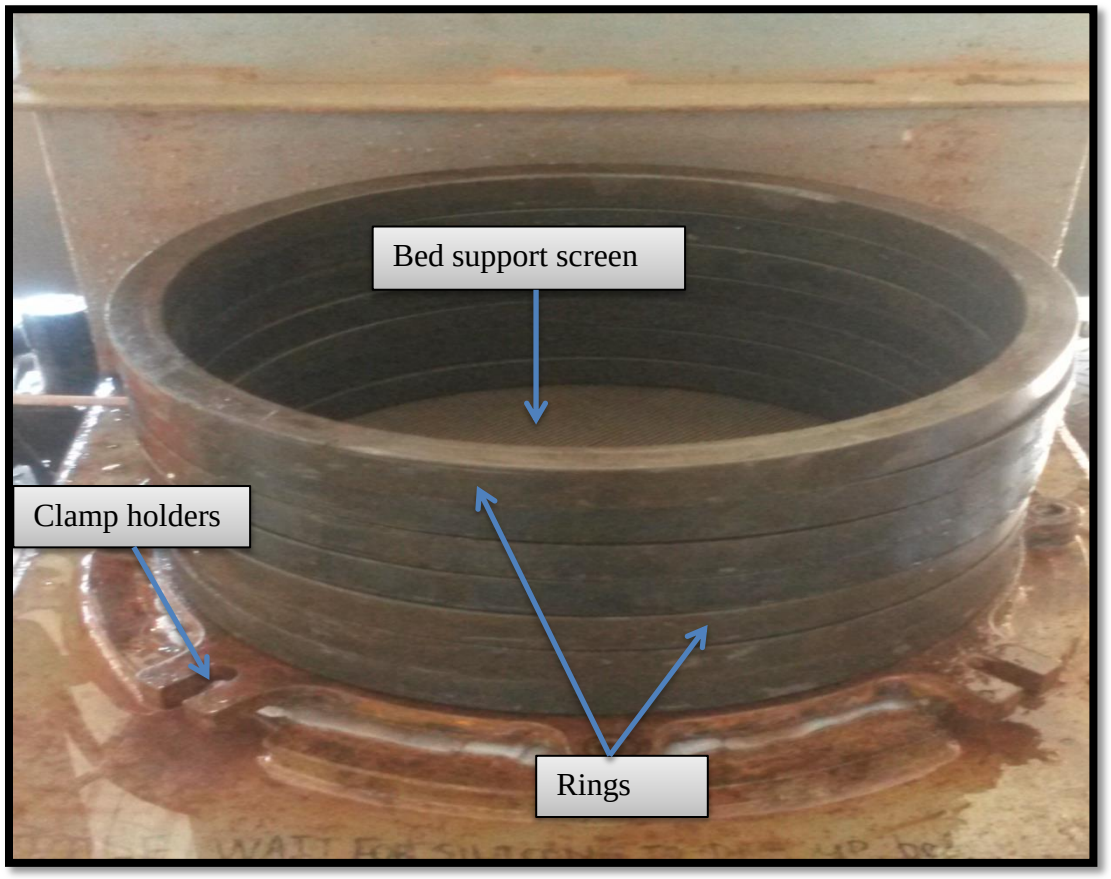

Figure 3: Makeup of the jig chamber setup

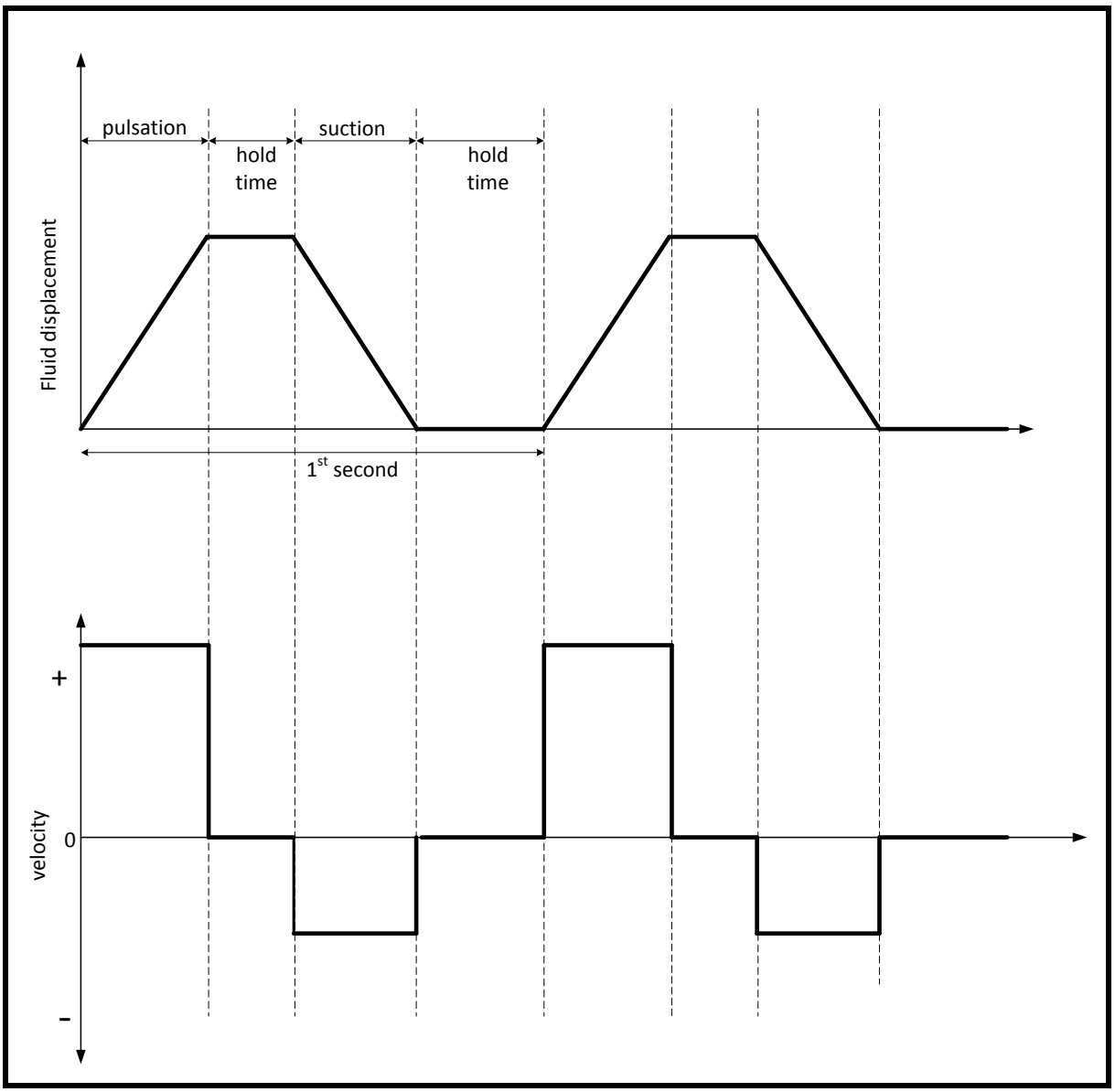

Figure 4: Jig cycles used in the tests

3.3. Test Procedures

3.3.1. Batch jigging tests

Once the jig equipment had been set up, the sample to be tested was poured into the chamber which was then flooded and jigged for 20 minutes with the jig cycle jig shown in Figure 4.

At the end of the experiment, the jig chamber was unclamped and the height of the particle bed was measured. The slices were removed progressively from the top of the bed by inserting a slicing device between each ring. The material collected from each layer was dried, weighed, bagged and tagged. The coal in each layer was then subjected to a float-sink analysis. After each test, all samples were screened into the different size classes in preparation for making up samples for the subsequent tests.

3.3.2. Float-Sink analysis

In order to split samples into different density fractions, a standard float-sink procedure was adapted using zinc chloride solutions. Six solutions with relative densities ranging from 1.3 to 1.8 with intervals of 0.1 were prepared as indicated in Table 2.

Table 2: Zinc chloride solution compositions

Density	$ZnCl_2$ vol%	Water vol%	Required $ZnCl_2$ vol for 8L solution	Required H_2O vol for 8L solution
1.3	30.77	69.23	3.79	4.21
1.4	38.44	61.56	4.73	3.27
1.5	45.48	54.52	5.60	2.40
1.6	51.90	48.10	6.39	1.61
1.7	57.69	42.31	7.10	0.90
1.8	62.85	37.15	7.74	0.26

For each density fraction two 5 litre beakers were setup, the first holding four liters for the purposes of the float-sink operation and the second holding two liters of solution for the purposes of rinsing the float fraction in preparation for the next stage in the analysis. The overall float-sink procedure is depicted graphically in Figure 5

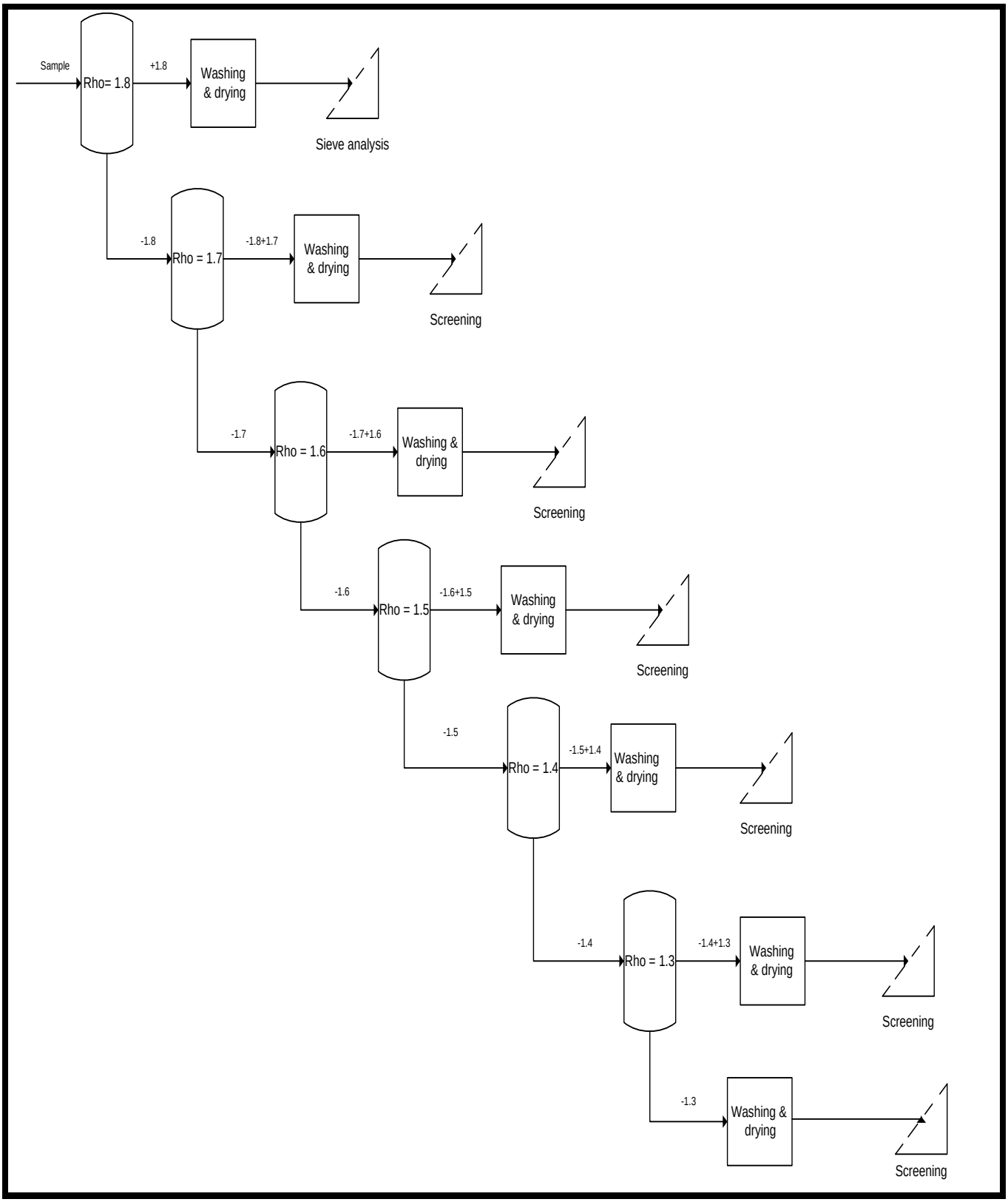

Figure 5: The float-sink analysis flow sheet

The dried sample poured out into the 1.8 S.G bath. The mixture was stirred to minimize the rafting phenomenon. This occurs either when heavier particles are carried on a bed of lighter particles making it difficult for them to freely settle or when lighter particles are under a bed of heavier particles hence preventing them from floating. The mixture was then given sufficient time to stand undisturbed ensuring that all material less than the density of the solution float and likewise all material denser than the medium to sink. The floats were then scooped out using a wire mesh strainer and rinsed in an intermediate solution with a density similar to that of the next float-sink stage. The rinsed product was then fed into the next stage of the process. The sinks were washed in a three stage wash setup before they were sun dried for an hour to ensure the removal of entrained zinc chloride solution. The process was repeated for all the six stages as depicted in Figure 5 and all subsequent layers from the jig were treated in the same way. After drying, all samples were weighed, bagged and tagged. Each sample obtained from the float sink analysis was screened to separate particles into different size classes in preparation for making up the sample for the next jig test.

3.4. Sample Preparation

3.4.1. Coal sample collection at Exxaro's Leeuwpan mine.

A sample of number two seam coal was collected from Exxaro`s Leeuwpan mine in Delmas, South Africa. The sample weighed about 100kg and had a top size of 50mm. The sample had been destoned i.e. it had been passed through a destoning jig to remove particles with an S.G. greater than 1.8.

3.4.2. Sample preparation for laboratory tests

Larger particles in the sample were crushed down to minus 25mm. A riffler was used to split the 100kg sample into smaller representative samples. This was done to ensure consistence of sample properties so that's results could be easily compared. The coal was then screened into five size fractions between 22.5mm and 6.7mm. The mass of each fraction was measured and recorded. Earlier work showed that between 8kg to 10 kg was an ideal sample size for test work with the 300mm Mintek jig. This gave a bed depth of between 130 and 150 mm. Knowing this, 9kg samples were prepared from the coal samples by mixing appropriate amounts of each size fraction to make up the desired size consist of the sample. Table 3 provides details of the 15

samples that were prepared. Each sample was made up of equal proportions (on mass basis) of the size classes indicated.

Table 3: Samples prepared

	Key		Top size (mm)					
	$D_{rep\ (mm)}$	R_s	A1	A2	A3	A4	A5	
bottom size (mm)			**22.5**	**19**	**16**	**13.2**	**9.5**	increasing particle size ↑
	B1	**19**	20.68	-	-	-	-	
			1.18	-	-	-	-	
	B2	**16**	18.97	17.44	-	-	-	
			1.41	1.19	-	-	-	
	B3	**13.2**	17.23	15.84	14.53	-	-	
			1.70	1.44	1.21	-	-	
	B4	**9.5**	14.62	13.44	12.33	11.20	-	
			2.37	2.00	1.68	1.39	-	
	B5	**6.7**	12.28	11.28	10.35	9.40	7.98	
			3.36	2.84	2.39	1.97	1.42	
	decreasing particle size and size range →							

In the table, D_{rep} represents the average particle size in a given sample i.e. it is denoted by the grey blocks in the table. R_s represents the size range of a given sample and is defined as the ratio of the largest to the smallest particles in the sample.

3.4.3. Design of the sample sets

The arrangement of samples in Table 3 allowed four different kinds of analysis to be undertaken. It allowed samples to be grouped in subsets which had similar properties. The first subset was assembled on the grounds of similar R_s ratios. This was done so that the effect of size on jig performance could be analyzed independently of R_s. Referring to columns (A1 to A5) and rows (B1 to B5) in Table 3, the subsets with about the same R_s ratio are as follows

- $R_s \approx 1.19$: A1B1, A2B2, A3B3
- $R_s \approx 1.4$: A1B2, A2B3, A4B4
- $R_s \approx 1.7$: A1B3, A3B4
- $R_s \approx 2.0$: A2B4, A4B5
- $R_s \approx 2.4$: A1B4, A3B5

The second subset brought together samples with relatively similar average particle sizes but differing size ranges. This was for the purposes of investigating the effect of size range on jig performance and model fits independent of particle size. The relevant subsets are as follows:

- $D_{rep} \approx 15mm$: A3B3, A1B4
- $D_{rep} \approx 17mm$: A2B2, A1B3

The third subset grouped all samples with the same top size but different bottom sizes together for the purposes of investigating how average particle size and size range affect the jig and model performance when considered simultaneously.

Finally, the last subset of samples was prepared to test which between the two, particle size and particle size range is jig performance was most sensitive to. This was achieved by comparing samples with the same bottom size but different top sizes.

3.5. Data analysis: Modeling the experimental data

All the data was recorded on an electronic spreadsheet (Microsoft excel). This section presents a sample of that data and how it was manipulated in order to address the research objectives of this project.

Table 4: Sample of washability data collected, -22.5mm+19mm

Class	**Mass (g)**				
	Layer 1	Layer 2	Layer 3	Layer 4	Layer 5
-1.3	0	0	0	0	85
-1.4+1.3	0	7	47	354	1215
-1.5+1.4	0	69	719	936	297
-1.6+1.5	26	517	579	86	5
-1.7+1.6	158	548	119	7	0
-1.8+1.7	346	256	15	0	0
+1.8	1268	174	4	0	0

Table 4 above is a sample of the data generated in a jig test. The tables for all the data sets can be found in Appendix A. For each test the reconstituted feed was determined from the data in the

table and this was used to plot the density distribution curve. This curve was then used to estimate the densities of the lightest and the heaviest particles in the sample respectively by extrapolation. From this data the volume of each density fraction in each layer was calculated. This volume data was used as the input to the MATLAB code used for fitting the model to the data.

3.5.1. Recovery-yield plots

It was found that the most convenient and clear way to present and evaluate the jig performance information was in the form of Recovery-Yield curves. An example of such a curve is shown in Figure 6. This graph shows the cumulative recovery of a given density fraction to the top product against the mass yield of solids to that product. For consistency across the tests the density fractions refed to in the figure are cumulative fractions, i.e. -1.3 to -1.8 g/cm^3. In each figure an idea of the exact separation of the fraction can be gauged by comparing it with the 'no-separation curve' which represents no stratification occurred during the jigging process. The further away the curves are from the no-separation line the better the separation. For the density fraction 1.3g/cm^3 anomalous results sometimes occured because of the small proportions of this fraction in all samples. The most distinct difference in performance is observed with the -1.4 g/cm^3 density which constituted a major proportion of the material fed to the jig.

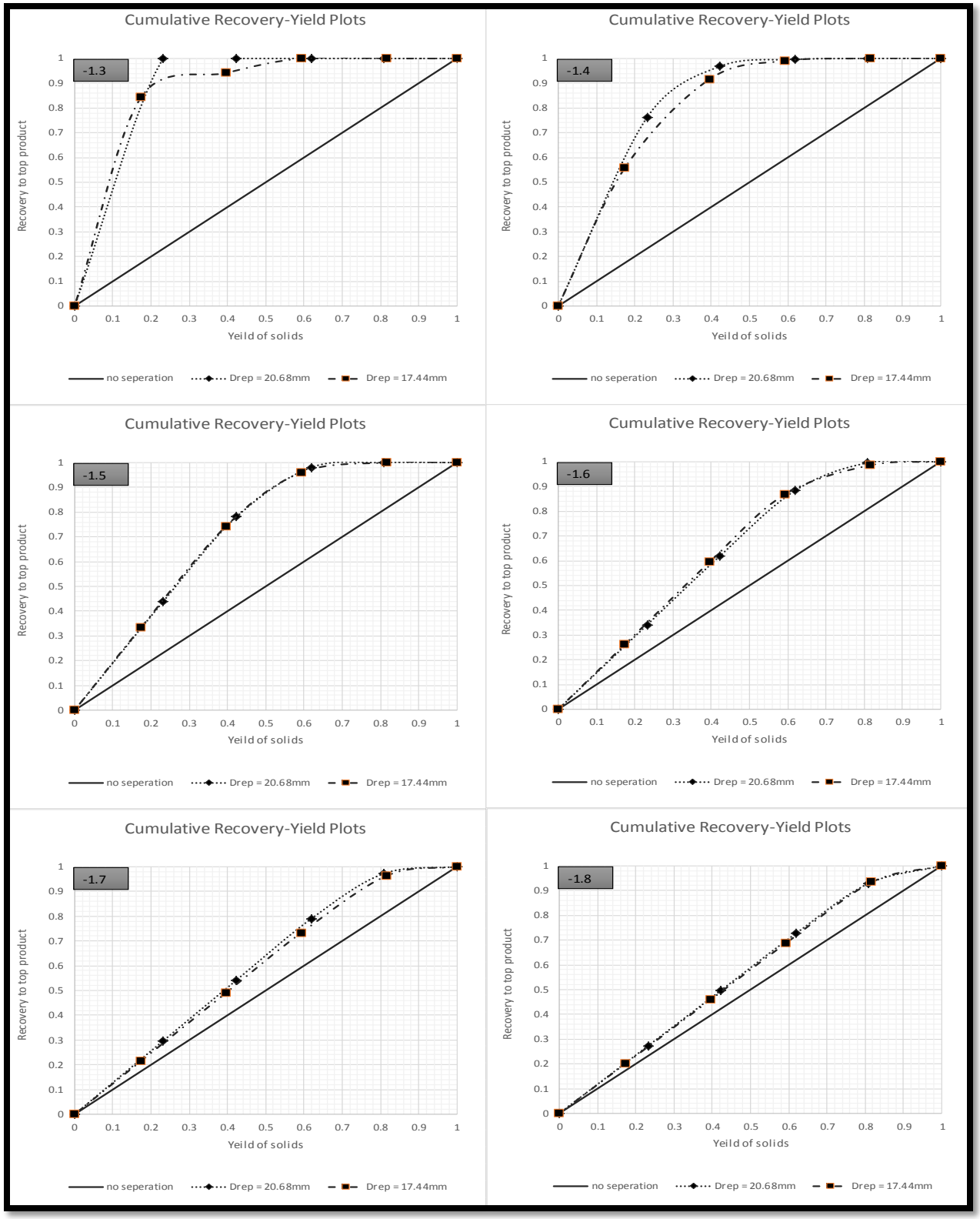

Figure 6: Sample Recovery-Yield curve

3.5.2. Partition curves

A partition curve shows how material of different specific gravity will split into one of the product streams. It allows the derivation of more quantitative indicators of jig performance namely the cut density, epm and the imperfection I_c. A partition curve for each test was developed by first plotting the associated cumulative recovery curve. Figure 7 illustrates how this was done.

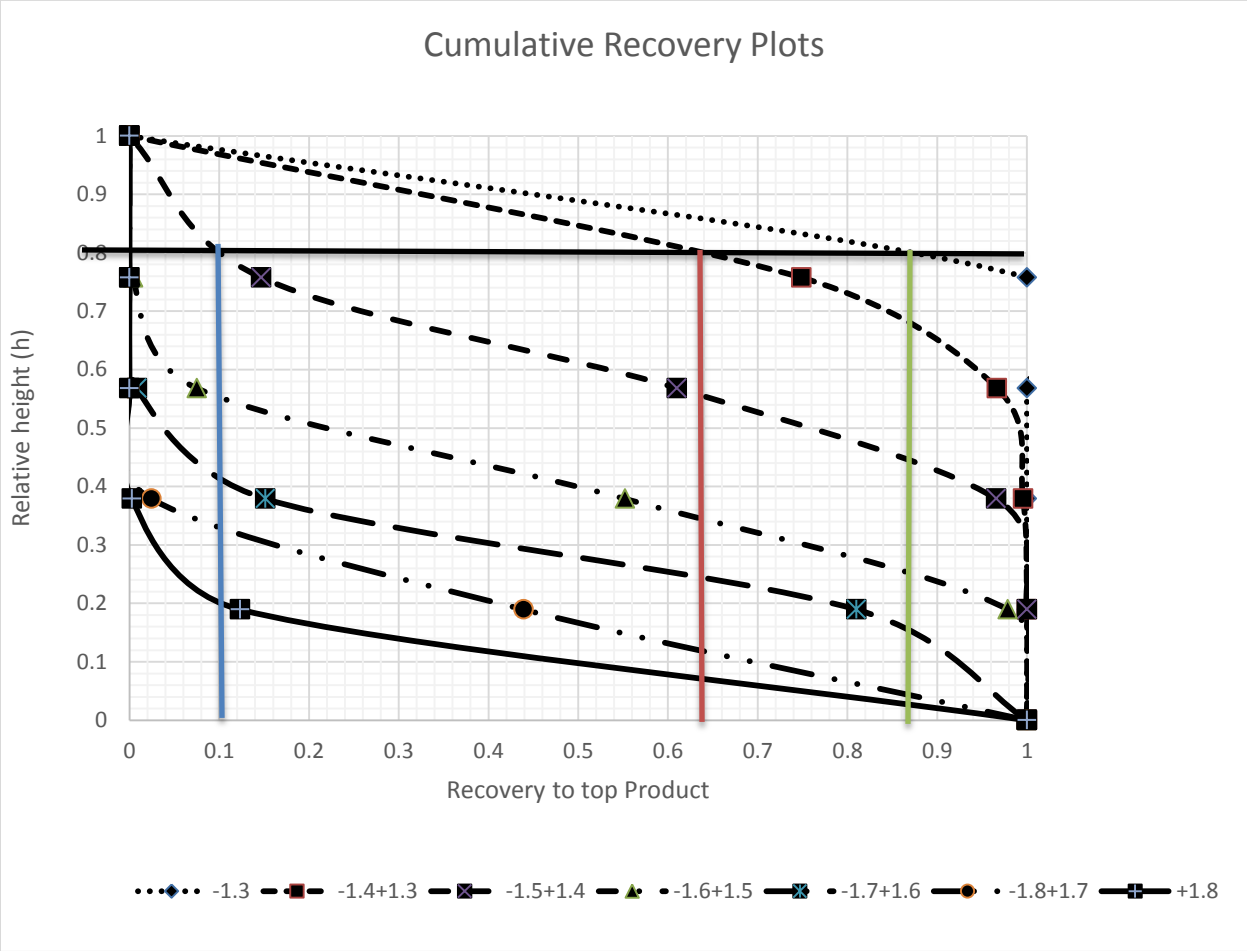

Figure 7: Typical cumulative recovery curve

A cumulative recovery curve such as shown in Figure 7 indicates the volumetric proportion of each density fraction in the bed that would report to the top product if the bed were to be split at a height h. Figure 7 illustrates the recoveries when the bed is split at h=0.8. The partition curve

associated with such a split is the plot of these recoveries vs. the density of the density fraction. Figure 8 is illustrative. A different partition curve is associated with splits at any value of h. Partition curves were developed and analyzed for values of h ranging from 0.1 to 0.9 in intervals of 0.1.

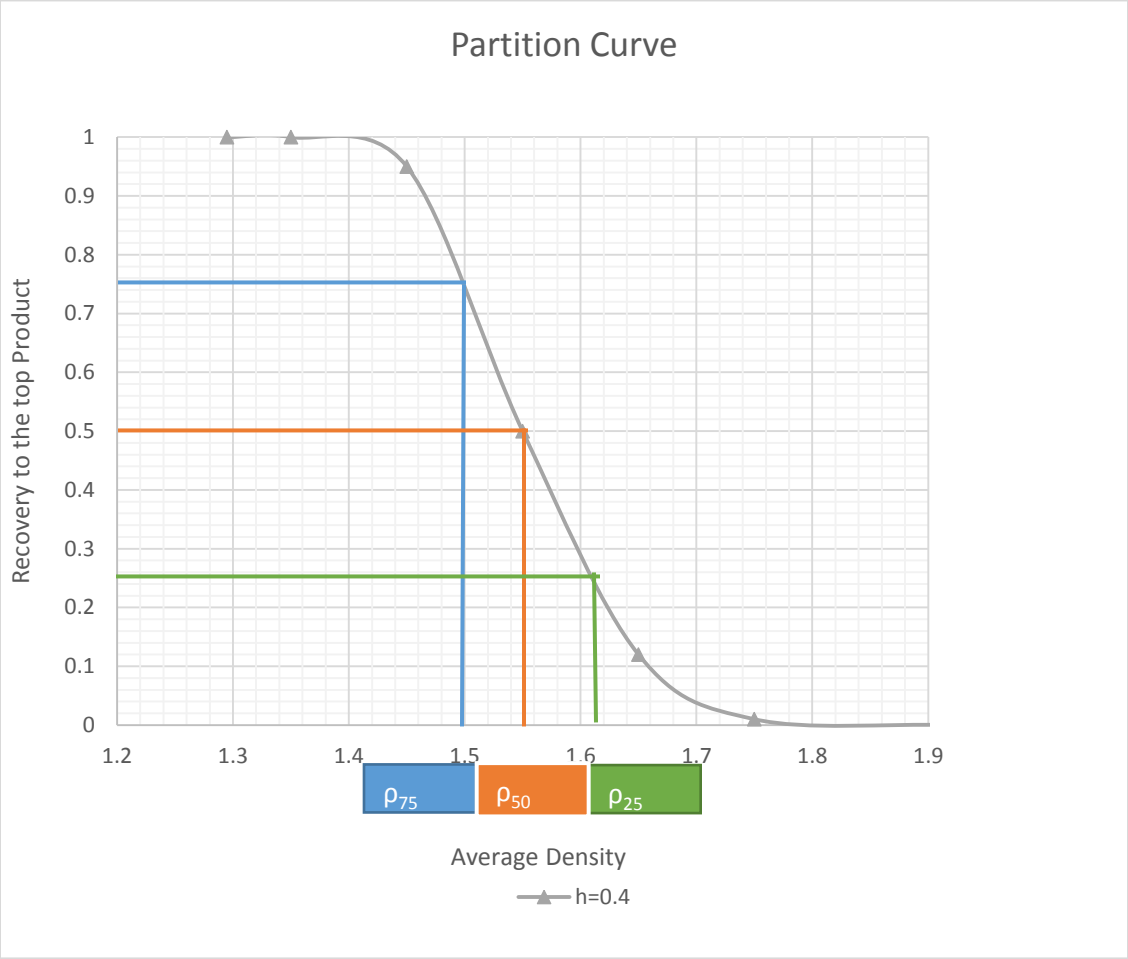

Figure 8: Typical partition curve

The partition curve gives a number of useful items of information. The first is the cut point which is denoted by ρ_{50}. This represents the density of the particles that have an equal chance of reporting either to the top or bottom product. The second is the Écart probable moyen (EPM) which is a measure used to quantify the sharpness of separation. The EPM is defined as

$$EPM = \left|\frac{\rho_{75} - \rho_{25}}{2}\right|$$

The terms ρ_{75} and ρ_{25} are the density of particles that have 75% and 25% probability of reporting to the top product. To enable general comparisons to be made, the EPM can be normalized by dividing it by the cut density, to give the imperfection (I_c) i.e. a normalized measure of separation efficiency given by the equation below.

$$I_C = \frac{\rho_{75} - \rho_{25}}{2\rho_{50}} = \frac{EPM}{\rho_{50}}$$

3.5.3. Solving the King model`s core equation

A MATLAB parameter estimation routine developed by **Woollacott, 2014** was used to solve the differential equations that represent the King Stratification model. It finds the stratification coefficient (α) that result in the best-fit between the model and the experimental data. This is achieved by minimizing the sum of squared differences SSD, between the experimental values $X(i)_{expr}$ and the model predicted ones $X(i)_{model}$. The objective function can be defined as follows

$$SSD = \sum_{i=1}^{n} \left[X(i)_{expr} - X(i)_{model}\right]^2$$

where n is the number of data points i.e. the number of density components multiplied by the number of layers sliced from the bed. The experimental values $X(i)_{expr}$ are associated with each density component j and each layer sliced from the bed during a test. An experimental value may be the concentration $C_j(i)$ in layer i, or the cumulative concentration $\overrightarrow{C_J}(i)$ of the component from that layer to the top of the bed, or the associated recovery of that density component, $\overrightarrow{R_J}(i)$. These are defined as follows

$$C_j^i = \frac{1}{t_i - b_i} \int_{b_i}^{t_i} C_j(h)\, dh$$

where $C_j(h)$ is the concentration of component j in the layer from h to h+dh and t_i and b_i are the heights of the top and bottom respectively for the i_{th} layer sliced from the bed.

$$\overrightarrow{C_j} = \int_{h_i}^{1} C_j \, dh$$

where, $h_i = h$ for the ith layer

and $$\overrightarrow{R_j} = \int_{h_i}^{1} R_j \, dh$$

where C_j^f is the feed concentration of component j

and

$$R_j^i = \frac{1}{C_j^f} \int_{b_i}^{t_i} C_j(h) \, dh$$

3.6. Limitations of the study

As shown in Figure 1, the Mintek jig has a jig chamber that is composed of 25mm ring elements that are stacked and clamped together to make up the jig chamber. Some of these rings were found not to be perfectly circular which resulted in the wall of a jig chamber that was sometimes irregular in places. It would be expected that this would create a degree of turbulence near the side walls of the jig chamber. This could potentially cause different particle behaviour near the walls. Figure 9 shows an instance where this wall effect was observed. To investigate this possibility, light colored particles were introduced into the jig chamber before jigging the coal in the normal way. In most cases the wall effect was not observed and when it was observed the effect was not very severe. Obviously the effect could not be observed or assessed on the 15 tests themselves. However, the effect constitutes a possible cause of the experimental error in the study.

Figure 9: The effect of turbulence in the jig chamber

A second cause of experimental error is the local scouring and remixing of particles that occurred when the bed was sliced. Because the particles were fairly coarse, the movement of the slicer through the bed inevitably jammed particles together causing a degree of scouring of particles from layers below the slicer. This effect was unavoidable and had to be accepted as a source of inherent experimental error.

Chapter 4: Results I: - Jig performance as a function of particle size and size range

4.1. Introduction

In this chapter, jig performance as a function of particle size and particle size range is investigated for a typical South African coal. The raw data collected from the batch jig tests and float-sink analysis is processed to provide the different performance parameters necessary to fully describe the jig performance in processing the coal. The parameters of interest are the cumulative recovery and the yield of solids. These were used to generate partition and recovery-yield plots for the different samples tested. Ultimately the variation of the EPM and the imperfection (I_c) with size and size range are determined and an empirical model for describing jig performance as a function of the cut density is presented. The data was analyzed from a number of perspectives to provide a holistic view of the effect of size and size range on jig performance.

4.2. Analysis of the Results

In order to address the question, "how does particle size and size range affect jig performance?" five indicators of separation performance were used – recovery–yield curves, partition curves, EPM and I_c (imperfection). Details of how each of these indicators was determined have been given in chapter 3 section 4.

The test data was analyzed from the following perspectives:

i. Influence of particle size on performance.
ii. Influence of size range on performance.
iii. Influence of both particle size and size range.
iv. Analysis of jig performance by reference to partition curves, EPM and I_c.

The first three perspectives focus on recovery-yield plots as a means of describing and comparing jig performance. The last perspective analyzes performance by reference to partition

curves, EPM and I_c. This allowed an extension of the analysis that enables a comparison of jig performance with the performance of other density separation processes.

4.3. The influence of particle size on jig performance

This section looks at the effect of particle size on jig performance for systems that had similar size ranges. Three data subsets with size ranges of about 1.2, 1.4, and 1.99 are investigated. The recovery-yield plots for these subsets are presented in Figures 10 to 12.

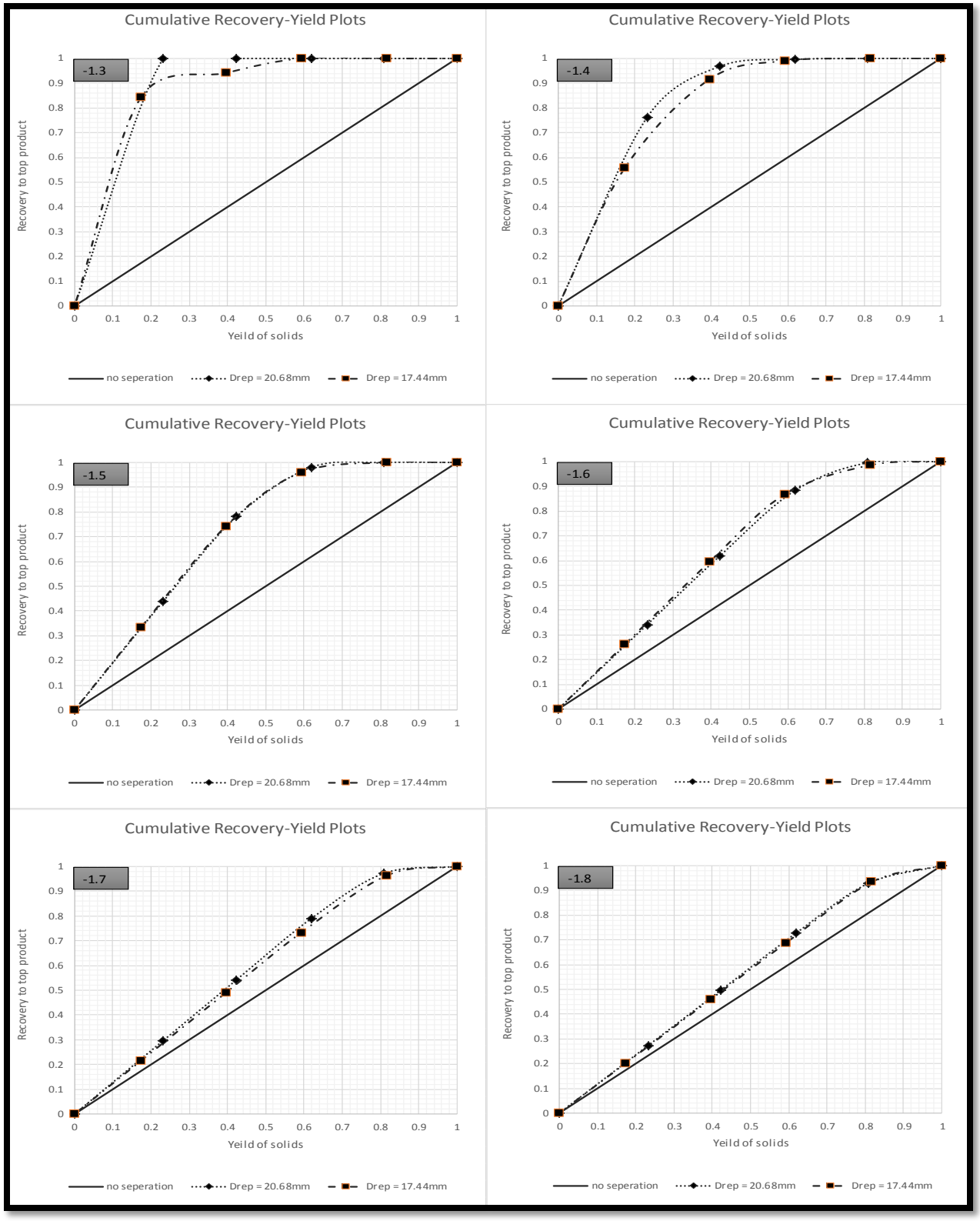

Figure 10: Effect of particle size on performance, Rs≈1.2

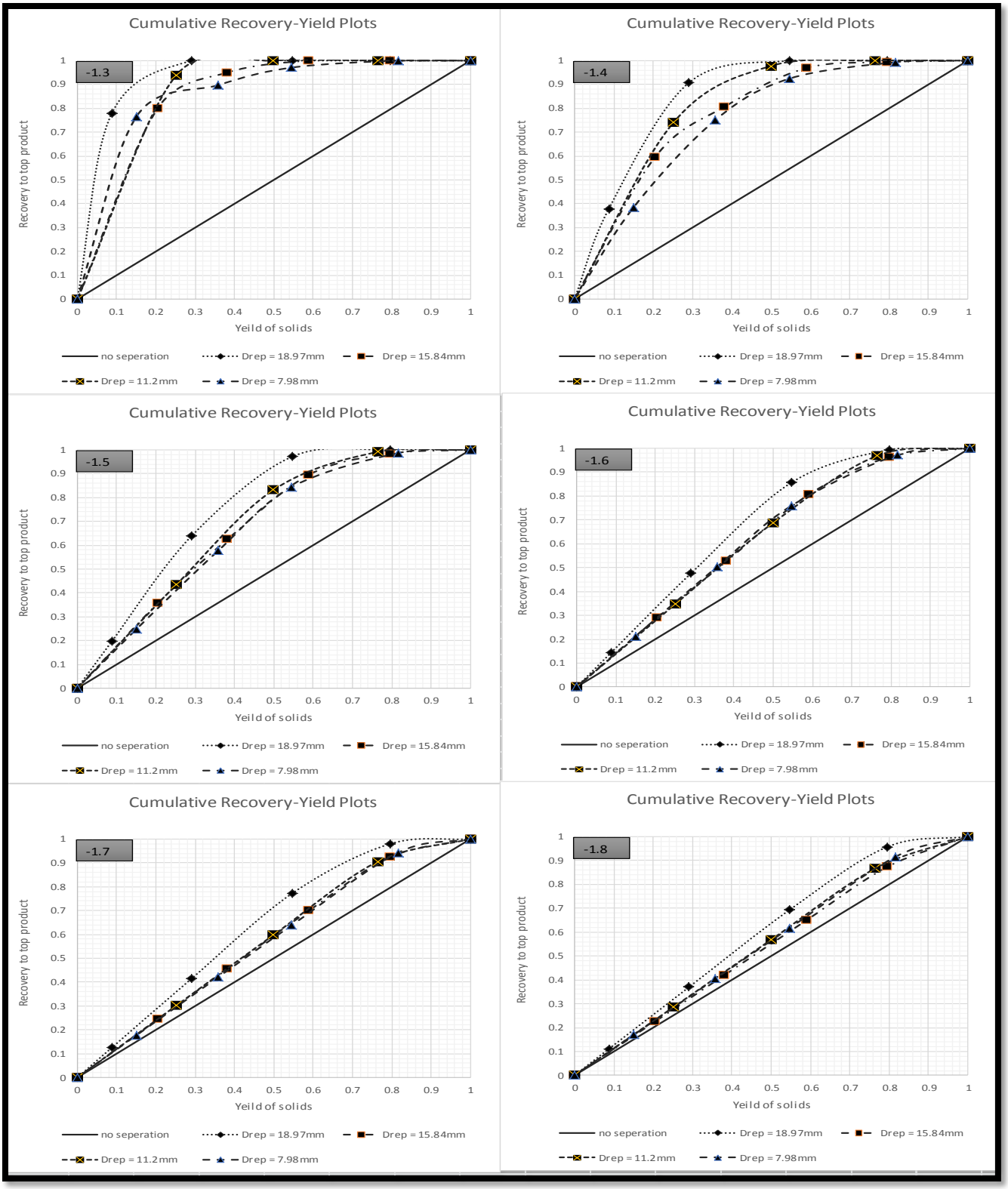

Figure 11: Effect of particle size on jig performance, Rs≈1.4

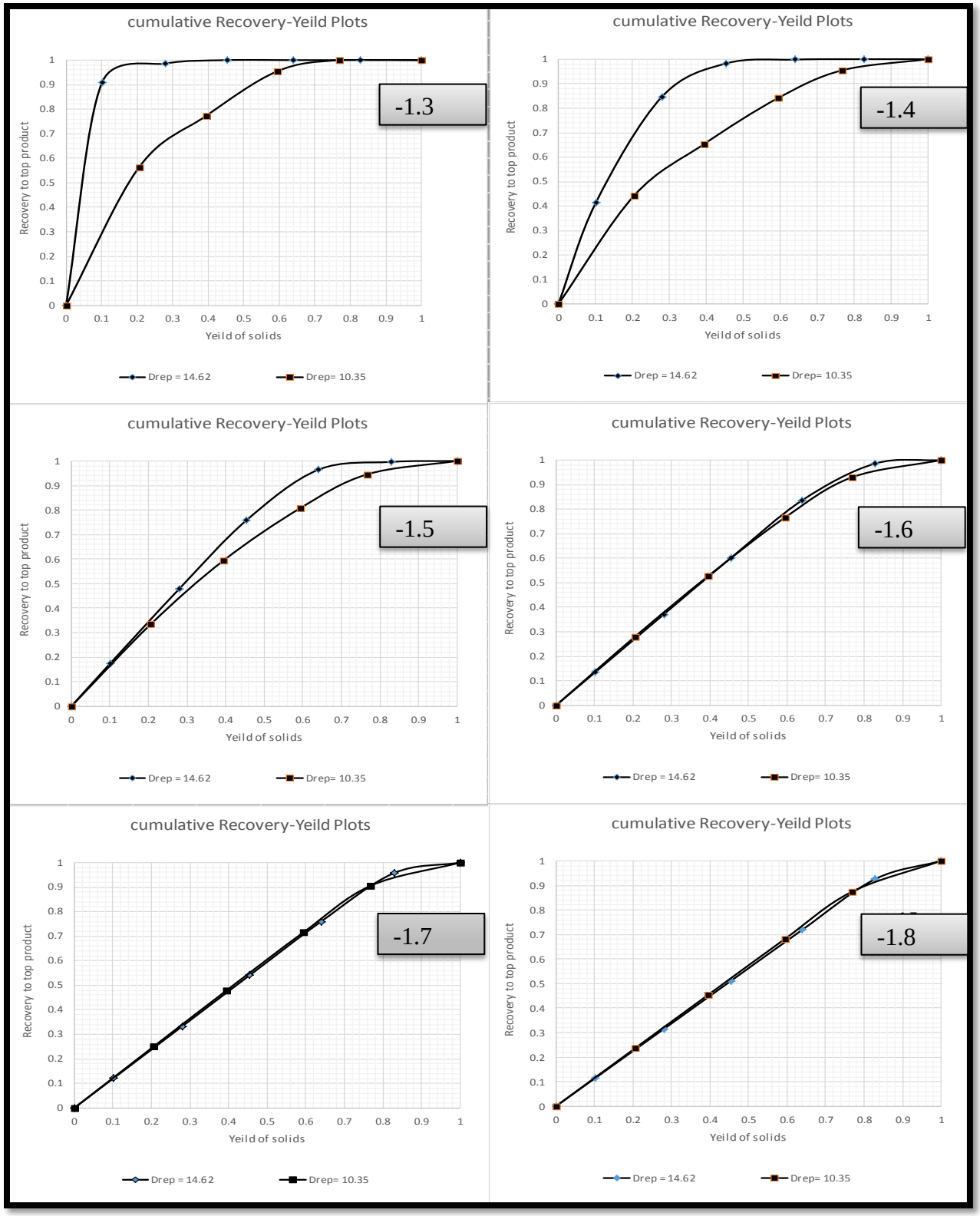

Figure 12: Effect of particle on jig performance, Rs≈1.9

It can be seen from Figures 10 to 12 that the recoveries to the top product are greater for systems of larger particles than for the systems of smaller particles. For example with a size range of 1.4 (Figure 11), the recovery when particles are larger was greater than when particles were smaller particles; e.g. considering the 1.4 g/cm^3 density fraction and a yield of 30%, the recovery with 18.97mm particles was 92%, 83% with 15.84mm particles, 72% with 11.2mm particles and only 67% with 7.98mm particles. The same trend is evident in Figures 10 and 12 for the density fractions -1.5, -1.4 and -1.3 g/cm^3. For the higher density fractions, -1.6 g/cm^3 and above, there is little variation in the recoveries for systems of different size because the higher density fractions constitute the majority of the material in the beds.

4.3. The effect of size range on jig performance

For the purposes of determining the effect of size range on jig performance, data for the subsets with relatively similar average particles sizes but varying size ranges (Rs) were compared. The relevant recovery-yield plots are presented in Figures 13 and 14.

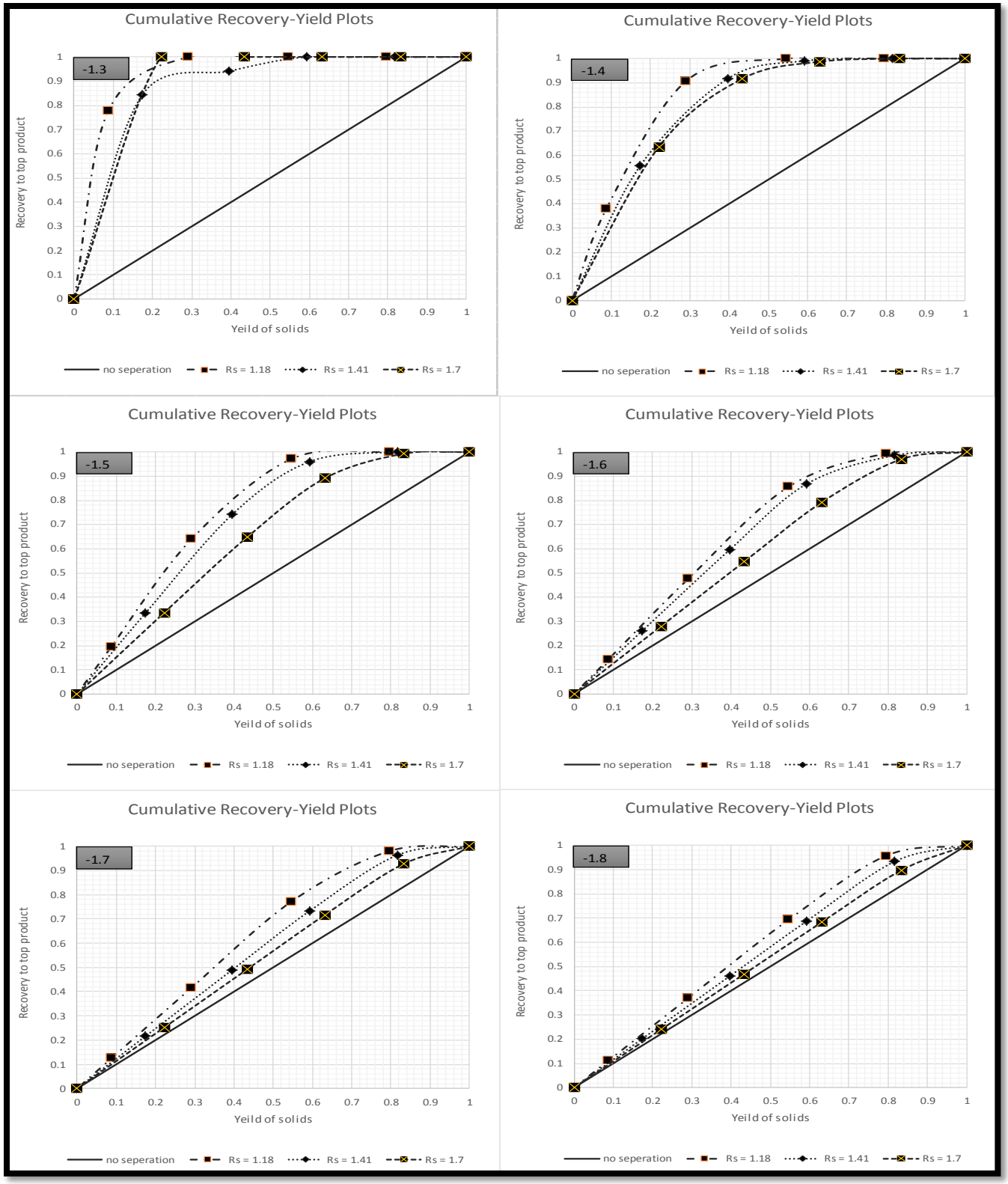

Figure 13: Effect of size range (R_s) on jig performance, Drep= 17mm

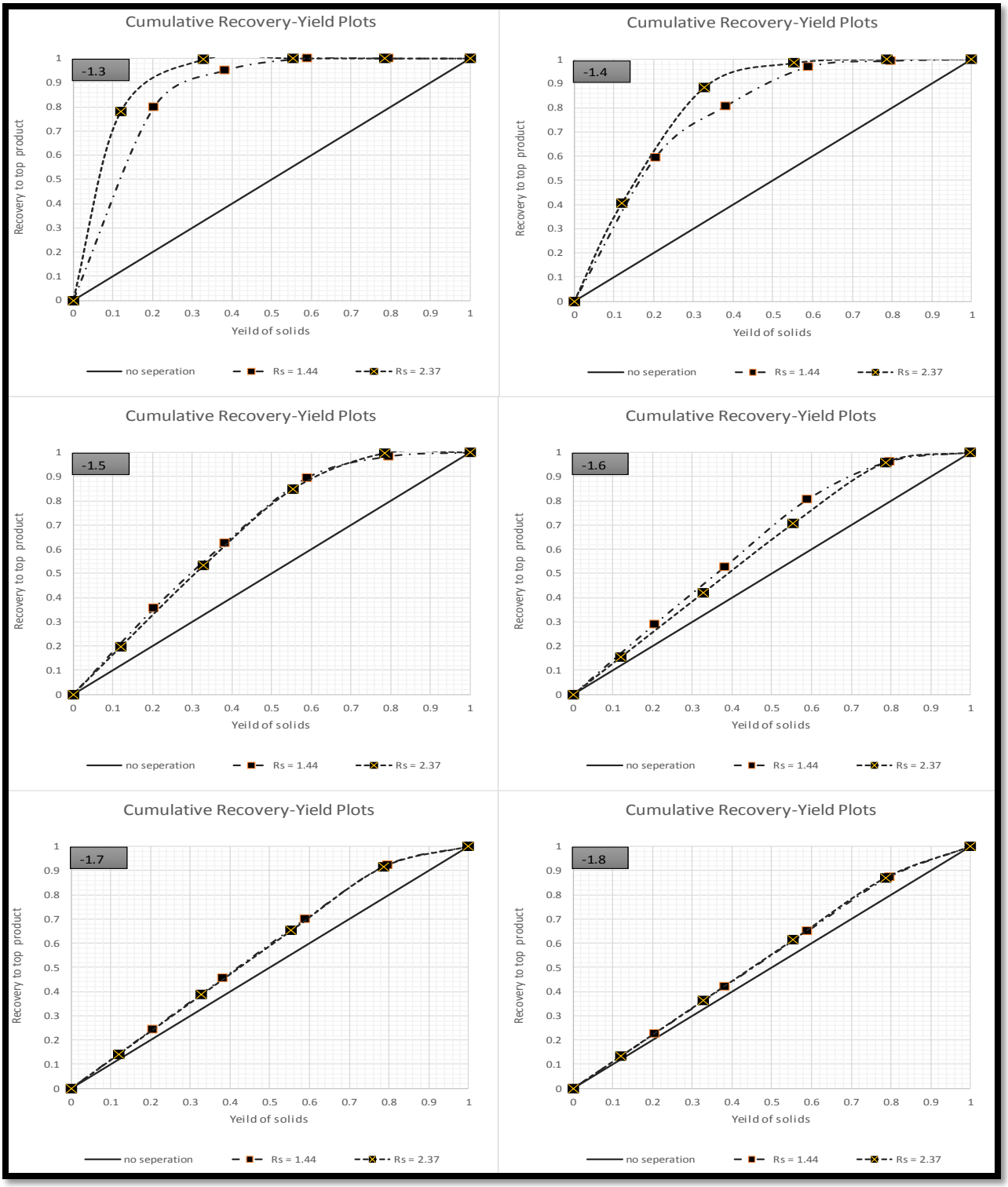

Figure 14: Effect of size range on jig performance, Drep= 15mm

It can be seen from Figures 13 and 14 that the jig performance has a negative correlation to the particle size range for the systems tested. That is to say that the jig performed better in stratifying the bed of particles when the ratio of the sizes of the smallest to largest particles in the sample was smaller.

This is most clearly demonstrated in Figure 13, by considering the 1.5 g/cm^3 density fraction and a yield of 40%. A recovery of 66% is achieved for the sample with the widest size range of 1.7., 91% for the sample with a range of 1.41 and 99% for the sample with the narrowest size range of 1.18.

Similarly, in Figure 14, with the density fraction 1.4 g/cm^3 and a yield of solids of 40% a recovery of 95% is achieved for the system with a size range of 1.44 and a significantly lower recovery of 81% is achieved for the sample with a size range of 2.57.

4.4. The combined effect of size and size range: the sensitivity of jig performance to size effects

Up to this point I have investigated the effect of size alone while size range is held constant and vice versa. However, in this section I take the analysis further by investigating the effect of these two simultaneously by looking at samples with the same bottom size but different top sizes. The data from four subsets were examined i.e. with bottom sizes of 6.7mm, 9.5mm and 13.2mm for top sizes of 13.2mm, 16mm, 19mm and 22.5mm respectively – see rows B3, B4 and B5 in Table 3. As can be seen from the table, both the average particle size and the size range R_s increase from left to right across each row.

Comparing jig performance for these subsets addresses the question as to whether particle size has a greater influence on jig performance than size range or vice versa. The logic is that since it has been established that jig performance has a positive correlation with particle size and negative one with size range, comparing data sets in which the size range and average size increase simultaneously should reveal which of the two trends is more dominant. If jig performance improves in this sequence then the positive effect of an increase in particle size must be greater than the negative effect of an increase in size range. Figures 15, 16 and 17

compare the recoveries of the density fractions -1.3 g/cm^3 and -1.5 g/cm^3 when the yield varies between 0.3 and 0.6.

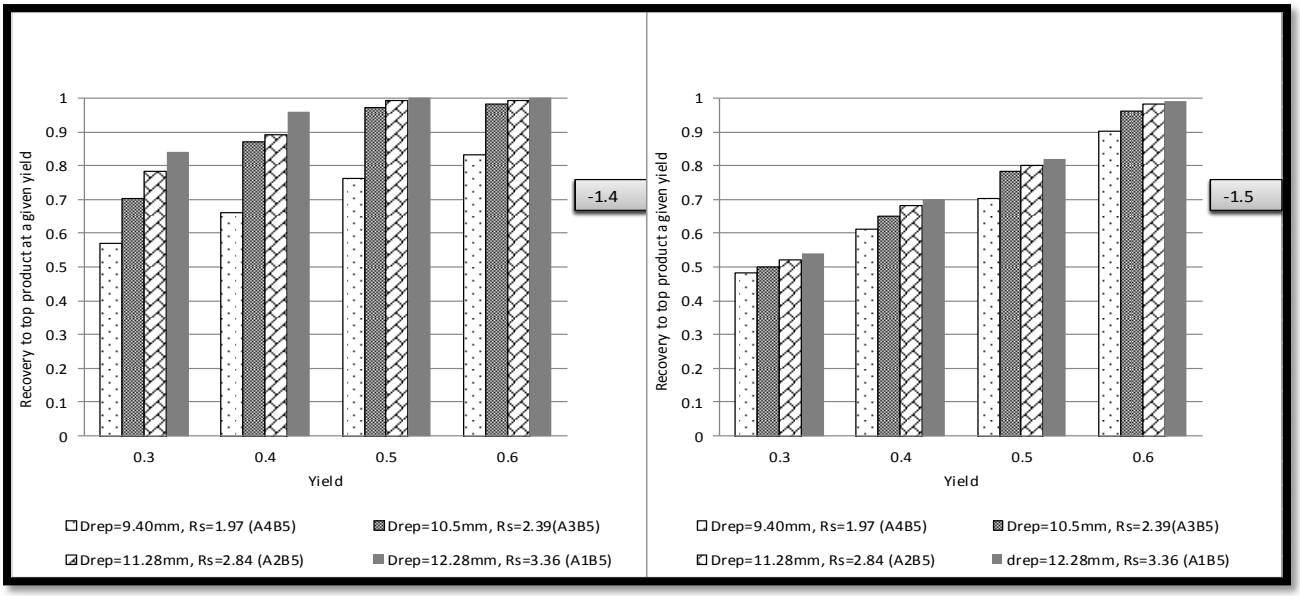

Figure 15: Recovery at a given yield for samples with a bottom size of 6.7mm

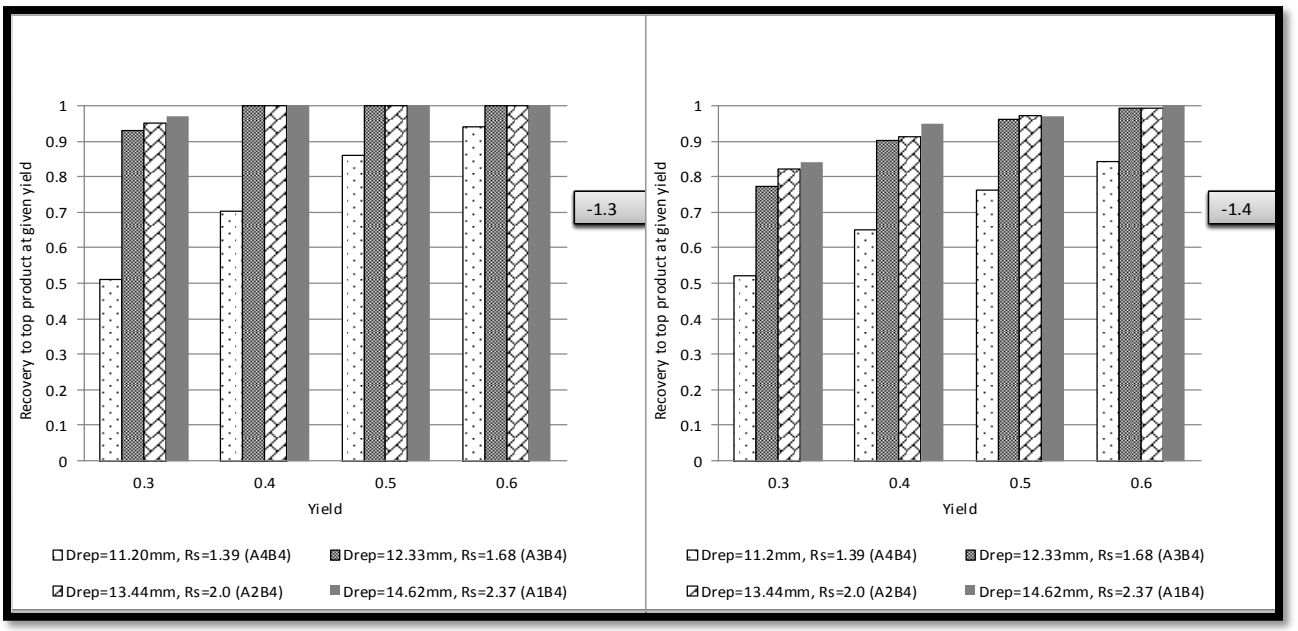

Figure 16: Recovery at a given yield for samples with a bottom size of 9.5mm

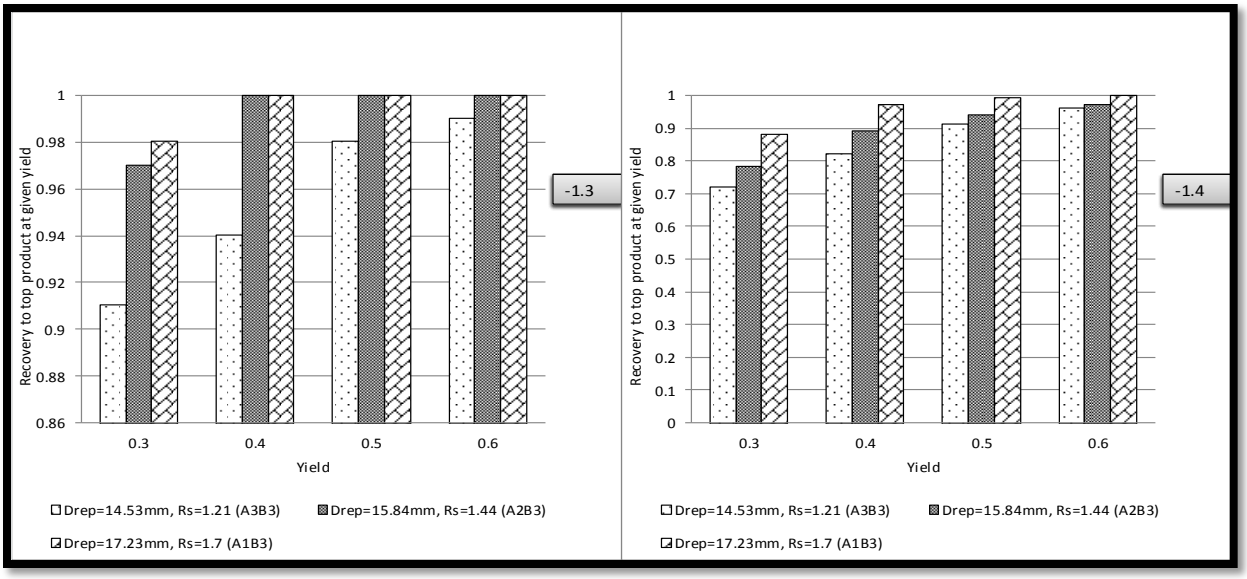

Figure 17: Recovery at a given yield for samples with a bottom size of 13.2mm

Since increasing either the particle size or size range has opposite effects on the jig performance, the one which results in the greatest change in jig performance when both are increased is the one which jig performance is most sensitive to. It is observed that in all cases, the recovery of the density fractions shown clearly improves with an increase in particle size. This suggests that jig performance is more sensitive to particle than it is to the width of the size range.

4.6. Quantifying the jig performance in terms of standard indicators

In this section I will use more general indicators of jig performance i.e. EPM and I_c (the imperfection) which allows a comparison with the performance of other density separators.

As indicated in section 3.5 splitting the bed at different heights yield different cut densities and epm values. Figure 18 indicates typically how these cut densities and epm values vary – each point representing the situation when the bed is split at a different h.

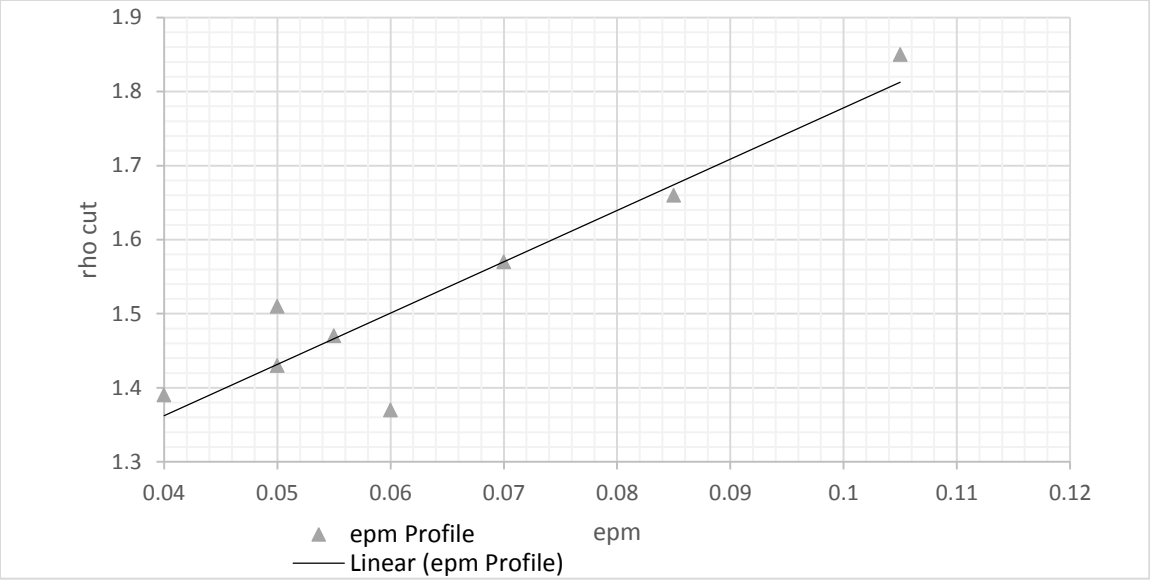

Figure 18: Typical relationship between epm and cut density

As can be seen, the relationship between cut density and epm appears to be linear with EPM increasing as the cut density increases. It has been shown by (**Gotfried, 1978**) that the EPM is directly proportional to the cut density and these results agree with his claim. Accordingly the relationship can be described by a linear equation obtained by an appropriate regression analysis. This was done for all the data sets and the results are presented in Appendix C. Figures 19 to 21 are typical of these results. They show fits to the subsets having the same size ratio i.e. 1.2, 1.4 and 1.98 but different average particle sizes.

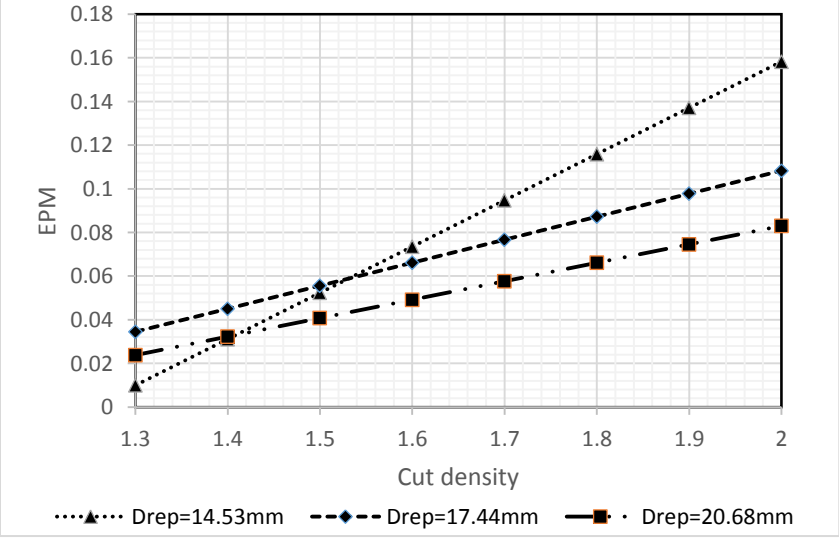

Figure 19: Effect of size on jig performance, EPM vs. cut density for Rs=1.2

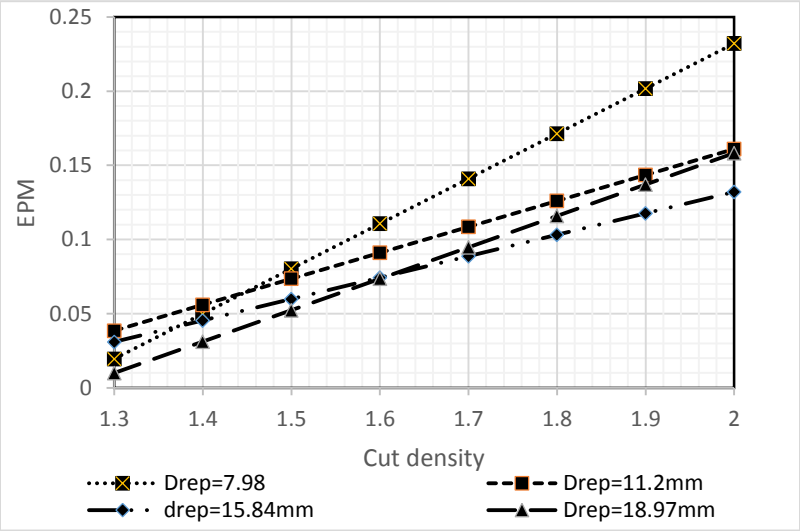

Figure 20: Effect of size on jig performance, EPM vs. cut density for Rs=1.4

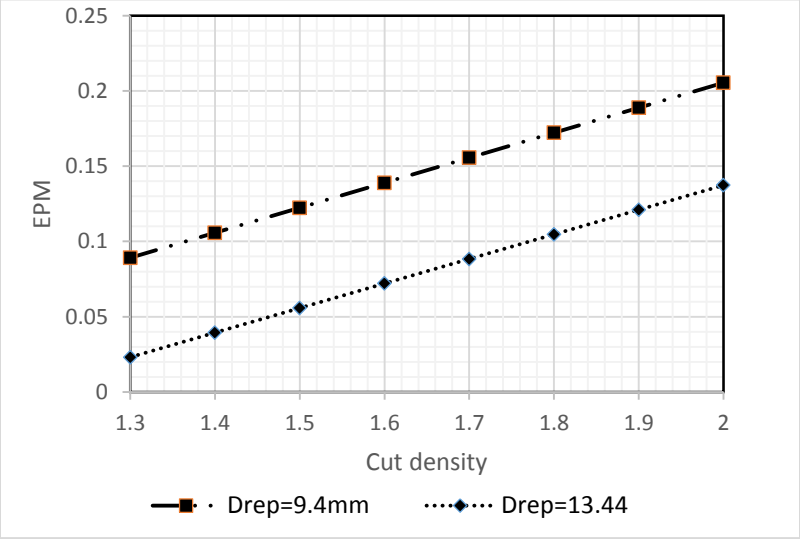

Figure 21: Effect of particle size on jig performance, EPM vs. cut density for Rs=1.98

It be seen in Figures 19 to 21 that the EPM of larger particles was lower than that of smaller particles at the same cut density. This means that better jig performance is achieved when processing larger particles relative to finer particles. This reinforces the findings obtained from the recovery-yield plots.

4.6.2. The effect of size range on EPM

Figures 22 and 23 present the linear fits of the epm-ρ_{cut} relationship where the average particle size was approximately the same but the size range differed.

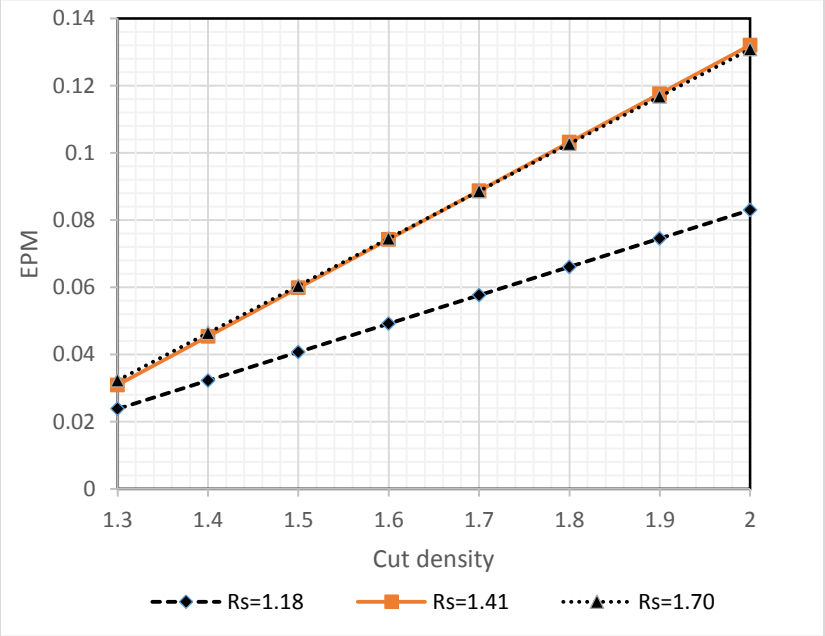

Figure 22: Effect of size range on jig performance, EPM vs. cut density for particle sizes of about 17mm

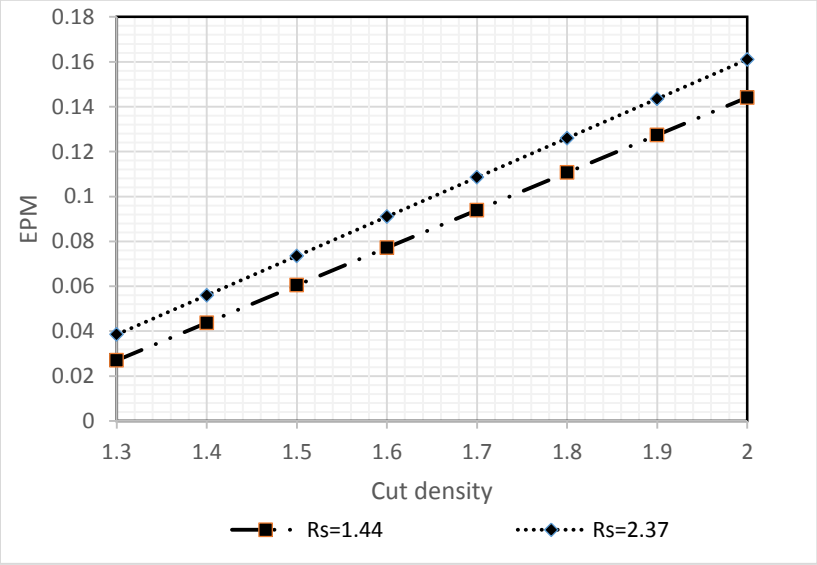

Figure 23: Effect of size range on jig performance, EPM vs. cut density for particle sizes of about 15mm

From Figures 22 and 23 it can be seen that the EPM increases as the size range increases indicating that jig performance decreases as the size range becomes larger. This too is in agreement with the findings from the recovery-yield plots.

4.6.3. Jig performance compared with other density separators

Table 5 presents data from **Wills, (1992)** that gives the typical ranges of EPM values for various density separators. It can be seen that the EPM values obtained in this project fall in the expected range. The very much better EPM values typically obtained with DMS separators are also apparent.

Table 5: Typical EPM values for different separation units, adapted from (Wills, 1992)

Process	Size ranges(mm)	EPM ranges
Shacking table		0.03-.11
Dense medium bath	6-100	0.01-0.02
Dense medium cyclones	0.2-9	0.01-0.04
Hydro cyclones		0.08-0.14
Baum jigs	1-25	0.03-0.12

The significance of the findings presented in this chapter are discussed in more detail in chapter six.

Chapter 5: Results II: - The veracity of the King stratification Model when particle size varies

5.1. Introduction

A good model of the performance of jig units has considerable value in investigating, in a cost effective way, how different operating conditions and feed conditions might influence separation performance. In this chapter the reliability of the King stratification model as a simulator of jig performance is tested in the context where particle size varies significantly.

King, (1987) and Tavares & King, (1995) have shown that the King stratification model is a good simulator for the jigging process for binary systems of cubic particles and for mixtures of coal and marble. **Woollacott *et al* (2014)** took the investigation further by investigating how well the King model fitted the experimentally measured concentration profiles for multi component systems of particles, with identical shapes and sizes; systems of two to seven components were investigated and good fits were obtained.

As an extension of that work, this chapter investigates how well the King model is capable of predicting the stratification behaviour of systems in which significant variation in particle size existed. It tests the extent to which the model can account for density stratification in contexts beyond that assumed in the formulation of the model, i.e. where it was assumed that all particles are essentially the same size.

To do this, the experimental data from the previous chapter were used. The model was fitted to the data from each test to obtain the appropriate value of the stratification parameter (α) and the concentration profile $C_j(h)$ for each density component j in the thin layer from h to h + dh. From this concentration profile, the model predicted values for the concentrations and recoveries associated with each density component in each layer sliced from the bed was determined as described in section 3.5.it is worth noting that the dotted line is the concentration profile as generated by the model the light circles represent the average concentration in the layer as calculated from the model data. Figures 24, 25 and 26 illustrate the kind of plots that were obtained.

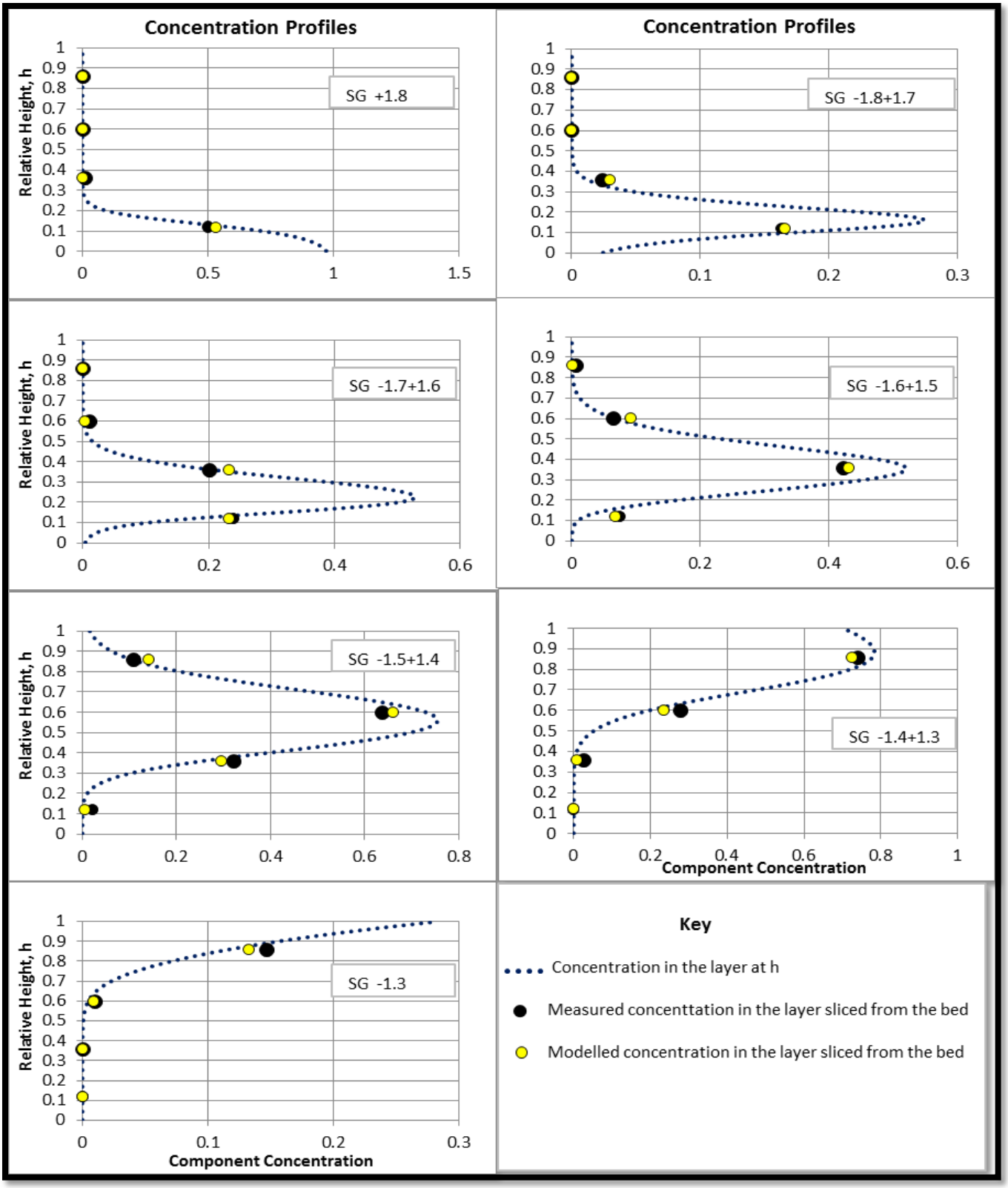

Figure 24: Typical concentration profile

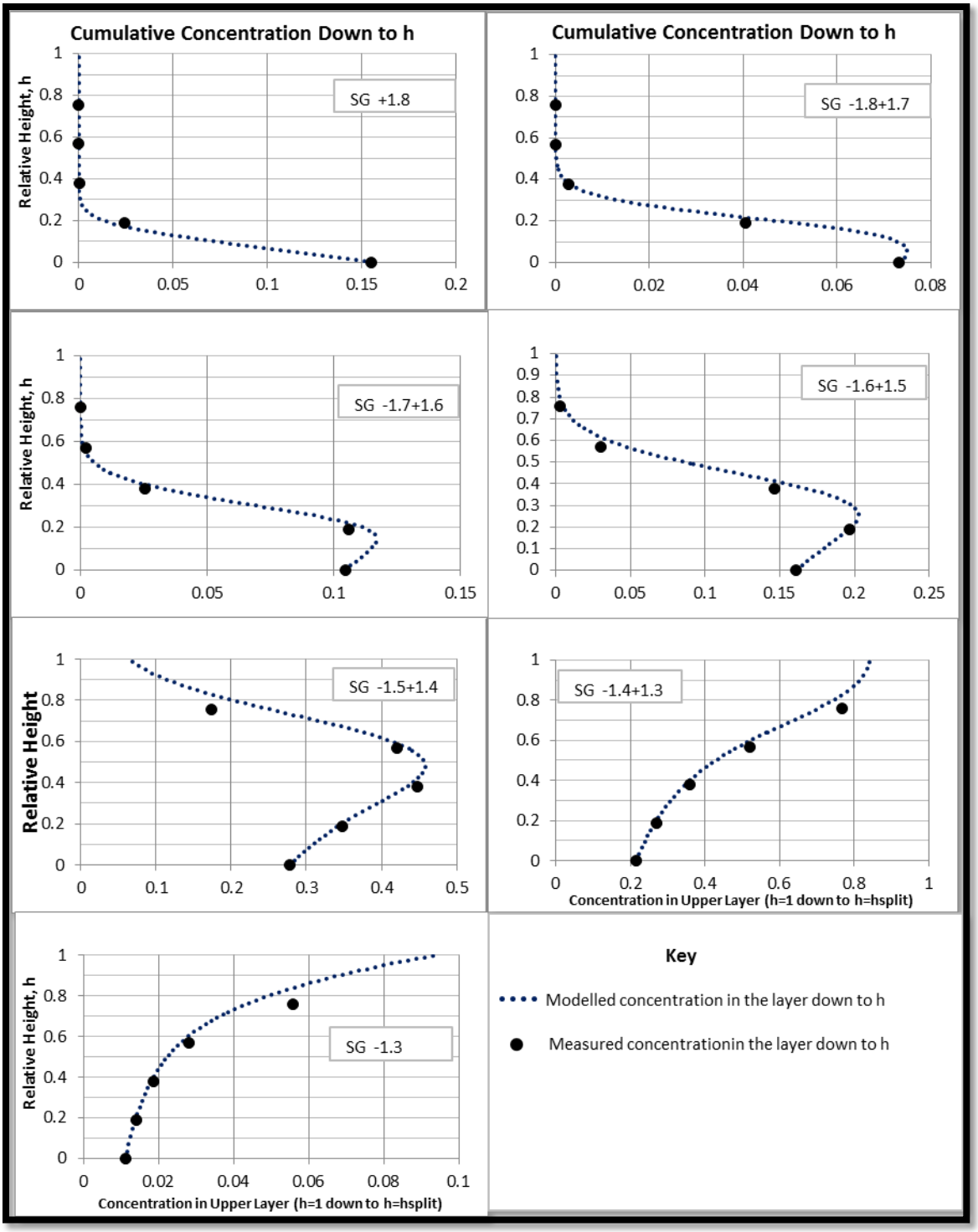

Figure 25: Typical cumulative concentration profile

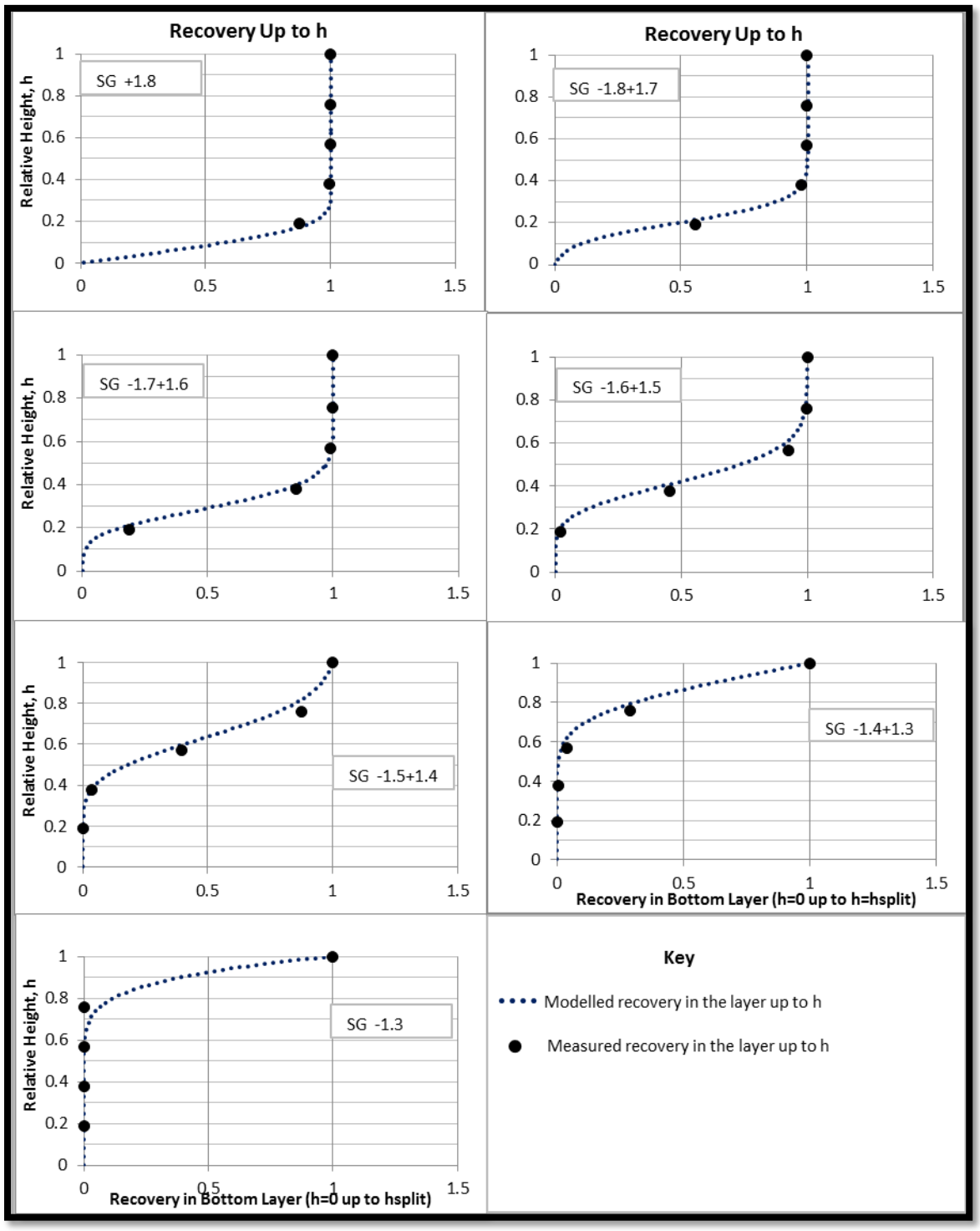

Figure 26: Typical recovery plots

Figure 24 shows the experimentally determined concentrations in the layer sliced from the bed (denoted by the dark circles) and the model predictions of these concentrations (denoted by the unfilled circles). These two points should coincide if the model fit is perfect. To provide perspective, the plot also shows the concentration profile $C_j(h)$ i.e. the concentration of component j in the layer from h to $h + dh$.

Figure 25 shows the predicted cumulative concentration $\overrightarrow{C_j}(h)$ in the top product from the jig, i.e. the concentration in the layers from $h = 1$ down to h. Figure 26 shows the predicted cumulative recovery $\overrightarrow{R_j}(h)$ to that top product. For perfect fits, the experimental points would coincide with these two plots. It is worth noting that all of the above best-fit plots were generated using a single value of the stratification parameter (α).

Plots of these kinds were generated to investigate how well the King model predicted the experimental data. In order to address the second research question, i.e. how well the King model describes stratification in the jig in contexts where particle size varies considerably, the investigation was conducted from the following perspectives

i. Varying particle size.
ii. Varying size range.
iii. Varying both particle size and size range simultaneously.

5.2. Analysis of goodness of fit

As will be seen, it was difficult to evaluate how well the model fitted the experimental data and a conventional statistical analysis could not be utilized. Accordingly, only a semi quantitative procedure was used.

In general an evaluation of the goodness of fit of a model to experimental data is based on the sum of squared differences (SSD) between model and experimental values. However, the sum of squared difference is a function of the number of data points involved and so SSD must be normalized if it is to be used as a comparative measure for assessing goodness of fit. In this study, all data sets involved the same number of density components and, with two exceptions

the same number of layers sliced from the particle bed. Accordingly, SSD was normalized as $\overline{SSD}$ by dividing by the number of layers.

In order to establish a basis for using $\overline{SSD}$ as a comparative measure of the goodness of fit, values associated with good, good to reasonable, reasonable and poor fits of the experimental data were determined by a visual analysis of all the model fits attempted – i.e. the equivalent of Figures 24 to 26 for each data set. In this visual analysis, the goodness of fit for each plot was evaluated by looking at how and by how much the experimental points deviated from the model generated profiles. The difference between what was considered to be a good fit, a reasonable fit and a bad fit in this investigation is discussed next.

5.2.1. Good fits

Figures 27 to 29 illustrate what were considered to be good fits of the experimental data. With regard to the plots of cumulative concentration and recovery profiles such as in Figures 27 and 28 respectively, a good fit is one in which the experimental points align very closely with the predicted profiles. With regard to the plots of concentration profiles such as in Figure 29, a good fit is one in which the experimental and model points (respectively the filled and unfilled circles) are reasonable close to one another. With good fits the values of $\overline{SSD}$ were all below 0.033.

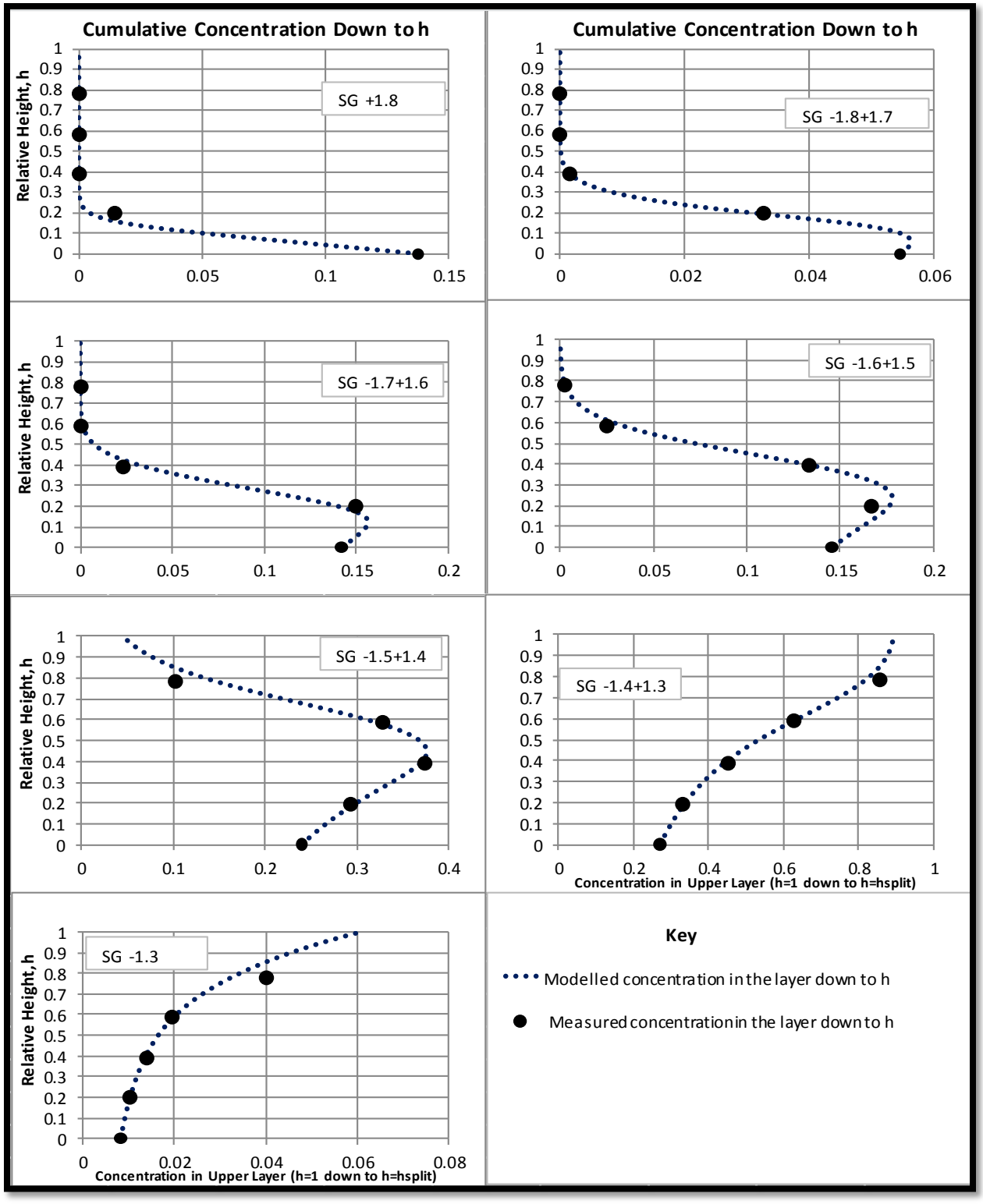

Figure 27: Typical Good fits: Cumulative concentration profiles for sample A2B2 (-19mm+16mm)

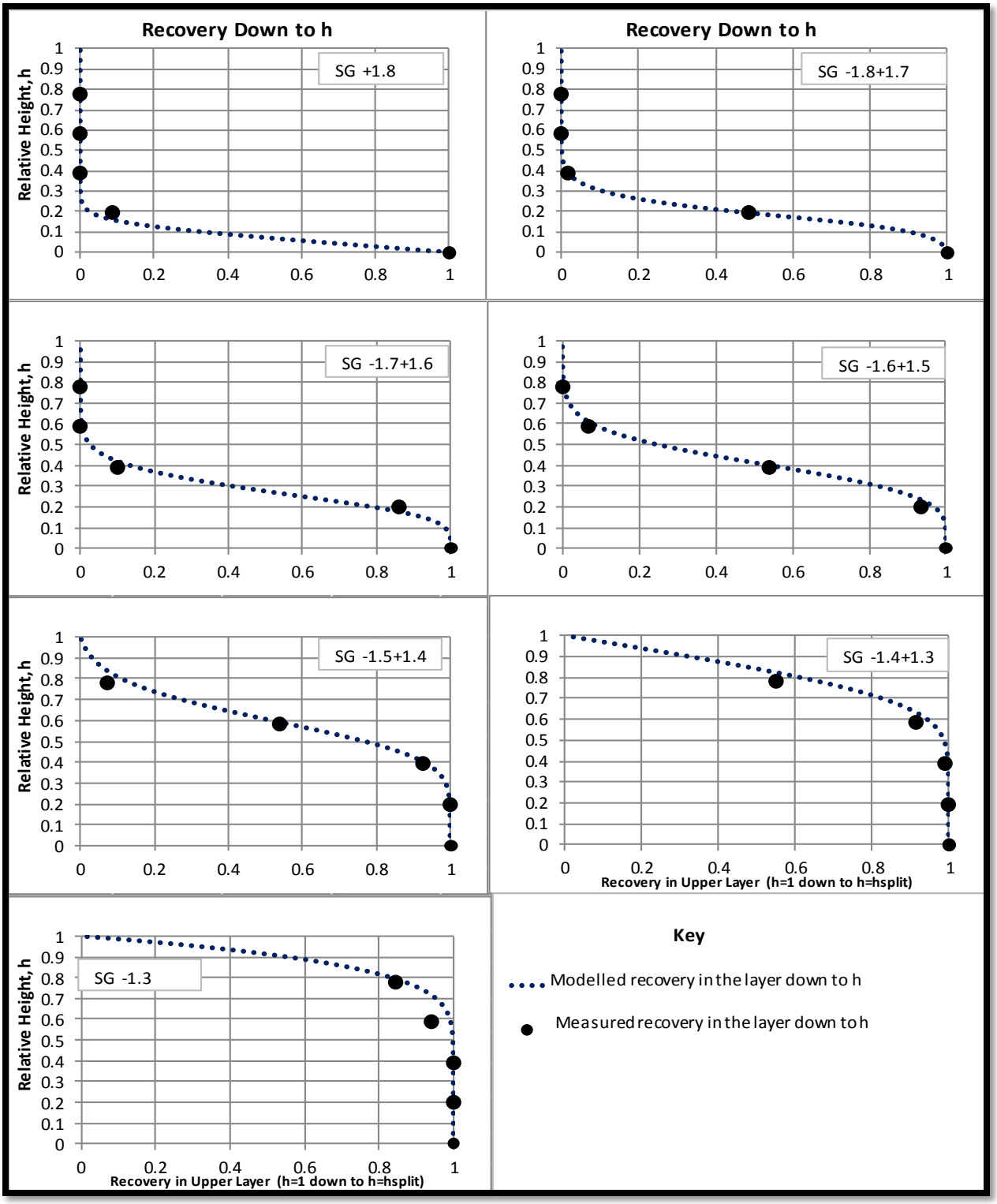

Figure 28: Typical Good fits: Cumulative recovery plots for sample A2B2 (-19mm+16mm)

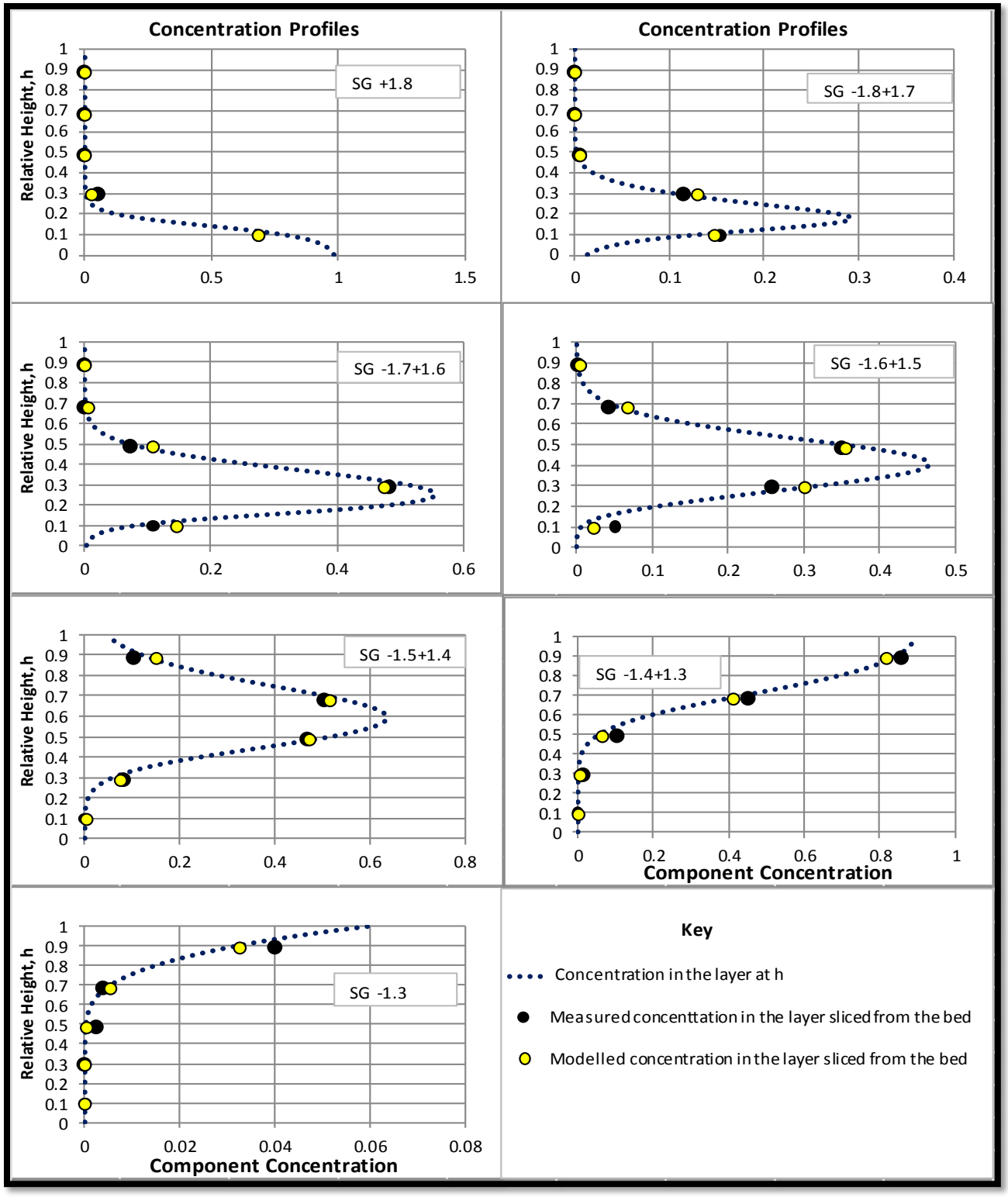

Figure 29: Typical Good Fits: Concentration profiles for sample A2B2 (-19mm+16mm)

5.2.2. Reasonable fits

Figures 30 to 32 illustrate what were considered to be reasonable fits of the experimental data. With regard to the plots of cumulative concentration and recovery profiles such as in Figures 28 and 29 respectively, the fit was considered to be reasonable if not more than three experimental points deviated from the model predicted profile. With regard to the plots of concentration profiles such as in Figure 32, the fit was considered to be reasonable if the experimental and model points (respectively the filled and unfilled circles) did not deviate by more than 0.1 at any point. With reasonable fits, the values of $\overline{SSD}$ ranged between 0.033 and 0.1.

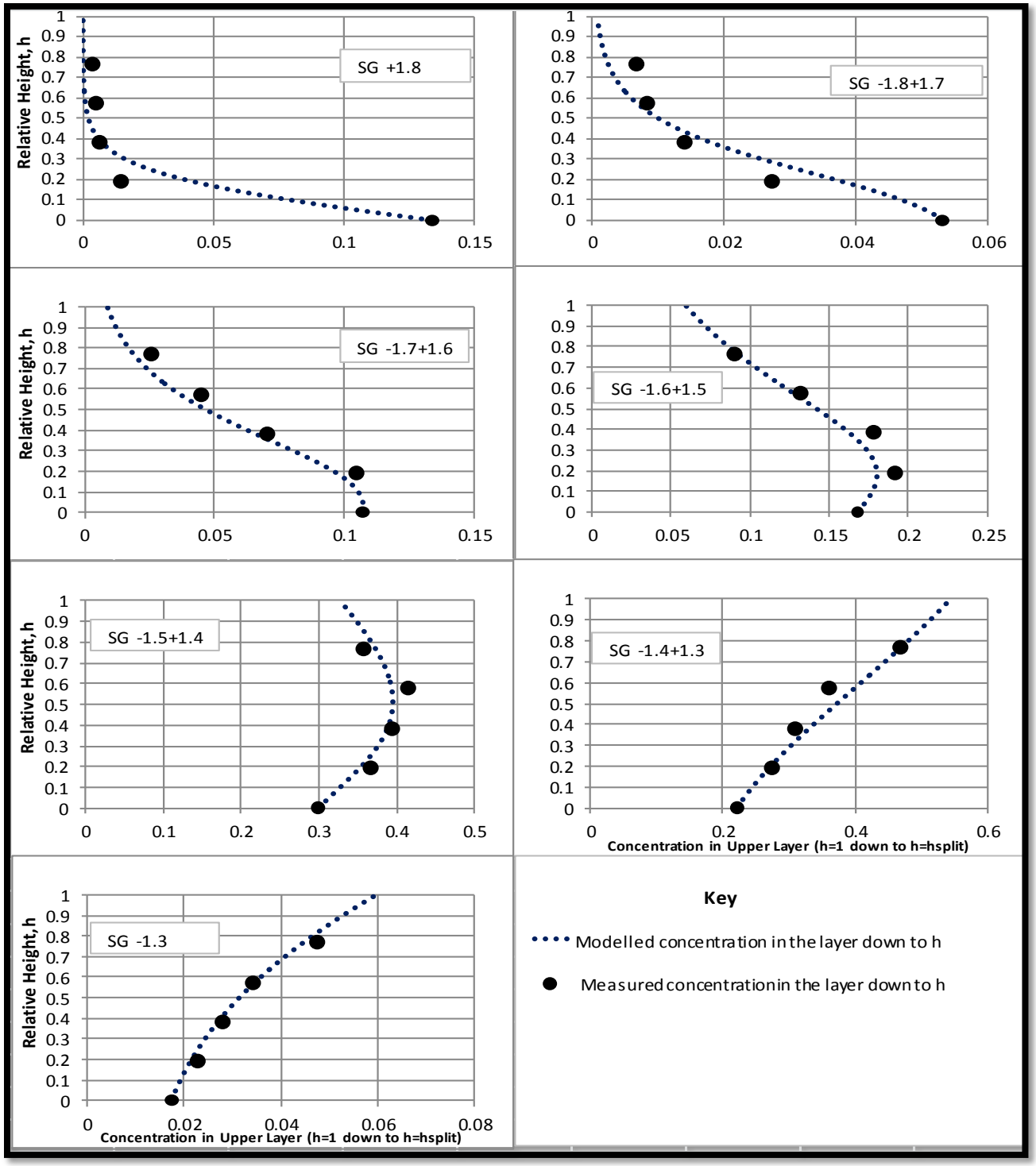

Figure 30: Typical reasonable fits: Cumulative concentration profiles for sample A4B5 (-13.2mm+6.7mm)

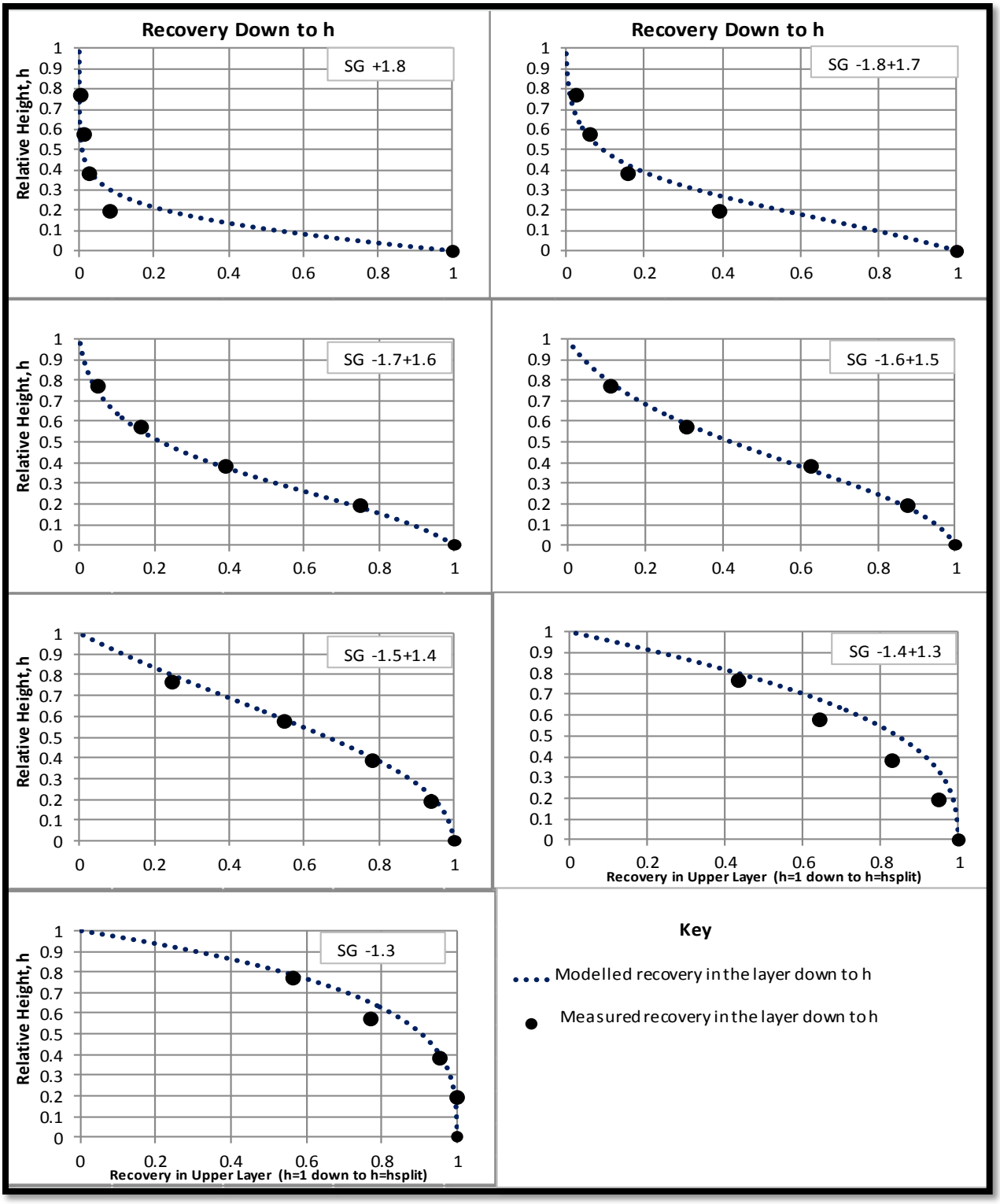

Figure 31: Typical reasonable fits: Cumulative recovery plots for A4B5 (-13.2mm+9.5mm)

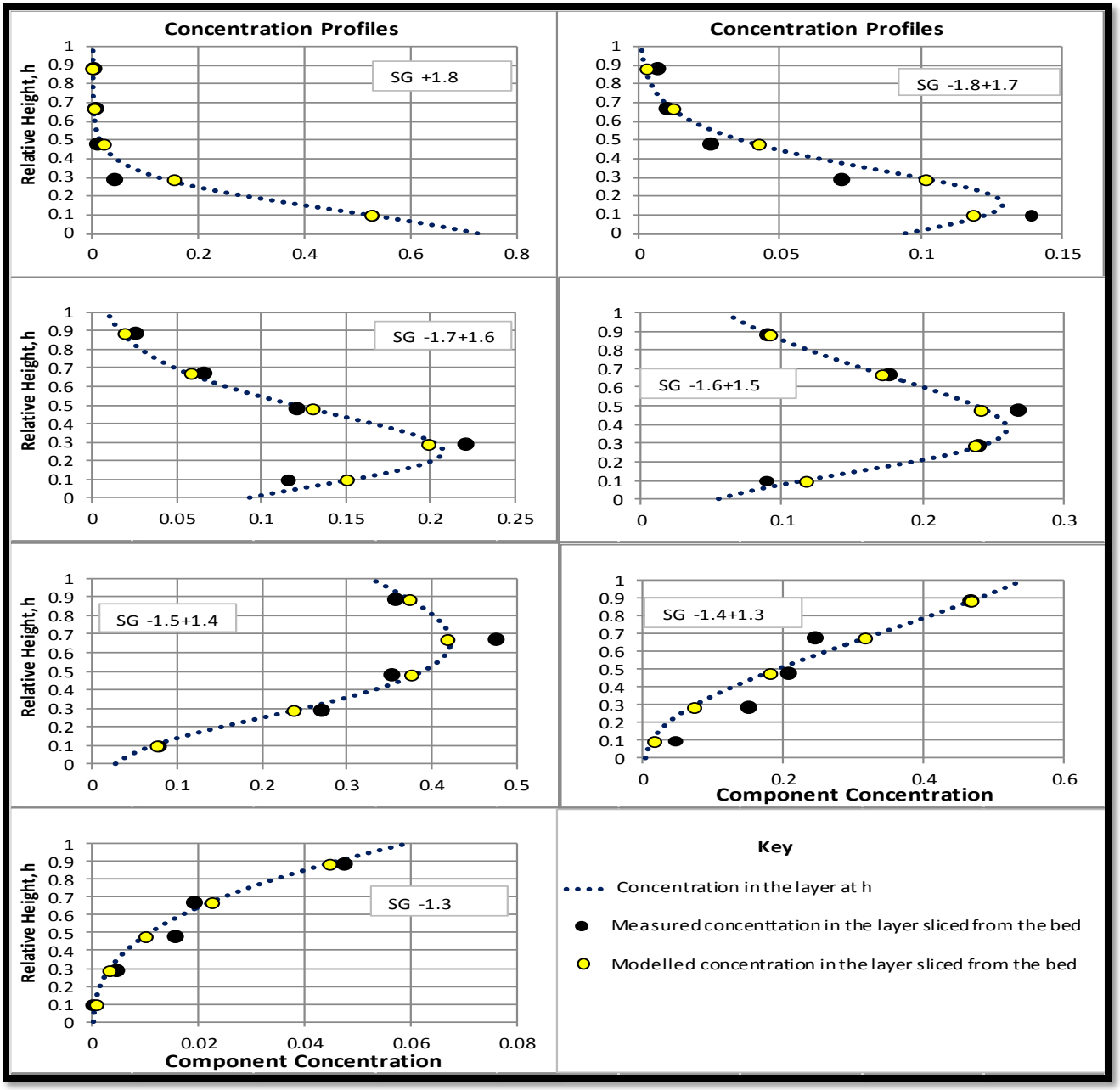

Figure 32: Typical reasonable fits: Concentration profiles for sample A4B5 (-13.2mm+6.7mm)

5.2.3. Poor fits

Figures 33 to 35 present examples where the model did not fit the data at all well. In all cases the values of $\overline{SSD}$ associated with such data sets were above 0.1.

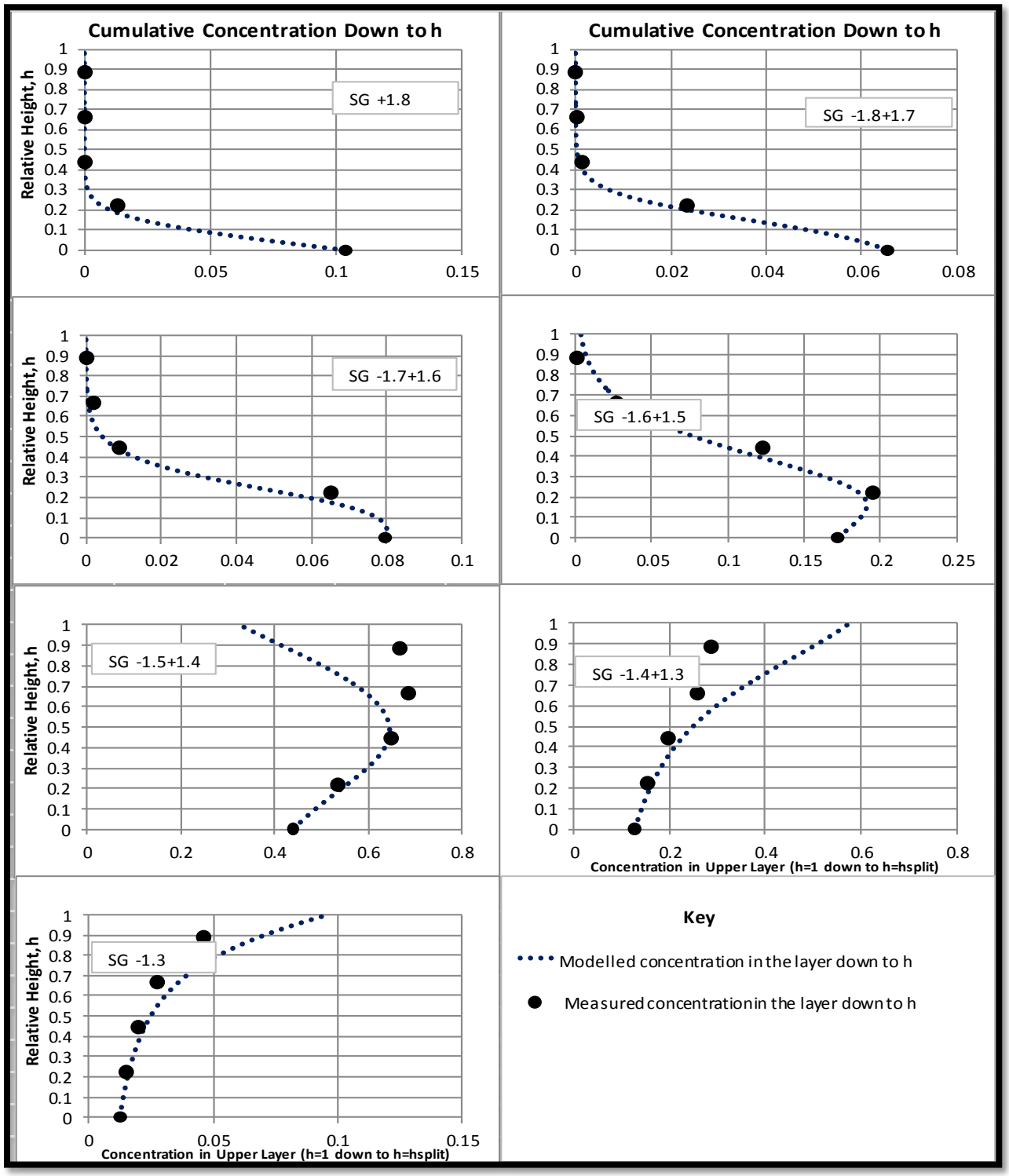

Figure 33: Typical poor fit- Cumulative concentration profiles for sample A2B5 (-19mm+6.7mm)

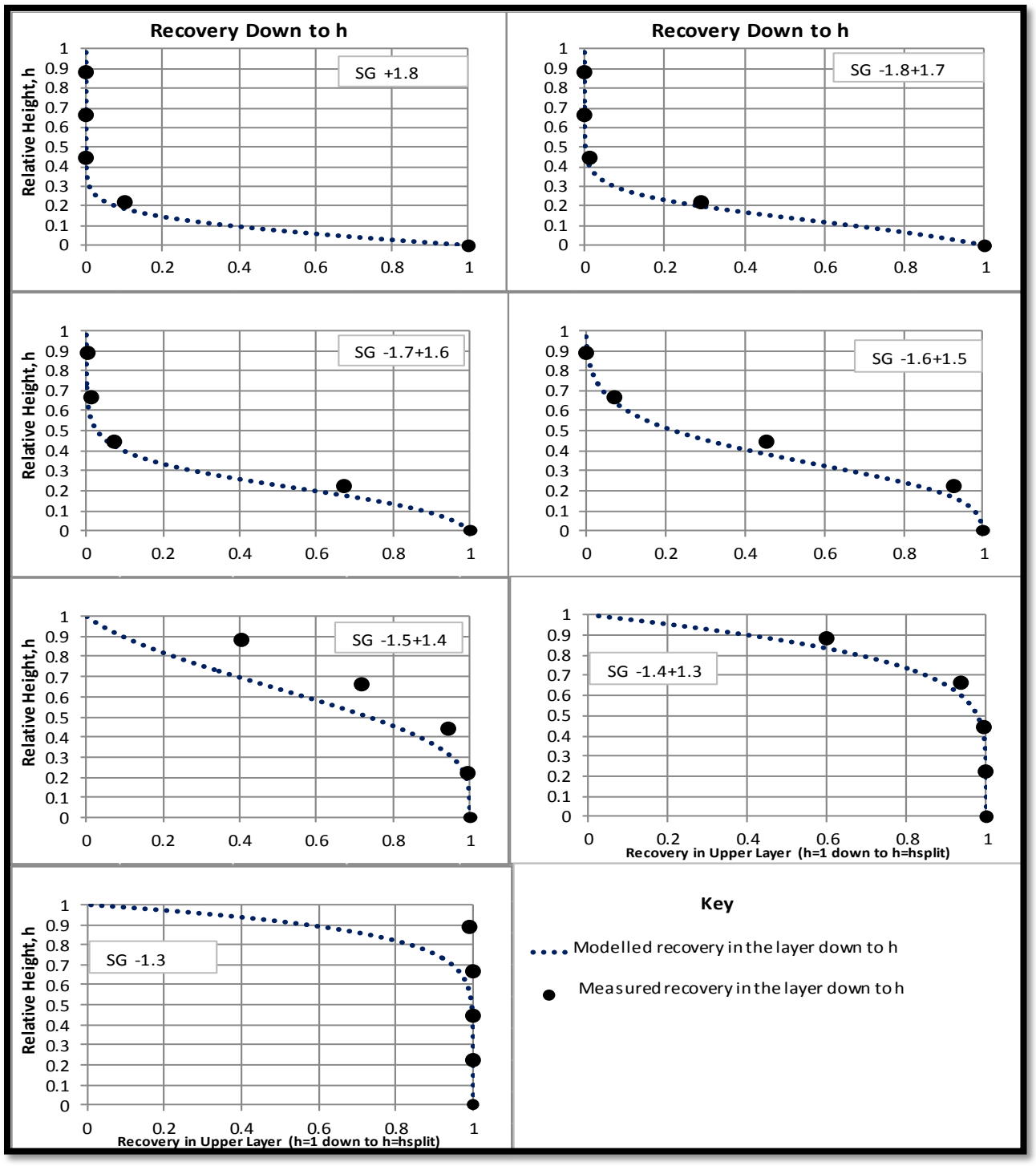

Figure 34: Typical poor fit-Cumulative recovery plots for sample A2B5 (-19mm+6.7mm)

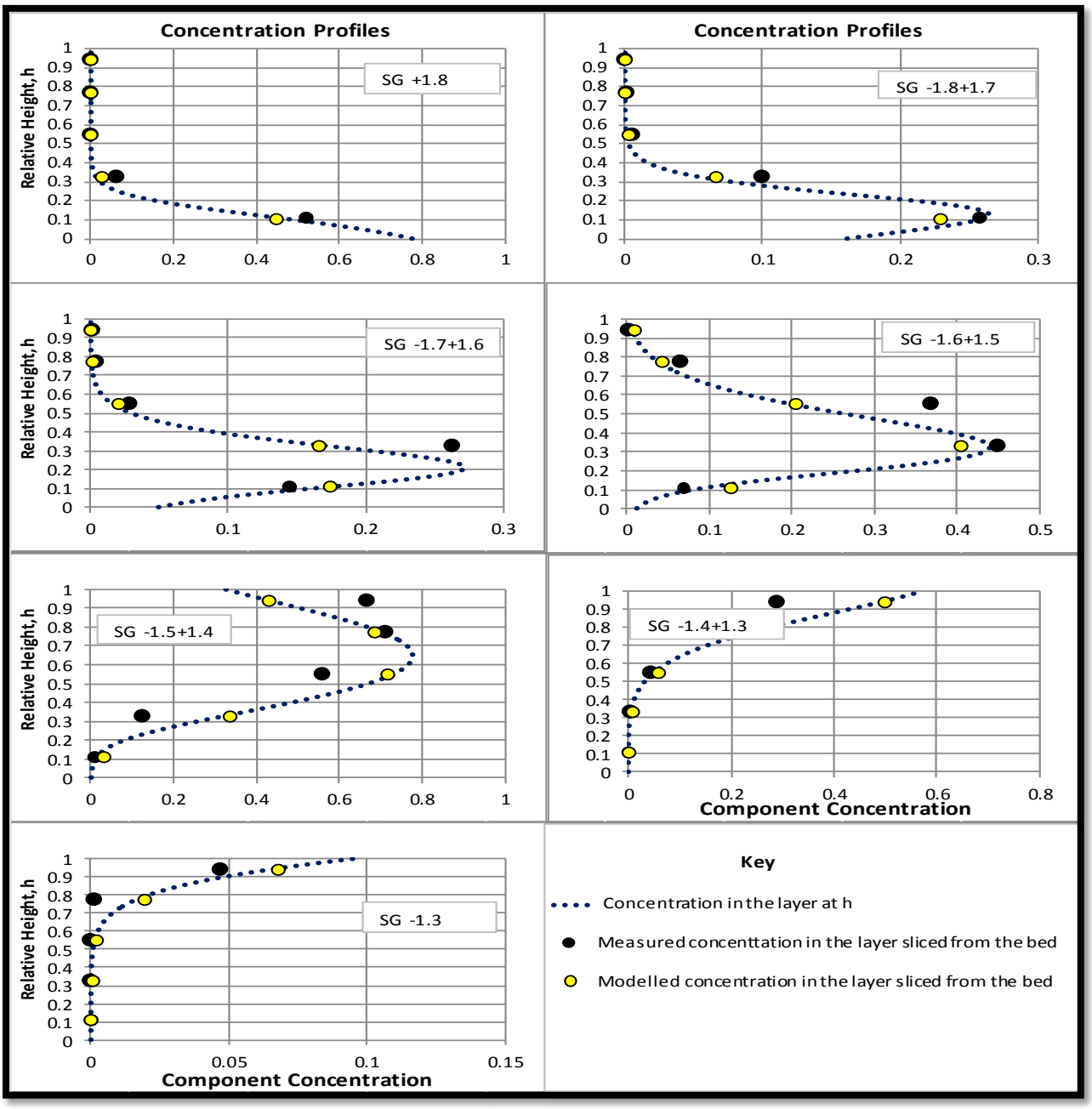

Figure 35: Typical poor fits: Concentration profiles for sample A2B5 (-19mm+6.7mm)

Table 6 presents the values of $\overline{SSD}$ obtained for each data set arranged according to the quality of fit. The associated plots and fits for each data set are presented in full in Appendix B. As can be seen from the table, the thresholds from good to reasonable fits and from reasonable to bad

fits occurs for values of $\overline{SSD}$ of about 0.3 and 0.6 respectively. To provide a graphical indication of the variation in the quality of the fits, the values of $\overline{SSD}$ are plotted against Drep in Figure 36. As can be seen from this figure and from Table 6 there is a fair degree of variation in the quality of the fits obtained. This set of data is now examined in more detail.

Table 6: Goodness of fit data for each data set ordered by Quality of fit and $\overline{SSD}$

Sample	Size Range (mm)		Drep (mm)	Rs	Alpha/Hbed	SSD	No. of Layers	$\overline{SSD}$	Quality of Fit
	top	*bottom*							
A4B4	13.2	9.5	11.2	1.39	1.173	0.033	4	0.008	Good
A3B5	16	6.7	10.4	2.39	0.767	0.051	5	0.010	Good
A1B1	22.5	19	20.7	1.18	0.905	0.054	5	0.011	Good
A2B2	19	16	17.4	1.19	0.810	0.091	5	0.018	Good
A1B3	22.5	13.2	17.2	1.70	0.690	0.127	5	0.025	Good
A2B4	19	9.5	13.4	2.00	0.797	0.085	5	0.017	Good to OK
A1B4	22.5	9.5	14.6	2.37	1.137	0.141	5	0.028	Good to OK
A2B3	19	13.2	15.8	1.44	0.425	0.165	5	0.033	Good to OK
A4B5	13.2	6.7	9.4	1.97	0.186	0.256	5	0.051	Reasonable
A1B5	22.5	6.7	12.3	3.36	0.495	0.229	5	0.046	Reasonable
A1B2	22.5	16	19.0	1.41	0.722	0.363	5	0.073	Bad
A3B4	16	9.5	12.3	1.68	0.235	0.418	5	0.084	Bad
A5B5	9.5	6.7	8.0	1.42	0.617	0.503	5	0.101	Bad
A2B5	19	6.7	11.3	2.84	0.638	1.173	5	0.235	Bad

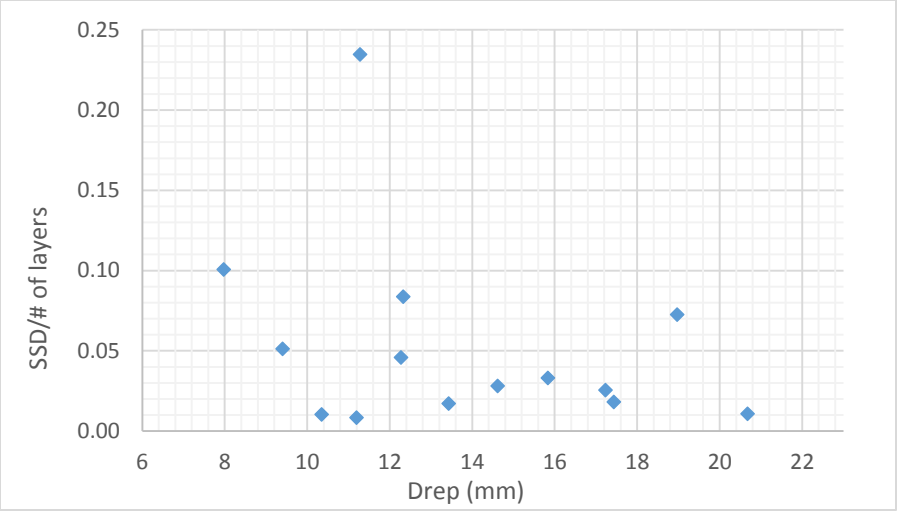

Figure 36: $\overline{SSD}$ (i.e. SSD/number of layers) for each data set plotted against Drep

5.3. The quality of fit when particle size varies

The first point to note from Table 6 and Figure 36 is the scatter in the values of $\overline{SSD}$ and that no clear trend is obvious. In the figure, the suggestion of a decrease in $\overline{SSD}$ with increasing particle size is probably spurious because any influence of size range on the quality of fit is hidden.

A similar conclusion is reached when the $\overline{SSD}$ values are plotted against Rs as in Figure 37. If the point for Rs equal to 2.84 were to be ignored as an outlier, it would appear that fits get better as the size range increases. This is the opposite of what is expected because as the size range increases the particle systems move further away from King's assumption that all particles have the same size and so the fits would be expected to get worse. However, any effect of particle size on the quality of fit is hidden in the figure. Also to be noted is that the fits obtained for the two data sets which had size ranges greater than 2.4 were not good.

To evaluate the quality of fits in a way that does not hide any influence that either particle size or size range may exert; reference is made to Table 7 where the data is ordered according to the top and bottom sizes of each data set.

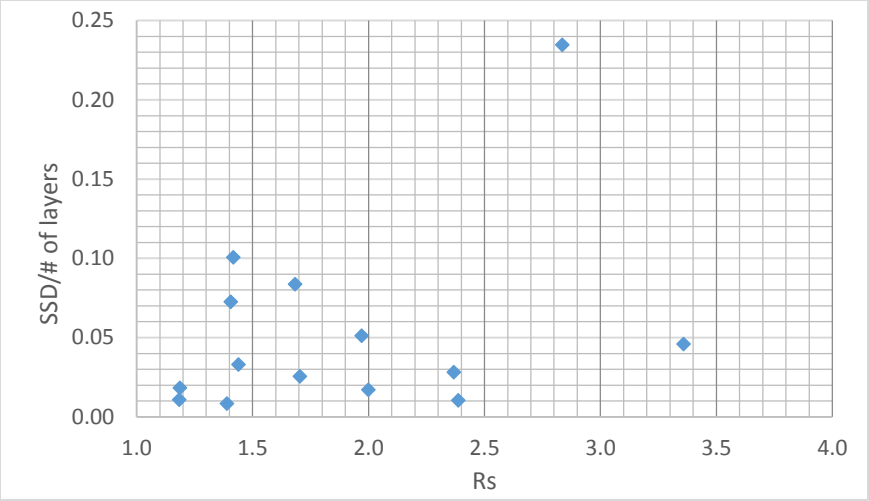

Figure 37: $\overline{SSD}$ for each data set plotted against Rs

Table 7: Values of $\overline{SSD}$ for each data set ordered by the top and bottom size of each data set

Sample	Size Range (mm)		Drep (mm)	Rs	Alpha/Hbed	SSD	No. of Layers	$\overline{SSD}$	Quality of Fit
	top	*bottom*							
A1B1	22.5	19	20.7	1.18	0.905	0.054	5	0.011	Good
A1B2	22.5	16	19.0	1.41	0.722	0.363	5	0.073	Bad
A1B3	22.5	13.2	17.2	1.70	0.69	0.127	5	0.025	Good
A1B4	22.5	9.5	14.6	2.37	1.137	0.141	5	0.028	Good to OK
A1B5	22.5	6.7	12.3	3.36	0.495	0.229	5	0.046	Reasonable
A2B2	19	16	17.4	1.19	0.810	0.091	5	0.018	Good
A2B3	19	13.2	15.8	1.44	0.425	0.165	5	0.033	Good to OK
A2B4	19	9.5	13.4	2.00	0.797	0.085	5	0.017	Good to OK
A2B5	19	6.7	11.3	2.84	0.638	1.173	5	0.235	Bad
A3B4	16	9.5	12.3	1.68	0.235	0.418	5	0.084	Bad
A3B5	16	6.7	10.4	2.39	0.767	0.052	5	0.010	Good
A4B4	13.2	9.5	11.2	1.39	1.173	0.033	4	0.008	Good
A4B5	13.2	6.7	9.4	1.97	0.186	0.256	5	0.051	Reasonable
A5B5	9.5	6.7	8.0	1.42	0.617	0.503	5	0.101	Bad

**The shading in the table highlights subgroupings with the same top size*

The expected trend of decreasing quality of fit as the size range increases is evident in Table 7 if the two 'Bad' data sets highlighted are overlooked. It appears from this table that variation in the quality of fits reflects the effect of both experimental errors arising from the limitations of the experimental procedure used (see section 3.6) and any discrepancies that arise when the model does not fit the experimental data well. Accordingly, little emerges from the comparison of the quality of fits beyond the following points:-

a) In general, the King model was able to fit 10 out of the 15 data sets well to reasonably well. Even when the fits were classified as poor, it was usually the case that the model predictions deviated from experimental data only in two or three out of the seven profiles. Overall, the extent to which the King model was able to fit experimental data is quite surprising given that particle size variation is ignored in its formulation.
b) It does appear that for size ranges above 2.4 the quality of fits obtained are not as good as those that were obtained for size ranges smaller than this.
c) Overall, it is apparent that both good to reasonable fits were obtained for data sets with size ranges up to 2.4. This matches with conventional jig practices whereby the maximum size range recommended in a jig feed is about 2.5. However, within this range some bad fits were also obtained.
d) It appears that the experimental equipment and procedures that have been utilized do not appear to be precise enough to show with confidence any clear trends with regard to whether or not the quality of model fits deteriorate as either the particle size or the size range vary.

5.4. The variation in the stratification parameter

An impressive feature of the King stratification model is that only a single parameter, the stratification parameter (α), is needed to predict the concentration profiles in a batch jig and the measures needed to predict the separation performance of that jig. As shown in section 2.5.9, the stratification coefficient is defined as

$$\alpha = \frac{ug\, V_\rho H_{bed}}{D}$$

King, 1987 claimed that the value of the stratification coefficient is independent of feed composition and the densities of the components in the feed. This has been validated to some extent by **Woollacott *et al,* 2014**. However the effect of particle size and particle size range on the parameter has not been tested. According to King the penetration velocity (u) and diffusion coefficient (D) in the above equation are strong functions of particle size, shape and the bed expansion mechanism but are unaffected by the particle density. In this section the influence of particle size effects on the stratification parameter is investigated.

As can be seen in the equation above, α is a function of the bed depth $\mathbf{H_{bed}}$. The bed depths in the tests carried out were similar but not identical. Therefore, to remove the influence of bed depth on the value of the stratification parameter, α was normalized by dividing by the bed depth associated with the test. This allows a more valid basis for comparing the values of α obtained when fitted the model to each data set. Tables 8 to 10 present the relevant data.

Table 8: The influence of particle size on the stratification parameter for a size range of about 1.19

Sample	Drep (mm)	Rs	Alpha	Quality of fit
A1B1	20.7	1.18	0.905	Good
A2B2	17.4	1.19	0.810	Good

Table 9: The influence of size on the stratification parameter for a size range of about 1.4

Sample	Description	Drep (mm)	Rs	α/Hbed (L/Kg.mm)	Hbed (mm)	Quality of fit
A1B2	-22.5mm+16mm	18.97	1.39	1.173	118.0	Good
A2B3	-19mm+13.2mm	15.84	1.41	0.722	129.5	Reasonable
A4B4	-13.2mm+9.5mm	11.2	1.39	0.617	104.0	Bad
A5B5	-9.5mm+6.7mm	7.98	1.44	0.425	126.0	Reasonable

Table 10: The influence of size on the stratification parameter for a size range of about 1.7

Experiment	Description	Drep	Rs	α/Hbed (L/Kg.mm)	Hbed (mm)	Quality of fit
A3B4	-22.5mm+13.2mm	12.3	1.68	0.235	130.0	Reasonable
A1B3	-16mm+9.5mm	17.2	1.70	0.690	116.0	Reasonable

As can be seen from these tables there is considerable scatter in the values of the stratification parameter. With very narrow size ranges (Table 8) its value seems to decrease as the particle size increased. In the case of the data sets with size ranges of about 1.4 (Table 9) the values are scattered and no trend is evident. With a size range of about 1.7 (Table 10) the values increase as the particle size increased.

Table 11 shows the effect of the size range on the stratification parameter. In this case, samples with relatively similar sizes but distinctly different size ranges are compared. Again the values are scattered and no clear trend could be observed.

Table 11: The influence of size range on the stratification parameter for particle sizes of about 11mm

Sample	Description	Drep	Rs	α/Hbed (L/Kg.mm)	Hbed (mm)	Quality of fit
A4B4	-13.2mm+9.5mm	11.2	1.39	1.173	104.0	Good
A3B4	-16mm+9.5mm	12.3	1.68	0.235	116.0	Bad
A3B5	-16mm+6.7mm	10.4	2.39	0.767	130.0	Good
A2B5	-19mm+6.7mm	11.3	2.84	0.638	113.0	Bad

The scatter in the values of the stratification parameter is again evident in the results of the replicate tests reported in Table 12. (The full set of data for these replicates is presented in Appendix B4.) The replicates were performed on three samples and the results show a fair amount of variation in the values of the stratification parameter for identical samples tested under identical conditions. This suggests that the observed scatter in the values of the stratification parameter probably stems from shortcomings in the experimental equipment and procedures, i.e.

these are not precise enough to reveal the nature of the variation in the stratification parameter associated with different particle sizes.

A detailed discussion of the significance of the findings reported in this chapter is presented in the next chapter.

Table 12: Results from replicate tests

Sample	Description	Drep (mm)	Rs	Alpha/Hbed	Hbed (mm)	Quality of fit
A1B1	-22.5mm+19mm	20.7	1.18	0.905	132.0	Good
A1B1 *repeat*	-22.5mm+19mm	20.7	1.18	0.728	132.0	Reasonable
A2B4	-19mm+9.5mm	13.4	2.00	1.085	129.5	Good to OK
A2B4 *repeat*	-19mm+9.5mm	13.4	2.00	0.797	135.0	Reasonable
A4B4	-13.2mm+6.7mm	9.4	1.97	0.186	130.5	Reasonable
A4B4 *repeat*	-13.2mm+6.7mm	9.4	1.97	0.719	130.5	Bad

Chapter 6: Discussion and Conclusion

6.1. Introduction

A typical South African coal was used for this study. The samples were obtained from Exxaro`s Leeuwpan mine in Delmas. The aim of the test work conducted on this coal was to find out how average particle size and the size ratio affect jig performance; how they affect the ability of the King Model to predict stratification behaviour in a batch jig and the stratification parameter (α). The findings of the investigation are summarized and discussed here.

6.2. Discussion of Results Relating to Jig Performance

The major findings relating to the influence of size and size range on jig performance are as follows;

- Jigging efficiency increases with an increase in particle size
- The coarser the size range the poorer the jig performance
- Jig performance is more sensitive to particle size than to size range
- EPM is directly proportional to the cut density

The investigation has shown that jigging efficiency increases as particle size increases. A number of investigators have reached the same conclusion for jigs and other density separation equipment (**Venkoba Rao *et al.*, 2003; Xia *et al*., 2007; Venkoba Rao, 2007; Chikerema, 2011**).

The actual cause of this phenomenon is not well understood. According to classical theories (**Gaudin, 1934**), separation performance can deteriorate as particle size decreases because the hydrodynamics shift in the direction from laminar to turbulent flow so that the settling ratio decreases. Others have suggested that the smaller the particles are the more their behaviour is affected by surface resistance relative to density differences (**Kelly and Spottiswood, 1982**). Some workers have also attempted to account for these behaviors by suggesting that smaller particles experience a different apparent viscosity than larger particles (**Kelly and Spottiswood, 1982**). On the other hand, according to **King, 1987,** dispersive forces act in the jig bed to de-stratify the bed. One of these dispersive forces has been identified by **Knight *et al.*, 1993.** They

showed that a convectional current is formed when particles in a fluid are subjected to an oscillating motion. These dispersive forces and convectional currents are experienced by all particles in the jig bed small and large alike. However larger particles have greater inertia as they move up and down in the jig chamber enabling them to resist the effect of these dispersive forces more effectively than smaller particles can. As a result misplacement of particles is likely to be more prevalent for smaller particles relative to larger ones. Hence the overall jigging efficiency decreases. This suggests that to maximize jig performance in industrial applications it would be beneficial to keep the feed size to the jig as large as is possible other factors such as liberation being equal. Although the phenomenon of decreasing separator performance with decreasing particle size is not adequately addressed by theory, its effect is well known.

The investigation also found that jig performance has an inverse relationship with size range i.e. the EPM increases as the size range increases. There is agreement between these findings and the literature (**Rao *et al,* 2003; Xia *et al,* 2007; Chikerema, 2011). Myburgh *et al*, 2014** reached the same conclusion i.e. they found that reducing the size range of the iron ore fed to industrial scale jigs significantly improved their performance. This phenomenon is both well-known and well understood. Because particle behavior in a bed is a function of both size and density, the greater the size range of particles in the bed the greater the extent to which bed stratification is the result of both particle size and density, i.e. density separation becomes confounded to an increasing degree by size segregation in the bed. Another reason may be because interstitial trickling **(Burt, 1964).** According to this mechanism during the down stroke of the jig the particles are sucked towards the bottom of the bed and as they settle the larger particles interlock forming channels. If these channels are large enough the heavier particles that are small enough are able to pass through the channels until they reach the bottom. Thus increasing the size range may increase the possibility that large enough channels are formed resulting in greater misplacement of particles. This in turn would reduce the performance of the jig.

One consequence of the agreement that has been found between the literature and the results just discussed is the confidence which it lends to the second aspect of the investigation; i.e. the

validation work performed on the King model has been done on data from particle systems that have behaved in an expected manner.

6.3. Discussion of results relating to the King Model

Most of the validation work that has been performed thus far on the King stratification model has been conducted on samples of mono size particles. This was appropriate to the assumptions used in the derivation of the model. **King, 1987, 2001**; **Tavares *et al.*, 1995;** and **Woollacott *et al.*, 2014** were able to endorse the mathematical appropriateness of the King stratification model by showing that it predicted well the stratification behaviour in batch jigs. The particles used in their tests were not spherical but were all essentially the same shape. This suggests that the requirement that particles must be spherical in nature for the model to apply can be abandoned.

As expected, it was found that cumulative concentration profiles resulted in better agreement between experimental and modeled values. This is because the discrete concentration profiles are more sensitive to experimental error. When slicing the particle bed, the slicer is forced through the bed and the particles that lie in the path of slicer are forced upwards or downwards into the layer above or below the slicer. In this process, particles can be misplaced to the wrong layer and can scour out particles from a lower layer. For the samples with larger average size particle misplacement errors would be expected to be greater because any particle displacement is likely to disturb adjacent particles more than would be expected with smaller particles. While such misplacement errors are associated with all the data in the study, the error is magnified when determining discrete concentration profiles of slices removed from the bed. This is because the slicing error occurs both at the top and the bottom of slice. When the data is cumulated from either the top or the bottom of the bed, the error diminishes because the only error is that associated with slicing the top or bottom of the combined layers

The work conducted in this study to investigate how well the King model was able to fit experimental data, appears to have been somewhat compromised by shortcomings in the experimental equipment and procedures. While the equipment and procedures were adequate for a credible demonstration of how jig performance was influenced by particle size effects, they appear to have been insufficiently precise to reveal the more subtle influences of particle size and size range on the stratification parameter and the quality of model fits. Consequently, there was

considerable scatter in both the indicators used to evaluate the quality of fit and in the values of the stratification parameter that were obtained from the model fits. As a result, only a limited number of conclusions can be drawn from this aspect of the investigation. These are as follows:-

- In general, the King Model was found able to predict stratification patterns far better than expected in contexts where there is a significant variation in particle size. The model fitted 10 out of the 14 data sets well to reasonably well.
- The model appears able to simulate stratification in jigs for the practical contexts where the size range in the feed is typically kept below 2.4.
- King model appears to be mathematically appropriate for the purposes of describing stratification phenomena under a much wider range of conditions than has been shown previously.
- No reliable indication was obtained with regard to the nature of the influence of size effects on the value of the stratification parameter.

6.4. Indications for Further Work

It was found that the test work was sufficiently reproducible to show quite clearly the trends associated with variation in particle size. However, the experimental error associated with the data generated was such that the stratification parameter values varied quite considerably for repeat tests performed under identical condition. This suggests that more refined equipment and/or experimental procedure are needed for a more accurate investigation of the effect of size variation on the stratification parameter.

6.4. CONCLUSION

Tests were conducted on a batch jig processing a typical South African coal as a means for investigating the effect of particle size and size range on the performance of a jig and the capability of the King model to simulate stratification when particle size effects are significant. Three research questions were posed. In addressing these questions, the following conclusions were drawn.

Question 1: How does particle size and size range affect jig performance?

It was found that jig efficiency increased with increasing particle size while increasing the ratio of the largest to smallest particles in a given sample resulted in a reduction in processing efficiency. It was also found, that jig performance is more sensitive to changes in particle sizes than it is to changes in size ranges. The study has revealed that improvements in jigging efficiency of between 10-20% in the jigging efficiency could be achieved by controlling the feed size and size ranges respectively.

Question 2: How well does the King model describe stratification behaviour in the jig for different particle sizes and sizes ranges?

The validation work conducted to test the capability of the King model showed that the King model is able to simulate stratification patterns reasonably to very well provided the size range is less than 2.5.

Question 3: How does the stratification parameter (α) in the King model vary with particle size and with particle size range?

It was found that the single, experimentally determined value of the stratification constant (α) was sufficiently capable of completely describing the stratification behaviour of a typical South African coal in a batch jig. No definitive trend could be observed with regard to the effect of variations in size and range on the stratification constant.

The significance of the findings of this study are as follows. The current understanding about the influence of size effects on jig performance has been confirmed. In addition, it has been shown that jig performance is more sensitive to changes in particle sizes than it is to changes in size ranges. Further it has been shown that the King model can be used with some confidence as a simulator for processes that are based on bed stratification provided the size and size range limitations of the model are met. In general, the King Model was found able to predict stratification patterns far better than expected in contexts where there is a significant variation in particle size.

References

Burt, R.O., 1984. Gravity Concentration Technology. Elsevier, Amsterdam, pp. 185- 220.

Caulkin, R., Jia, X., Fairweather, M., Williams, R.A., 2010. Geometric aspects of particle segregation. Physical Review E81, 051302.

Chikerema, P., 2011. Effects of particle size, shape and density on the performance of an air fluidized bed in dry coal beneficiation. MSc thesis University of the Witwatersrand.

de Jong, T.R.P., Witteveen, H.J., Dalmijn, 1996. Penetration velocities in a homogenous jig bed. International Journal of Process Engineering 46, pp.277-291.

Dempers, J., 2006. Eskom perspectives: expansion of power generation in the Waterburg. Influence of Waterburg coal qualities on Matimba boilers. Presented at the fossil fuel foundation of South Africa conference: The Waterburg coal field 2006 and beyond. 22-23 August 2006.

Falcon, L.M., Falcon, R.M.S., 1987. The petrographic composition of Southern African coals in relation to friability, hardness, and abrasive indices. Journal of the South African Institute of Mining and Metallurgy, vol.87, no.10,pp323-336

Gaudin, A.M., 1934, Principles of Mineral Dressing. McGraw-Hill New York.

Gotfried, B.S., 1978. Generalizations of distribution data for characterizing the performance of float sink coal cleaning devices. International Journal of Mineral Processing 5, 1-

Kelly, E.G., Spottiswood., D.J. 1982. Introduction to Mineral Processing. John Wiley and Sons, Ney York. Pp.79, 87-88.

King, R.P., 1987. A Quantitative Model for gravity Separation Unit Operations that rely on Stratification. APCOM 87. Proceedings of the Twentieth International Symposium on the application of Computers and Mathematics in the Mineral Industry. Volume 2: Metallurgy, Johannesburg, SAIMM. Pp.141-151.

King, R.P., 2001. Modeling and simulation of mineral processing systems. Butterworth-Heinemann, Linacre House, Jordan Hill, Oxford OX2 8DP, pp. 233-264.

Knight, J.B., Jarger, H.M., Nagel, S.R., 1993. Vibration-Induced Size Separation in Granular Media: The Convection Connection. Physical Review Letters vol. 70, number 24

Kuang, Y., Zhou, J., Wang, L., Yang, C., 2008. Laws of motion of particles in a jigging process. Journal of China University of Mining and Technology 18, pp. 0575-0579.

Lin, I.J., Krush-Bram, M., Rosenhouse, G., 1997. The beneficiation of minerals by magnetic jigging, Part 1. Theoretical aspects. International Journal of Mineral Processing 50, 143-159.

Mayer, F.W., 1964. Fundamentals of a potential energy theory of the jigging process. Paper presented at the proceedings of the 7th International Mineral Processing Congress

Mehrotra, S.P., Mishra, B.K., 1997. Mathematical modeling of particle stratification in jigs. Jamshedpur proceedings, pp. 202-217.

Myburgh, H.A., Nortje, A., 2014. Operation and performance of the Sishen Jig Plant. The journal of The South African Institute of Mining and Metallurgy 114, pp. 569-574.

Myburgh, H.A., 2010. The influence of control and mechanical conditions of certain parameters on jigging. The journal of The South African Institute of Mining and Metallurgy 110, pp. 655-661.

Rong, R.X., Lyman, G.J., 1993. A new energy dissipation theory of jig bed stratification. Part 1: energy dissipation analysis in a pilot scale Baum jig. International Journal of Mineral Processing 37, pp.165- 188.

Rong, R.X., Lyman, G.J., 1993. A new energy dissipation theory of jig bed stratification. Part 2: a key energy parameter determining bed stratification. International Journal of Mineral Processing 37, pp.189-207

Rong, R.X., 1990. Fundamental studies of the stratification mechanism in the jig, Ph.D. Thesis, Julius Kruttschnitt Mineral Research center, University of Queensland.

Tavares, L.M., King, R.P., 1995. A useful model for the calculation of the performance of batch and continuous jigs. Coal Preparation vol. 15, pp. 99-128.

Venkoba Rao, B., 2007. Extension of particle stratification model to incorporate particle size effects. International Journal of Mineral Processing 85, pp.50-58

Venkoba Rao, B., Kapur, P.C., Rahul, L., 2003. Modeling thee size density partition surface of dense medium separators. International Journal of Mineral Processing 72, pp.443-453

Viduka, S.M., Feng, Y.Q., Hapgood, K., Schwarz, M.P., 2013. Discrete particle simulation of solid separation in a jigging device. International Journal of Mineral Processing 123, pp.108-119.

Viduka, S.M., Feng, Y.Q., Hapgood, K., Schwarz, M.P., 2013. CFD-DEM investigation of particle separations using a sinusoidal jigging profile. Advanced Powder Technology 24, pp. 473-481

Wagner, N.J., Tlotleng, M.T., 2012. Distribution of selected trace elements in density fractioned Waterburg coal from South Africa. International Journal of Coal Geology 94, 225-237.

Wills, B.A., 1992. Mineral Processing Technology 5th edition. Pergamon Press Ltd, Headington Hill Hall, Oxford OX3 0BW, England. Pp.411-425.

Woollacott, L.C. A validation study of the King stratification model. *In press.*

Woollacott, L.C., 2014. *Private Communication*.

Xia, Y.K., Peng, F.F., Wolfe, E., 2007. CFD simulation of fine coal segregation and stratification in jigs. International Journal of Minerals Processing 82, pp. 164-176.

Appendices

Appendix A: Washability Data

The data that was generated form the float-sink analysis is presented here.

Table 13: Washability data for -22.5mm+19mm, Hbed=132mm

Class	Mass (g)				
	layer 1	layer 2	layer 3	layer 4	layer 5
-1.3	0	0	0	0	85
-1.4+1.3	0	7	47	354	1215
-1.5+1.4	0	69	719	936	297
-1.6+1.5	26	517	579	86	5
-1.7+1.6	158	548	119	7	0
-1.8+1.7	346	256	15	0	0
+1.8	1268	174	4	0	0

Table 14: Washability data for -22.5mm+16mm, Hbed=118mm

Class	Mass(g)				
	layer 1	layer 2	layer 3	layer 4	layer 5
-1.3	0	0	0	4	14
-1.4+1.3	0	0	93	532	369
-1.5+1.4	0	83	865	716	158
-1.6+1.5	29	493	587	40	0
-1.7+1.6	77	459	132	2	0
-1.8+1.7	152	492	36	0	0
+1.8	1485	353	8	0	0

Table 15: Washability data for -22.5mm+13.2mm, Hbed=130mm

Class	Mass(g)				
	layer 1	layer 2	layer 3	layer 4	layer 5
-1.3	0	0	0	0	141
-1.4+1.3	0	27	149	590	1193
-1.5+1.4	36	481	1066	937	253
-1.6+1.5	157	605	283	48	8
-1.7+1.6	347	400	31	8	0
-1.8+1.7	293	102	0	0	0
+1.8	708	46	0	0	0

Table 16: Washability data for -22.5mm+ 9.5mm, Hbed=130mm

Class	Mass(g)				
	layer 1	layer 2	layer 3	layer 4	layer 5
-1.3	0	0	2	96	349
-1.4+1.3	0	27	177	762	364
-1.5+1.4	11	586	1130	468	41
-1.6+1.5	223	781	215	33	0
-1.7+1.6	312	204	21	3	0
-1.8+1.7	373	60	6	0	0
+1.8	871	11	0	0	0

Table 17: Washability data for -22.5mm+ 9.5mm, Hbed=124mm

Class	Mass(g)				
	layer 1	layer 2	layer 3	layer 4	layer 5
-1.3	0	0	16.3	16.6	64.2
-1.4+1.3	4.4	29.3	131.2	268.7	489
-1.5+1.4	12.8	208.4	590.4	1035.1	519
-1.6+1.5	75.6	504.5	673.8	306.4	53.3
-1.7+1.6	123.7	432.7	164.2	54.8	5.5
-1.8+1.7	210.1	356	24.2	20.9	5.2
+1.8	1325.1	237	17.8	0	0

Table 18: Washability data for -19mm+ 16mm, Hbed=128mm

Class	Mass(g)				
	layer 1	layer 2	layer 3	layer 4	layer 5
-1.3	0	0	3	5	43
-1.4+1.3	0	17	131	643	960
-1.5+1.4	0	126	638	776	122
-1.6+1.5	69	427	510	71	3
-1.7+1.6	234	853	110	0	0
-1.8+1.7	157	215	8	0	0
+1.8	1200	116	0	0	0

Table 19: Washability data for -19mm+ 13.2mm, Hbed=129.5mm

Class	Mass(g)				
	layer 1	layer 2	layer 3	layer 4	layer 5
-1.3	0	0	1	3	16
-1.4+1.3	9	33	219	286	790
-1.5+1.4	54	308	824	738	523
-1.6+1.5	133	505	399	197	106
-1.7+1.6	313	640	84	73	10
-1.8+1.7	453	137	21	5	0
+1.8	846	29	0	0	0

Table 20: Washability data for -19mm+ 9.5mm, Hbed=129.5mm

Class	Mass(g)				
	layer 1	layer 2	layer 3	layer 4	layer 5
-1.3	0	0	0	21	274
-1.4+1.3	0	3	154	683	1135
-1.5+1.4	12	226	945	746	160
-1.6+1.5	63	626	380	45	8
-1.7+1.6	169	546	74	9	0
-1.8+1.7	278	212	8	0	0
+1.8	1182	157	0	0	0

Table 21: Washability data for -19mm+ 6.7mm, Hbed=113mm

Class	Mass(g)				
	layer 1	layer 2	layer 3	layer 4	layer 5
-1.3	0	0	0	1	87
-1.4+1.3	0	6	55	315	559
-1.5+1.4	13	179	788	1088	1395
-1.6+1.5	104	688	553	104	2
-1.7+1.6	233	428	44	7	1
-1.8+1.7	440	173	8	1	0
+1.8	952	110	0	0	0

Table 22: Washability data for -16mm+ 9.5mm, Hbed=116mm

Class	Mass(g)				
	layer 1	layer 2	layer 3	layer 4	layer 5
-1.3	0	4	10	10	8
-1.4+1.3	67	288	333	520	374
-1.5+1.4	81	591	563	714	256
-1.6+1.5	159	627	202	134	47
-1.7+1.6	253	181	42	27	6
-1.8+1.7	260	81	6	6	2
+1.8	883	59	6	4	0

Table 23: Washability data for -16mm+ 6.7mm, Hbed=116mm

Class	Mass (g)				
	layer 1	layer 2	layer 3	layer 4	layer 5
-1.3	0	0	0	19	241
-1.4+1.3	0	33	169	606	1125
-1.5+1.4	13	352	886	830	153
-1.6+1.5	99	724	291	65	17
-1.7+1.6	292	372	42	14	0
-1.8+1.7	307	158	8	0	0
+1.8	1019	59	0	0	0

Table 24: Washability data for -13.2mm+ 9.5mm, Hbed=104mm

Class	Mass(g)			
	layer 1	layer 2	layer 3	layer 4
-1.3	0	0	13	197
-1.4+1.3	0	38	385	1038
-1.5+1.4	30	510	944	161
-1.6+1.5	112	719	103	11
-1.7+1.6	383	364	17	0
-1.8+1.7	278	46	0	0
+1.8	940	17	0	0

Table 25: Washability data for -13.2mm+ 6.7mm, Hbed=104mm

Class	Mass(g)				
	layer 1	layer 2	layer 3	layer 4	layer 5
-1.3	0	5	20	23	62
-1.4+1.3	72	174	275	306	635
-1.5+1.4	130	332	501	636	523
-1.6+1.5	157	316	407	253	141
-1.7+1.6	218	309	195	100	43
-1.8+1.7	277	107	44	16	12
+1.8	1203	70	18	13	7

Table 26: Washability data for -13.2mm+ 6.7mm, Hbed=126mm

Class	Mass(g)				
	layer 1	layer 2	layer 3	layer 4	layer 5
-1.3	0	21	53	95	553
-1.4+1.3	17	154	382	833	403
-1.5+1.4	44	459	745	500	80
-1.6+1.5	91	541	156	75	20
-1.7+1.6	252	939	56	17	0
-1.8+1.7	238	68	15	7	0
+1.8	1133	51	6	0	0

Appendix B: Stratification patterns

In this section the full set of the stratification patterns obtained for all the samples tested are presented. Appendix B1 shows the concentration profiles, Appendix B2 shows the cumulative concentration profiles while Appendix B3 shows the recovery plots respectively.

Appendix B1: Concentration Profiles

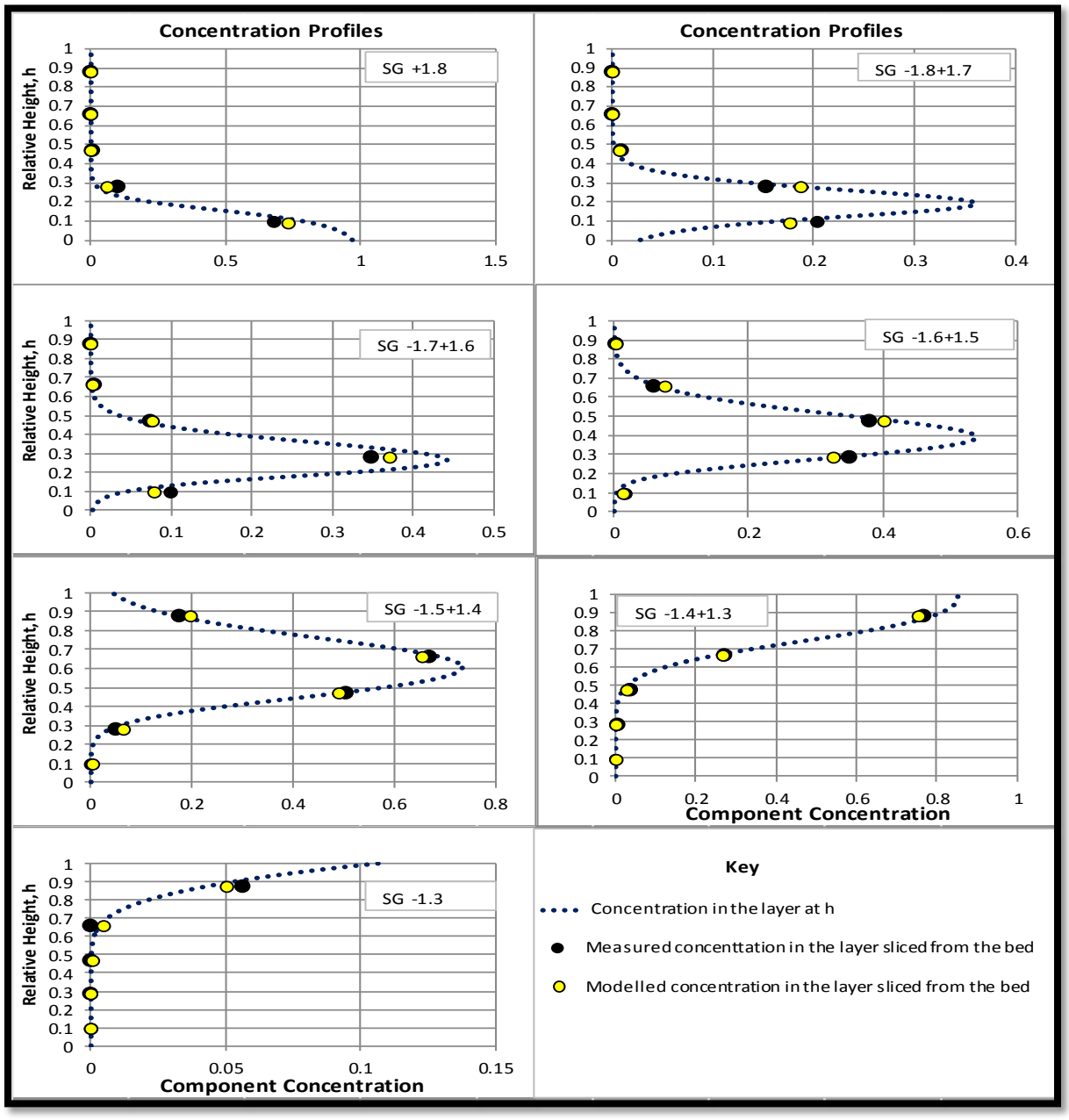

Figure 38: Concentration profile for sample A1B1 (-22.5mm+19mm)

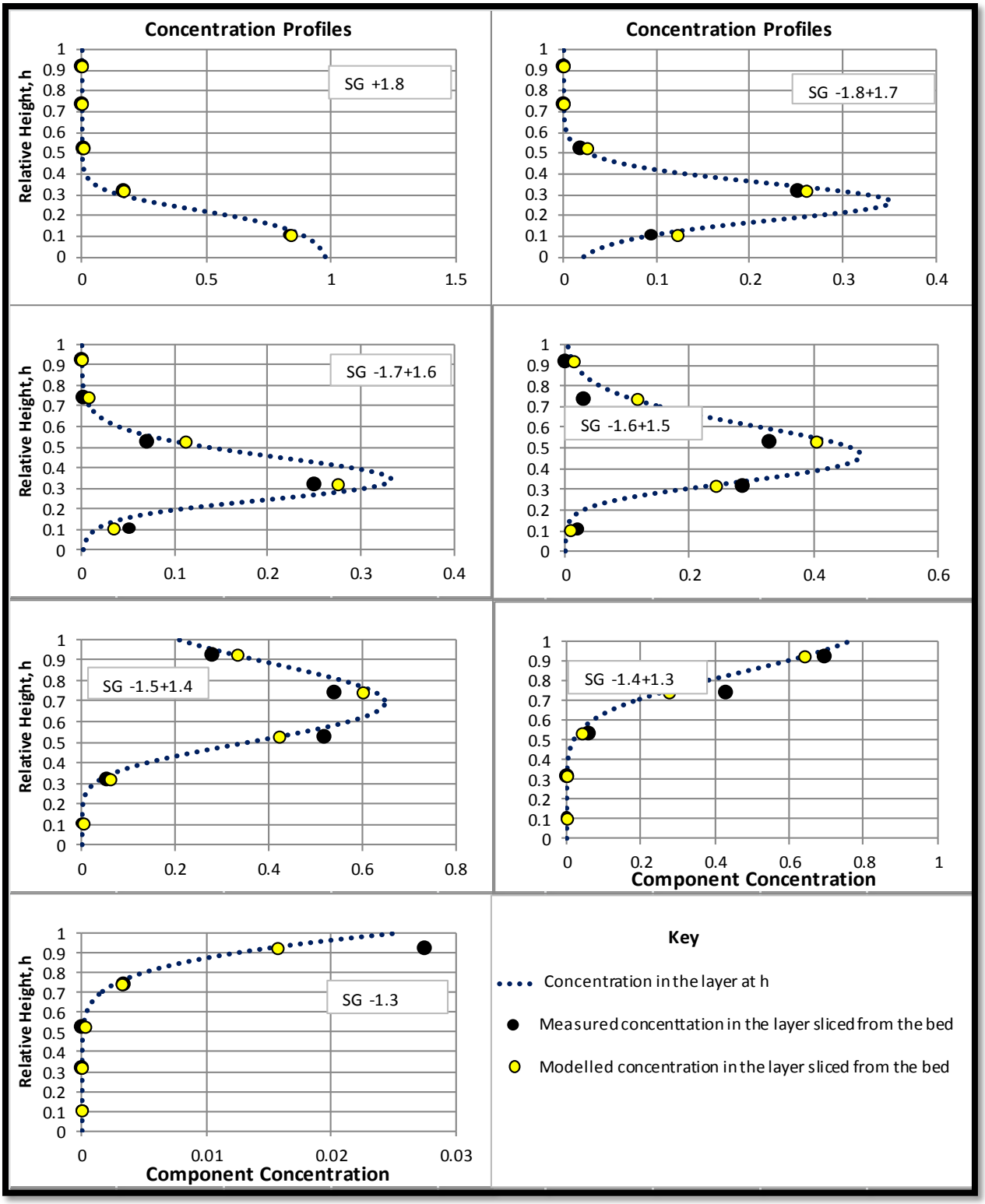

Figure 39: Concentration profile for sample A1B2 (-22.5mm+16mm)

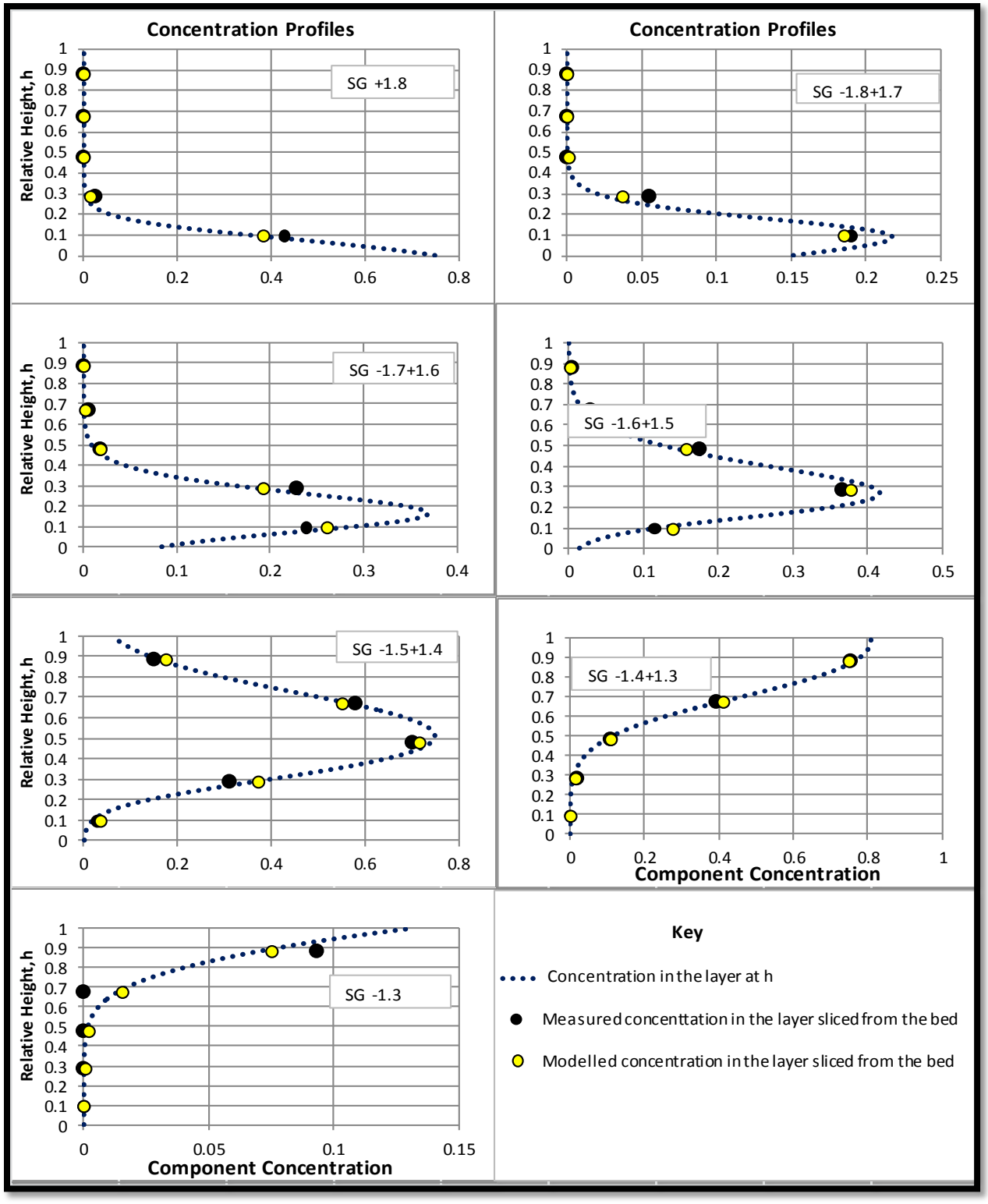

Figure 40: Concentration profile for sample A1B3 (-22.5mm+13.2mm)

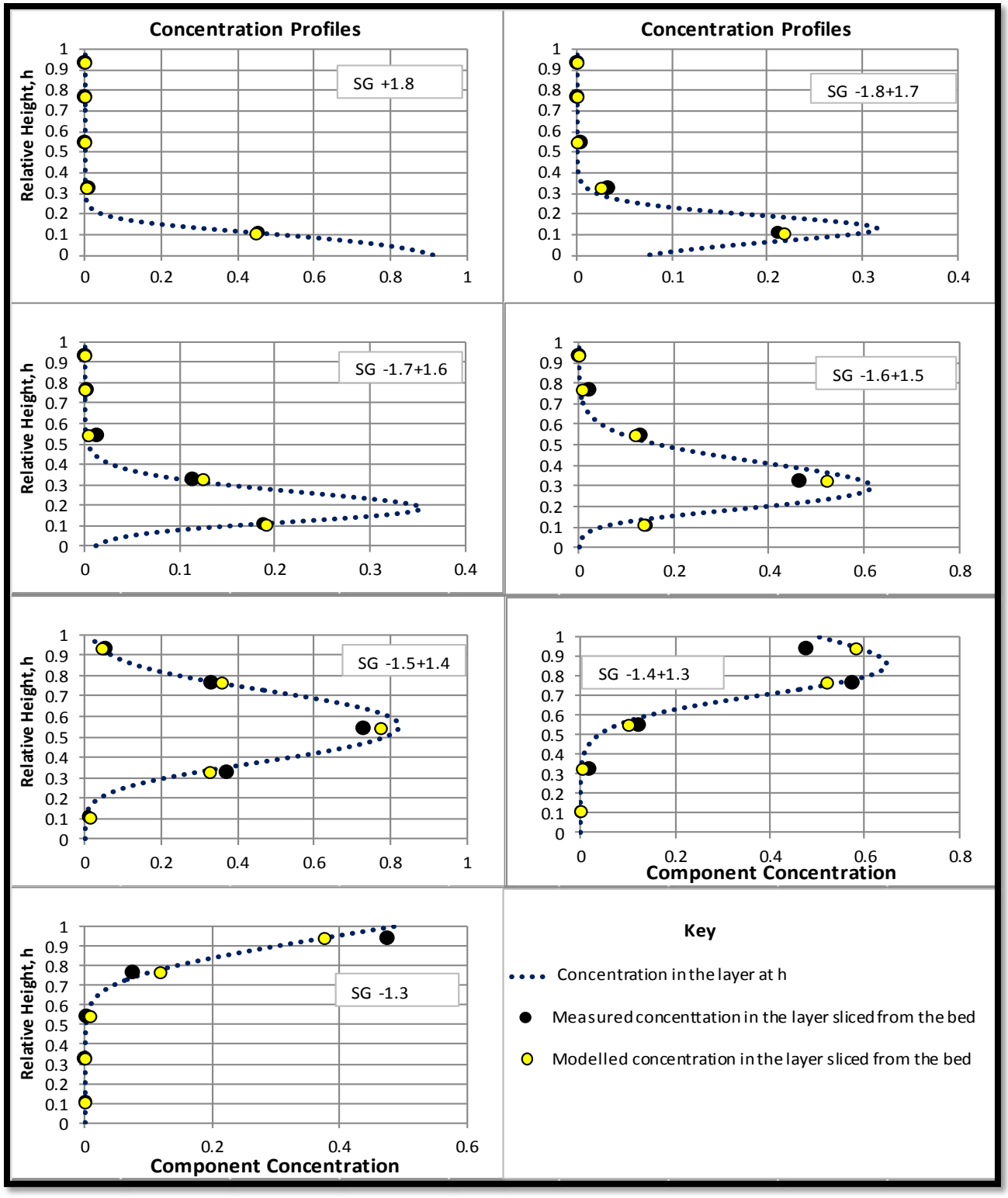

Figure 41: Concentration profile for sample A1B4 (-22.5mm9.5mm)

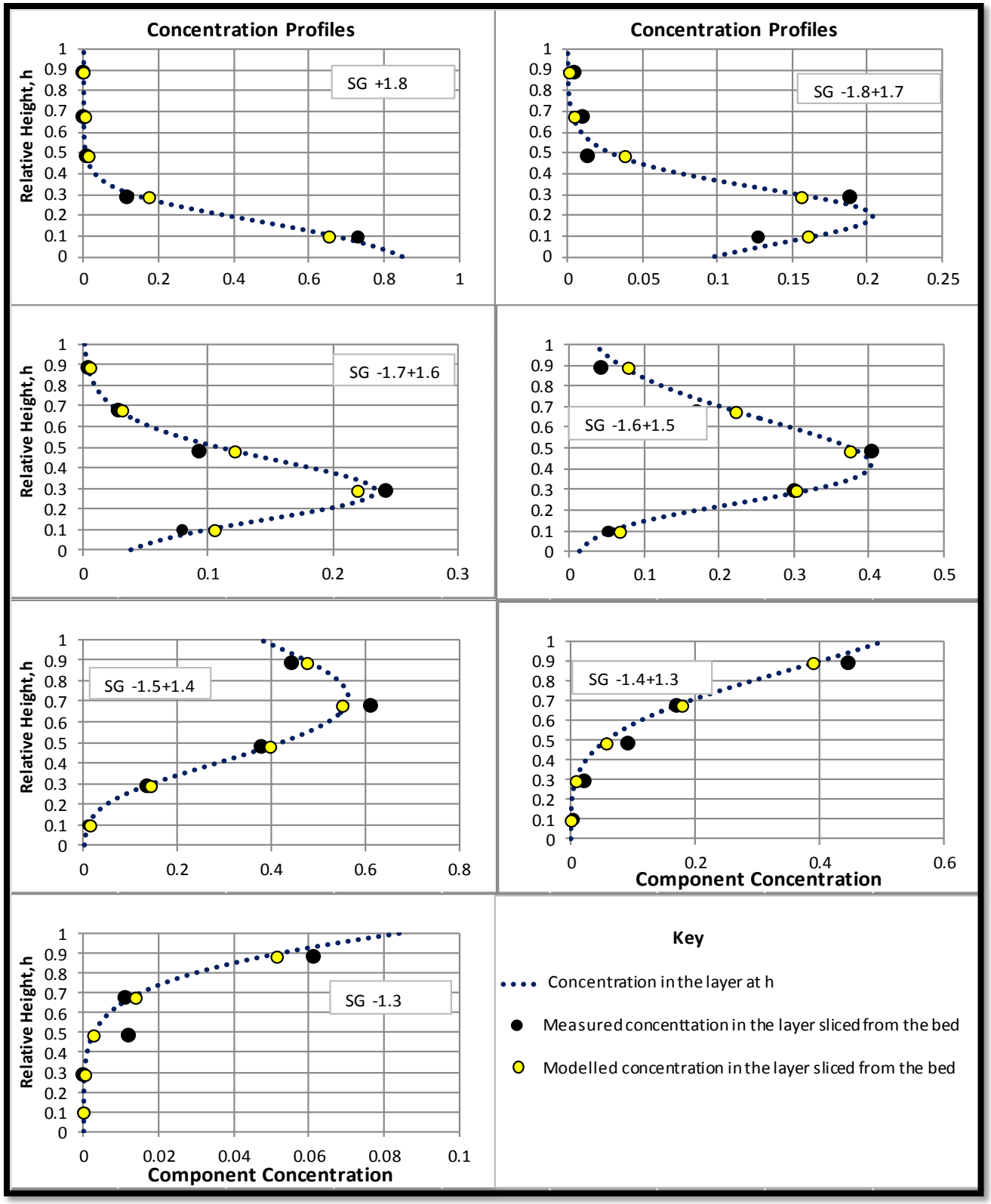

Figure 42: Concentration profile for sample A1B5 (-22.5mm+6.7mm)

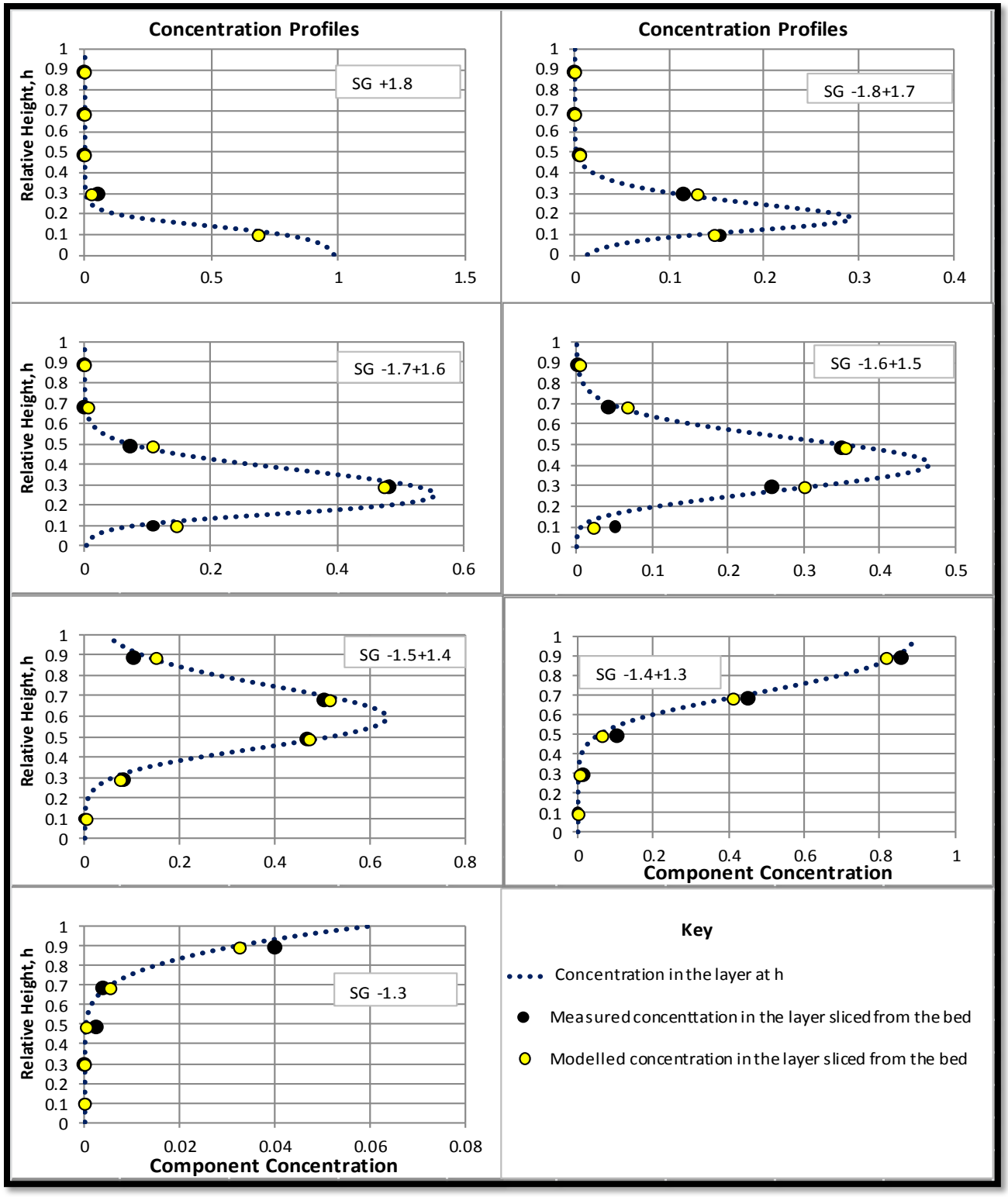

Figure 43: Concentration profile for sample A2B2 (-19mm+16mm)

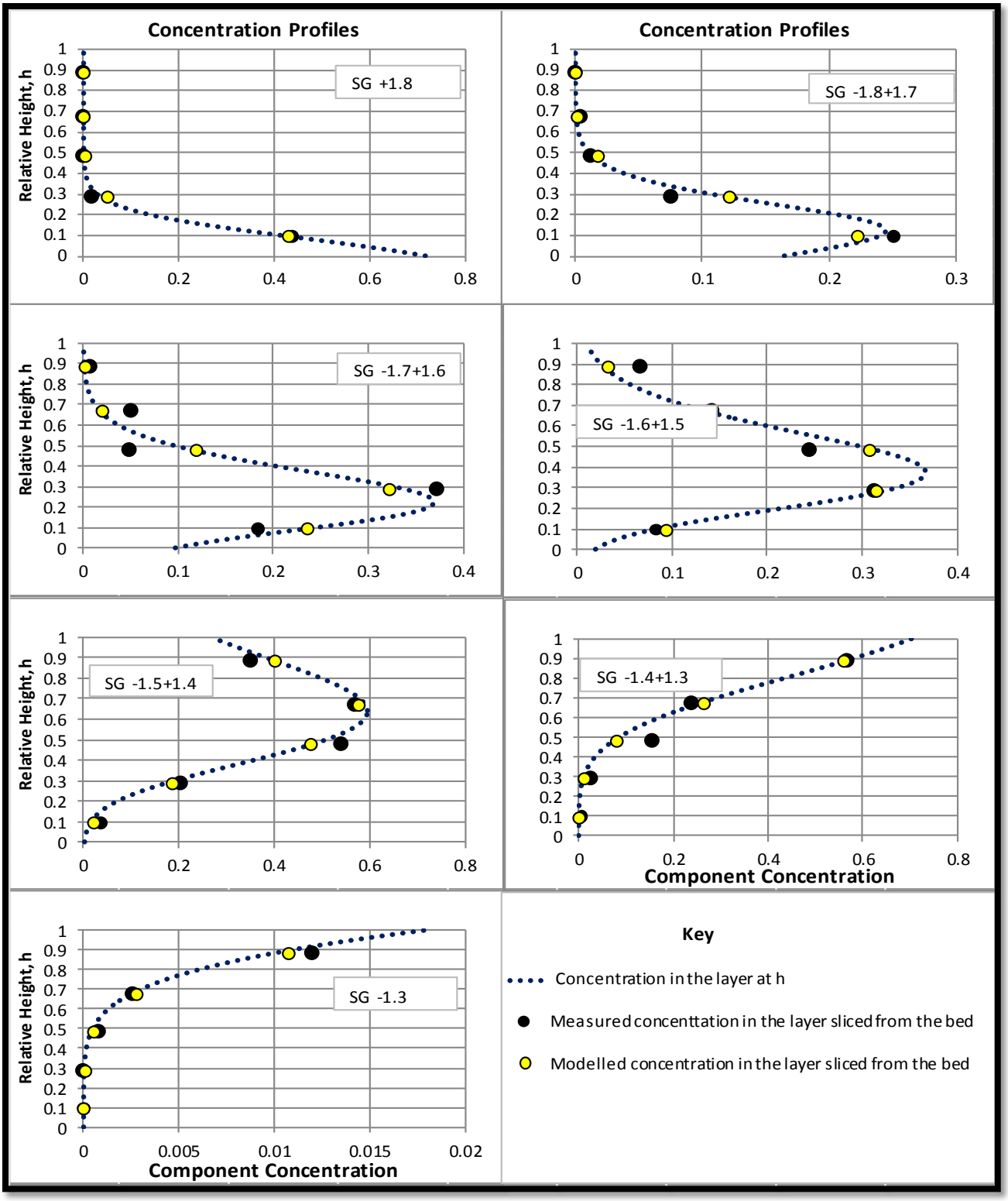

Figure 44: Concentration profile for sample A2B3 (-19mm+13.2mm)

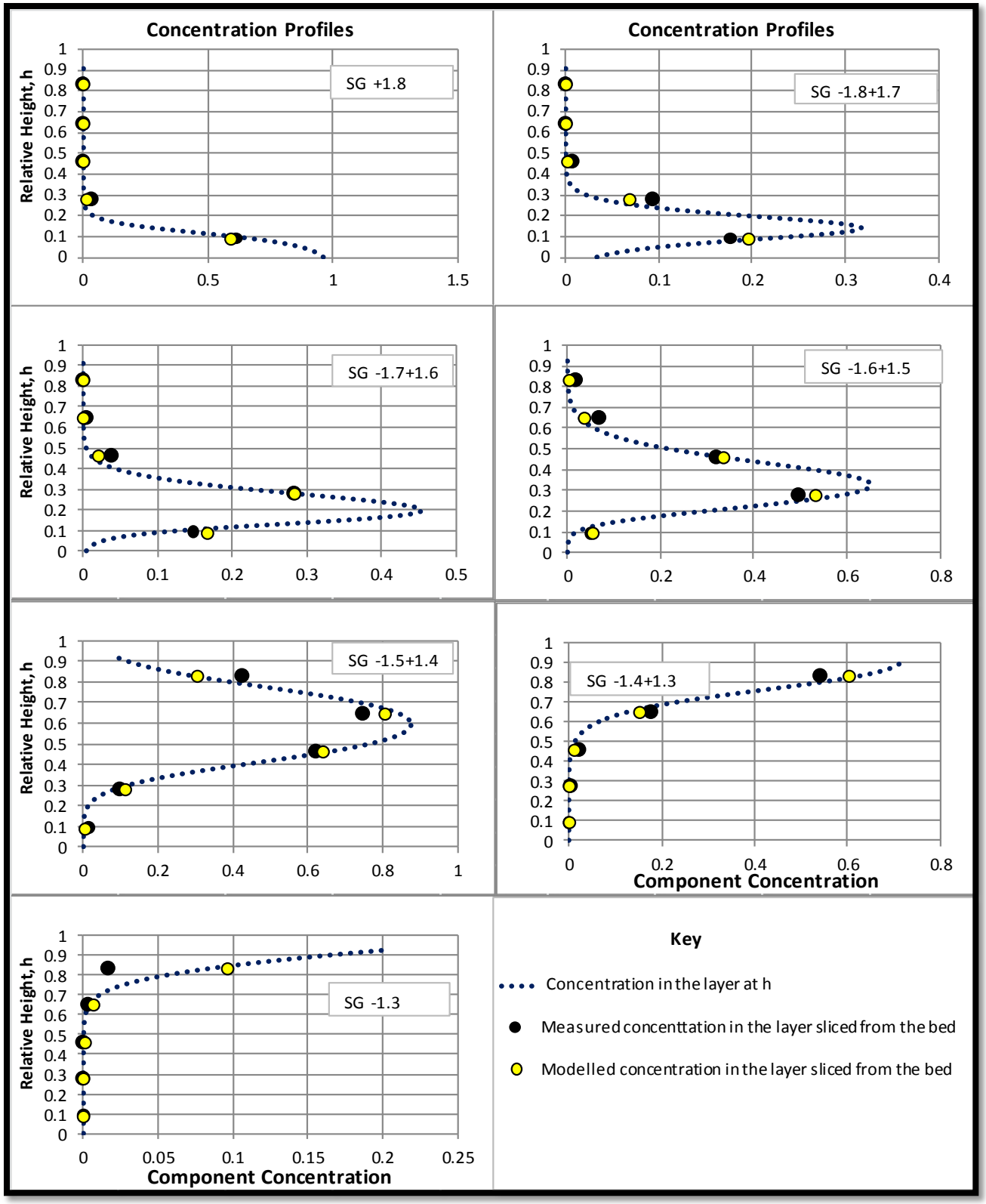

Figure 45: Concentration profile or sample A2B4 (-19mm+9.5mm)

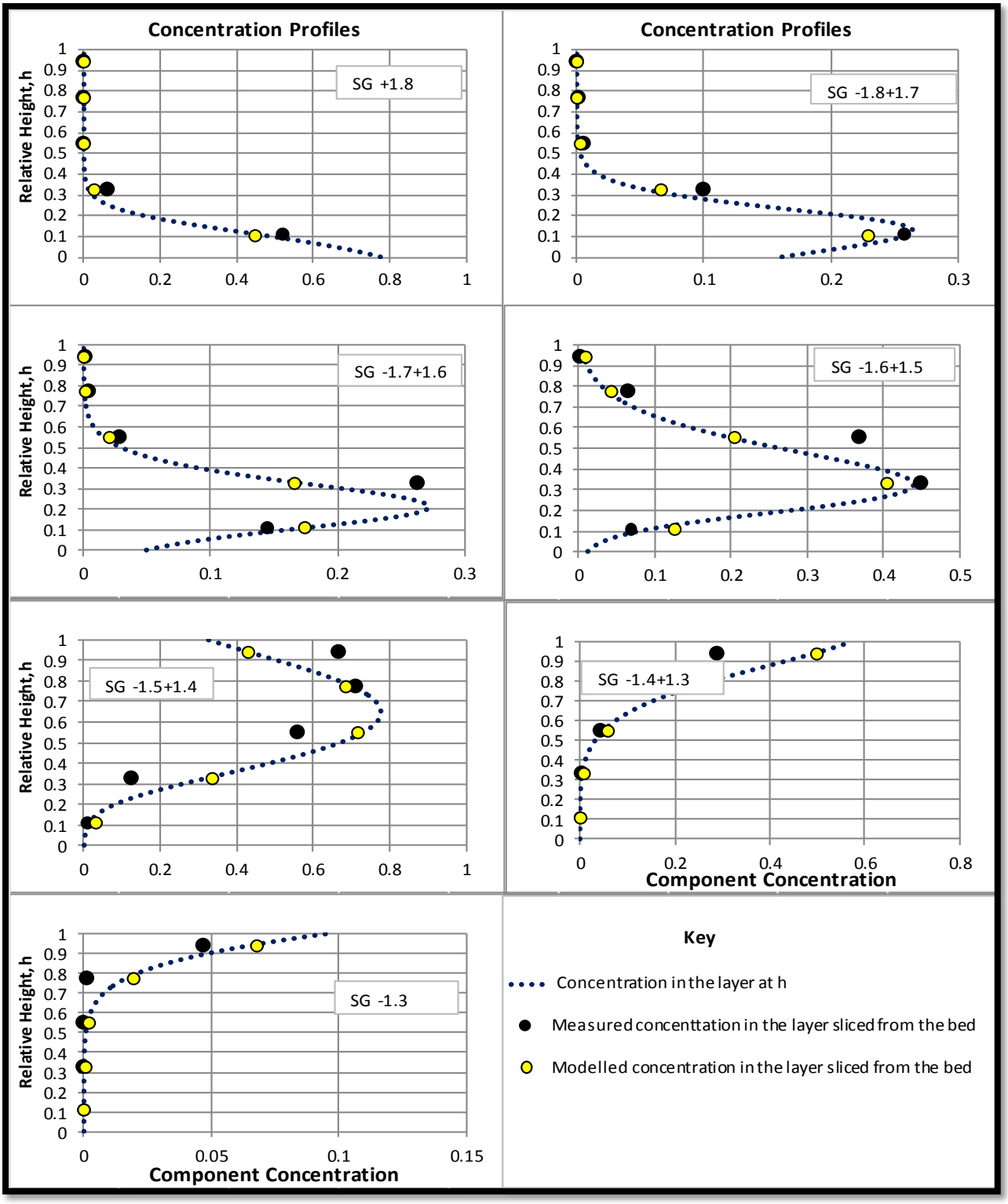

Figure 46: Concentration profile for sample A2B5 (-19mm+6.7mm)

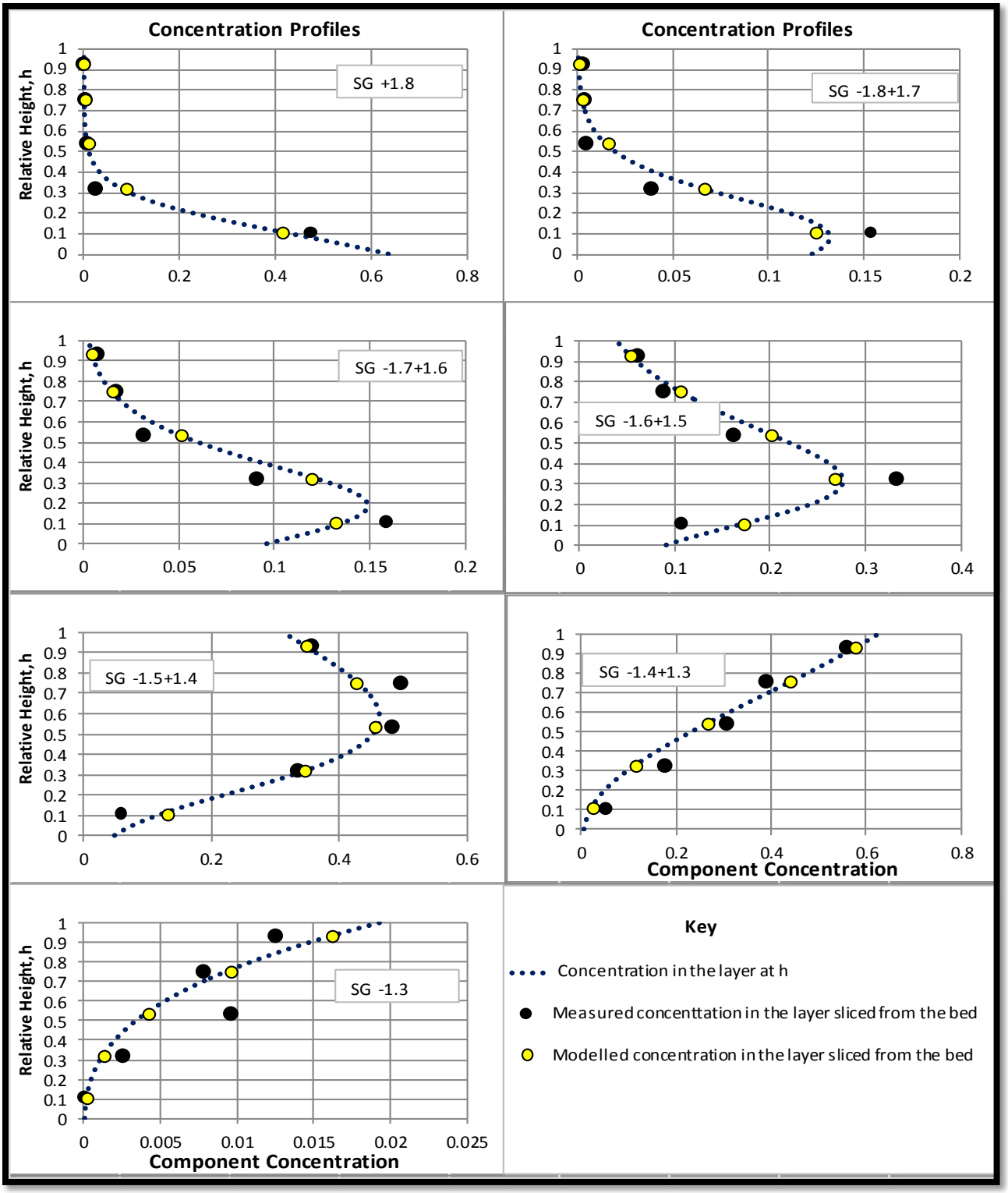

Figure 47: Concentration profile for sample A3B4 (-16mm+9.5mm)

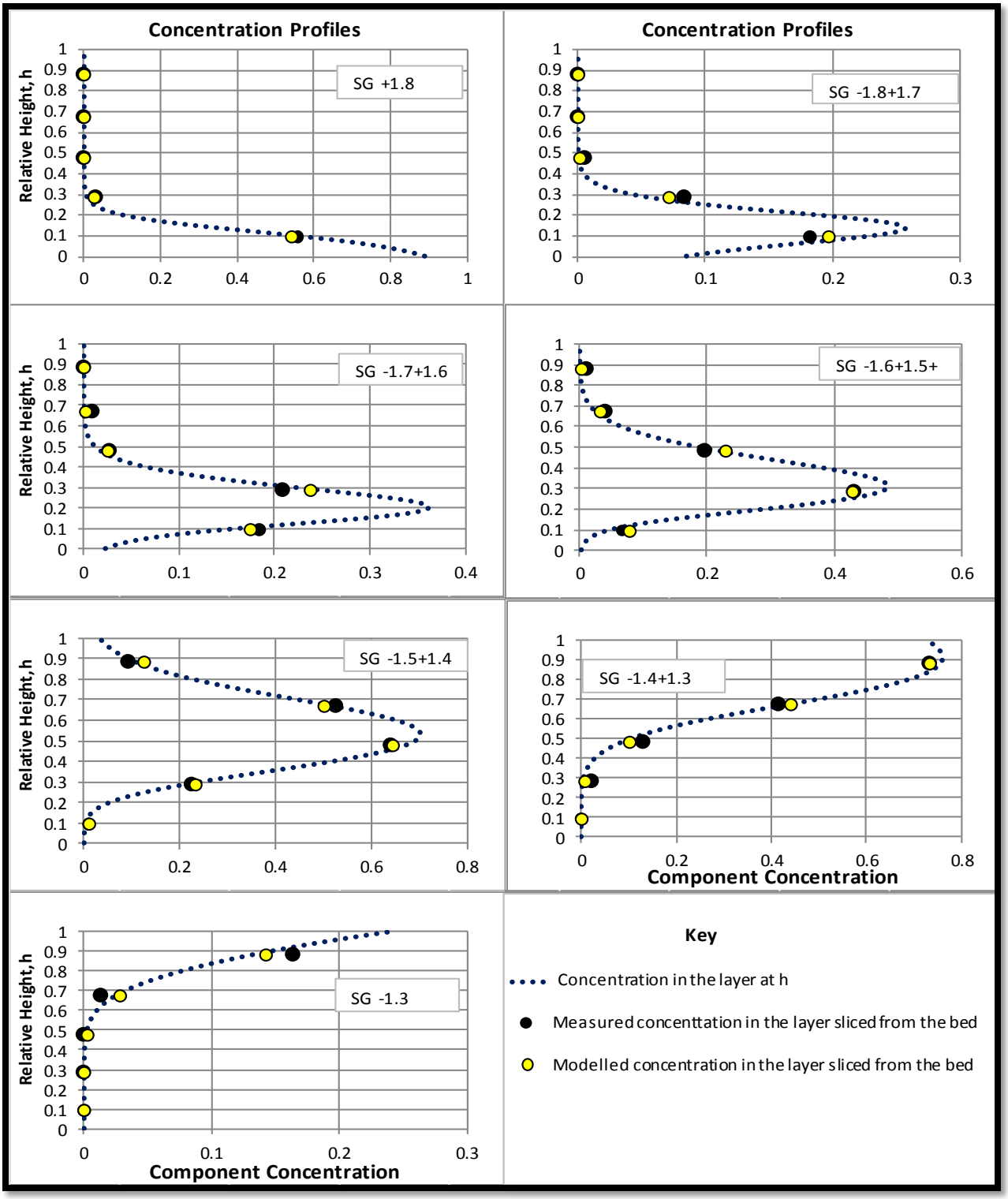

Figure 48: Concentration profile for sample A3B5 (-16mm+6.7mm)

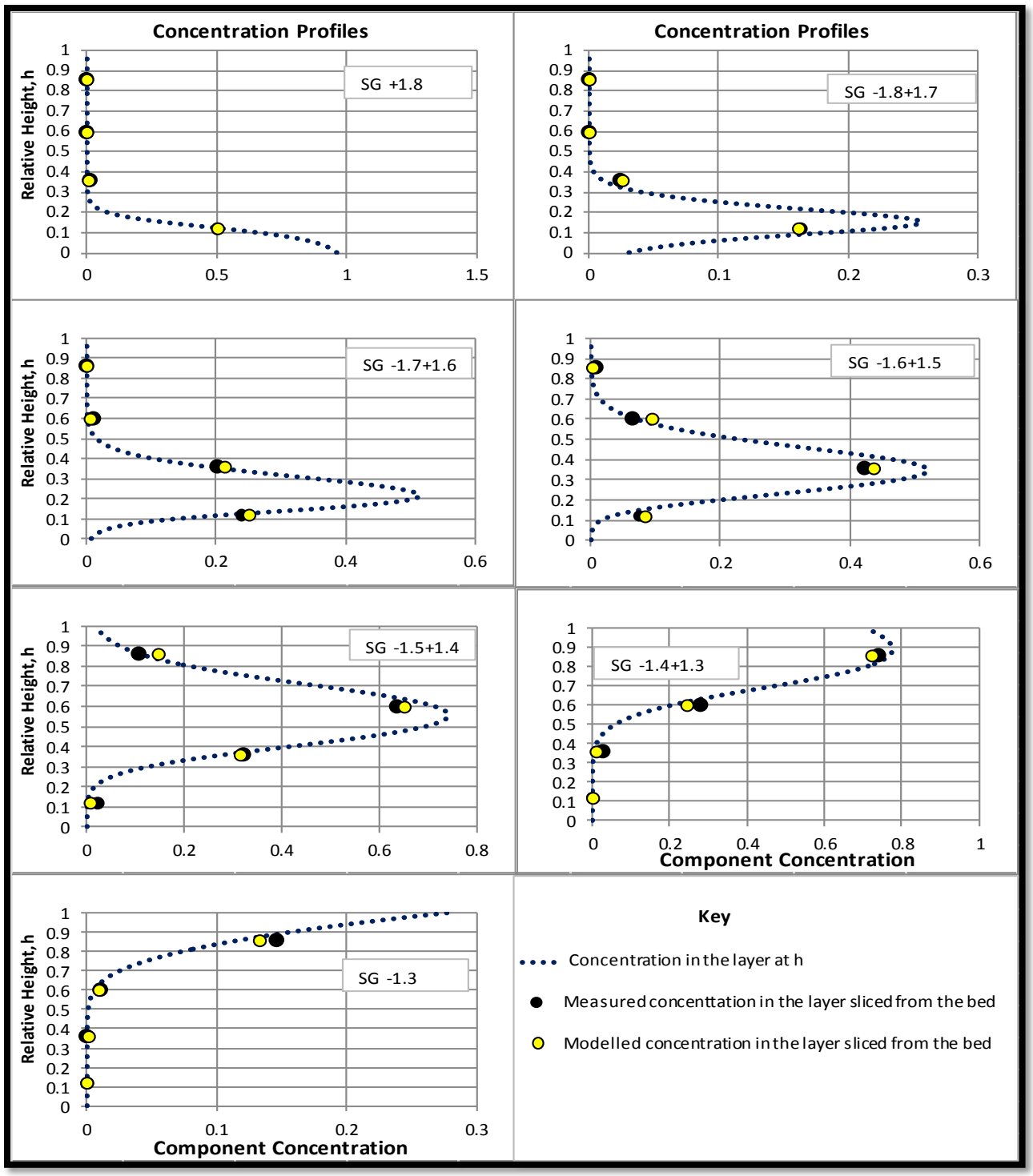

Figure 49: Concentration profile for sample A4B4 (-13.2mm+9.5mm)

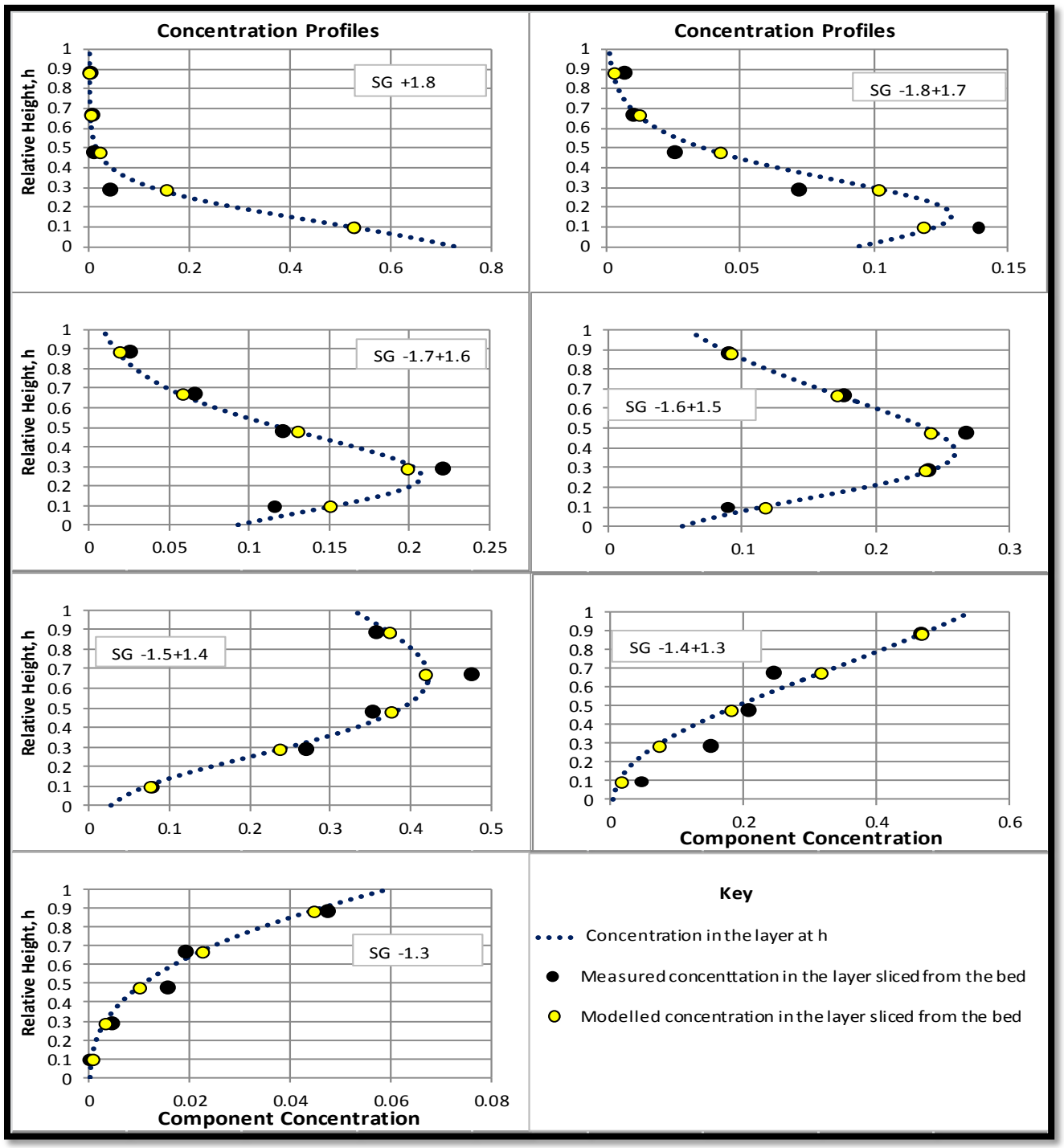

Figure 50: Concentration profile for sample A4B5 (-13.2mm+6.7mm)

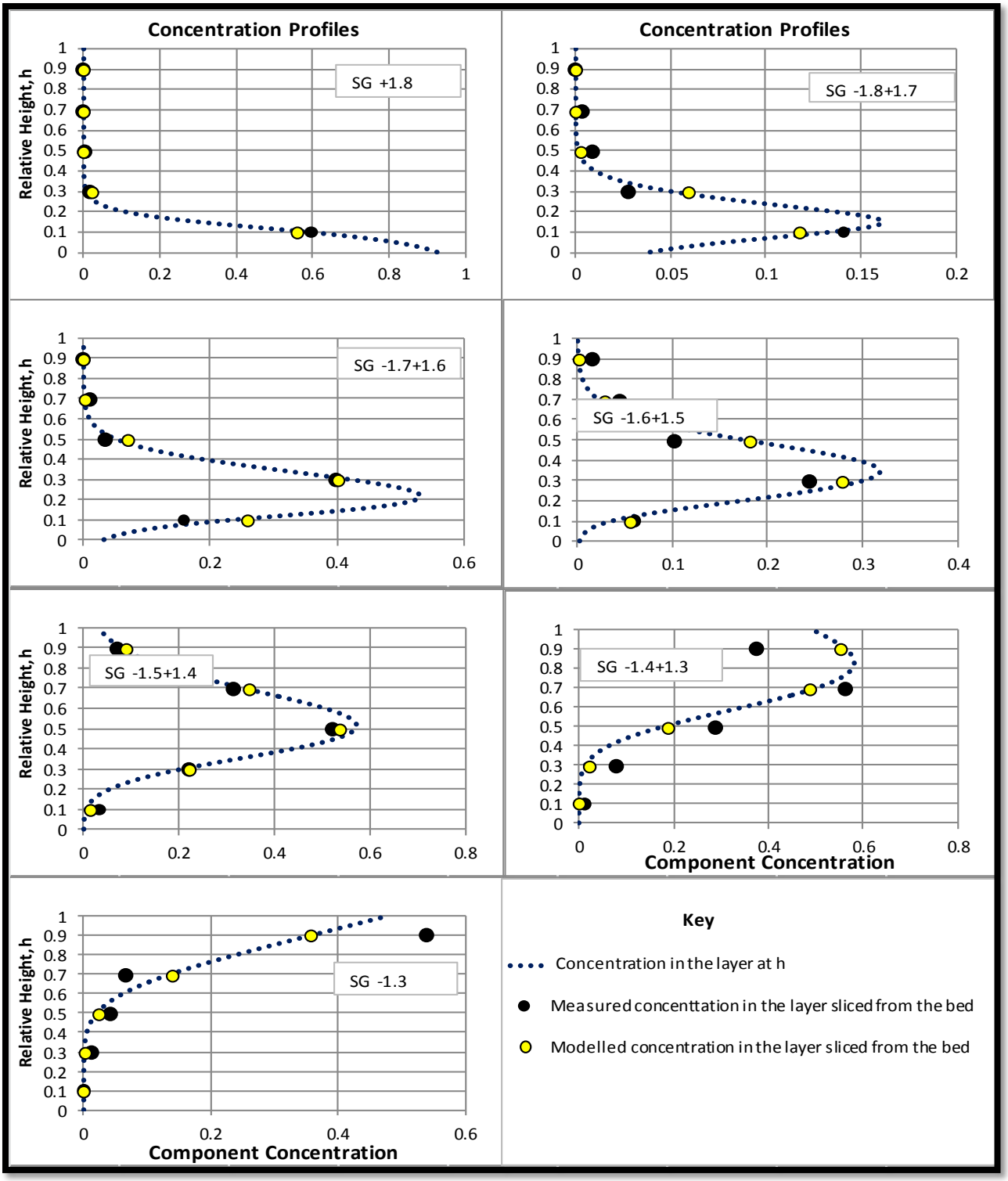

Figure 51: Concentration profile for sample A5B5 (-9.5mm+6.7mm)

Appendix B2: Cumulative concentration profiles

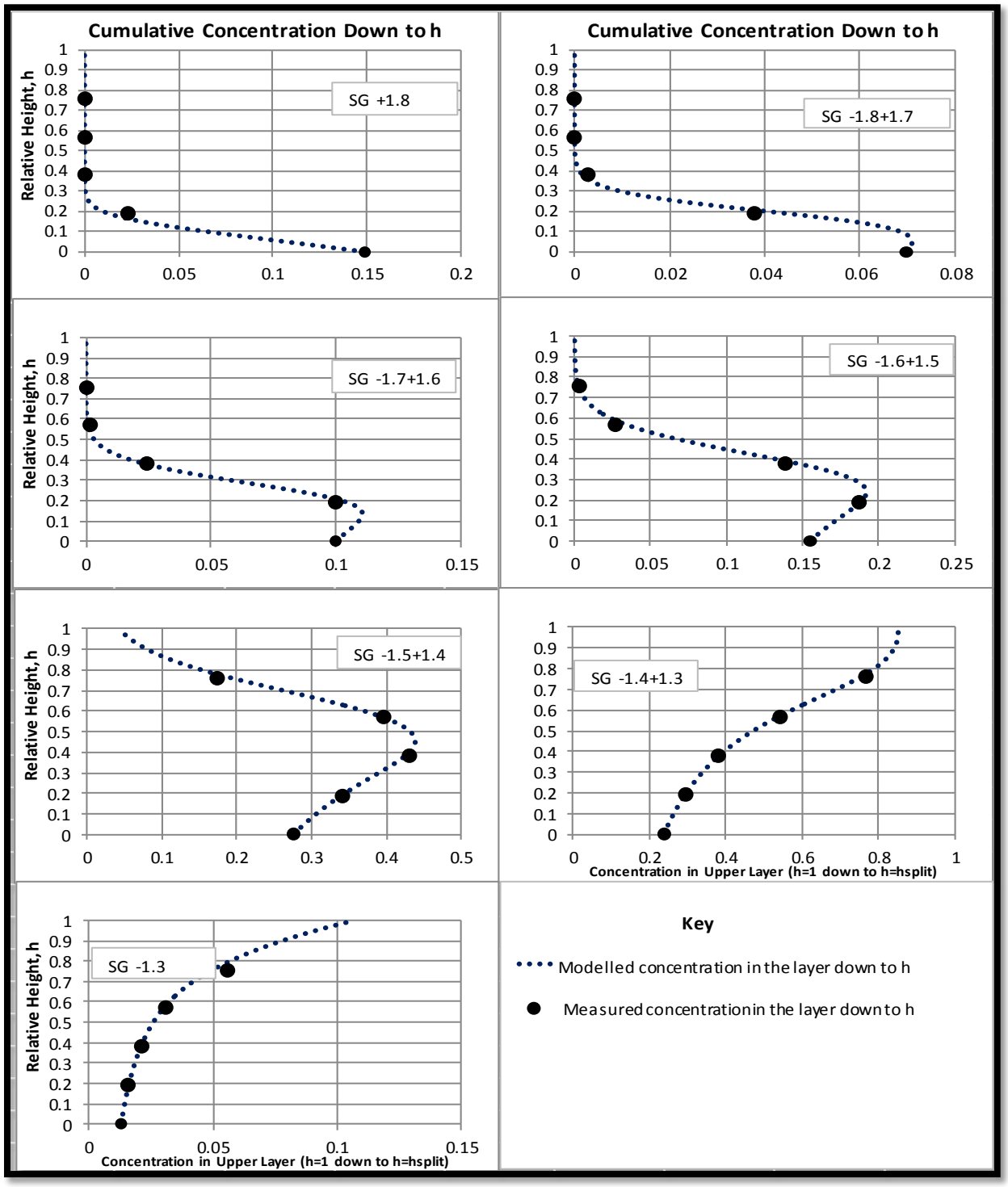

Figure 52: Cumulative concentration profile for sample A1B1 (-22.5mm+19mm)

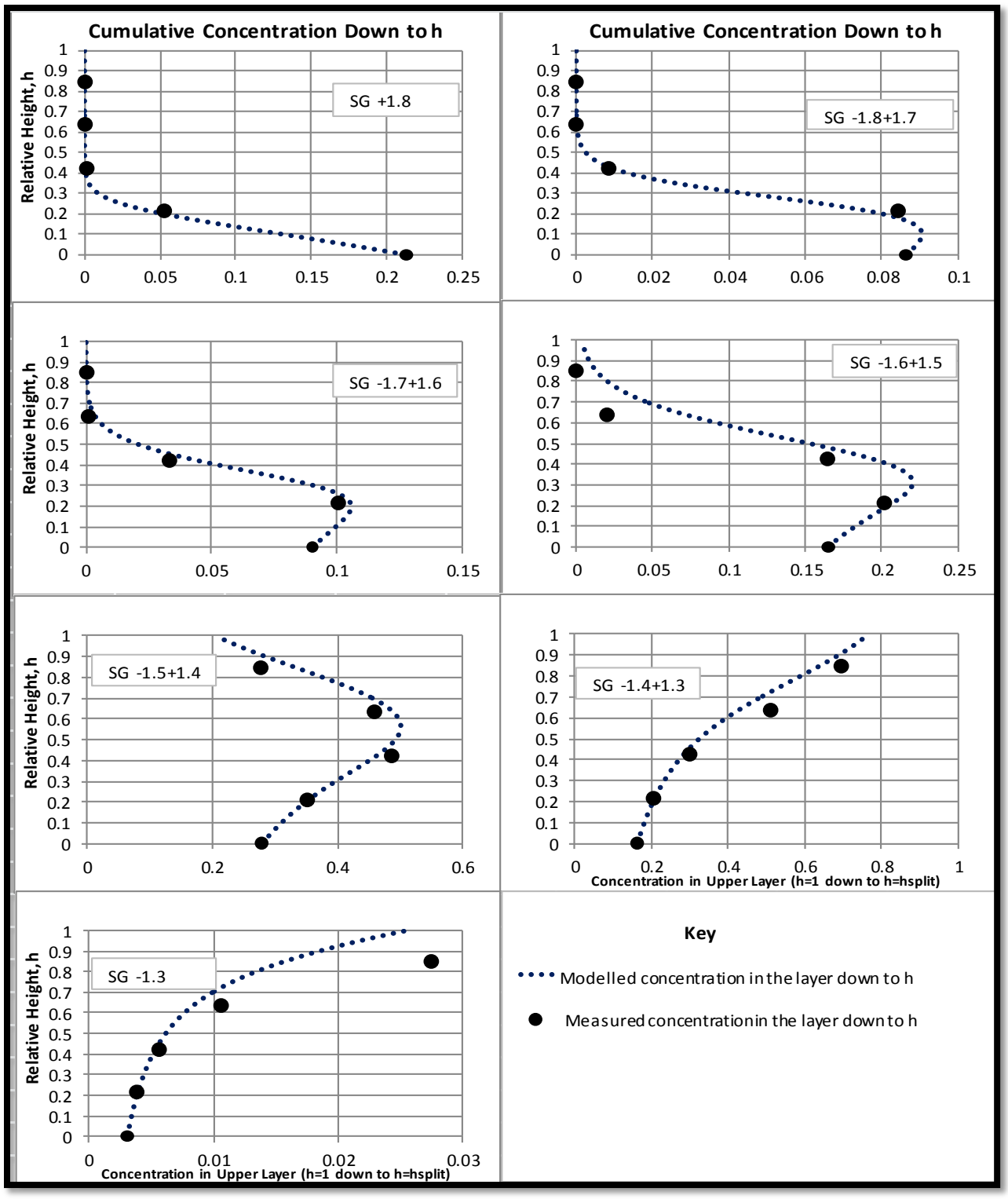

Figure 53: Cumulative concentration profiles for sample A1A2 (-22.5mm+16mm)

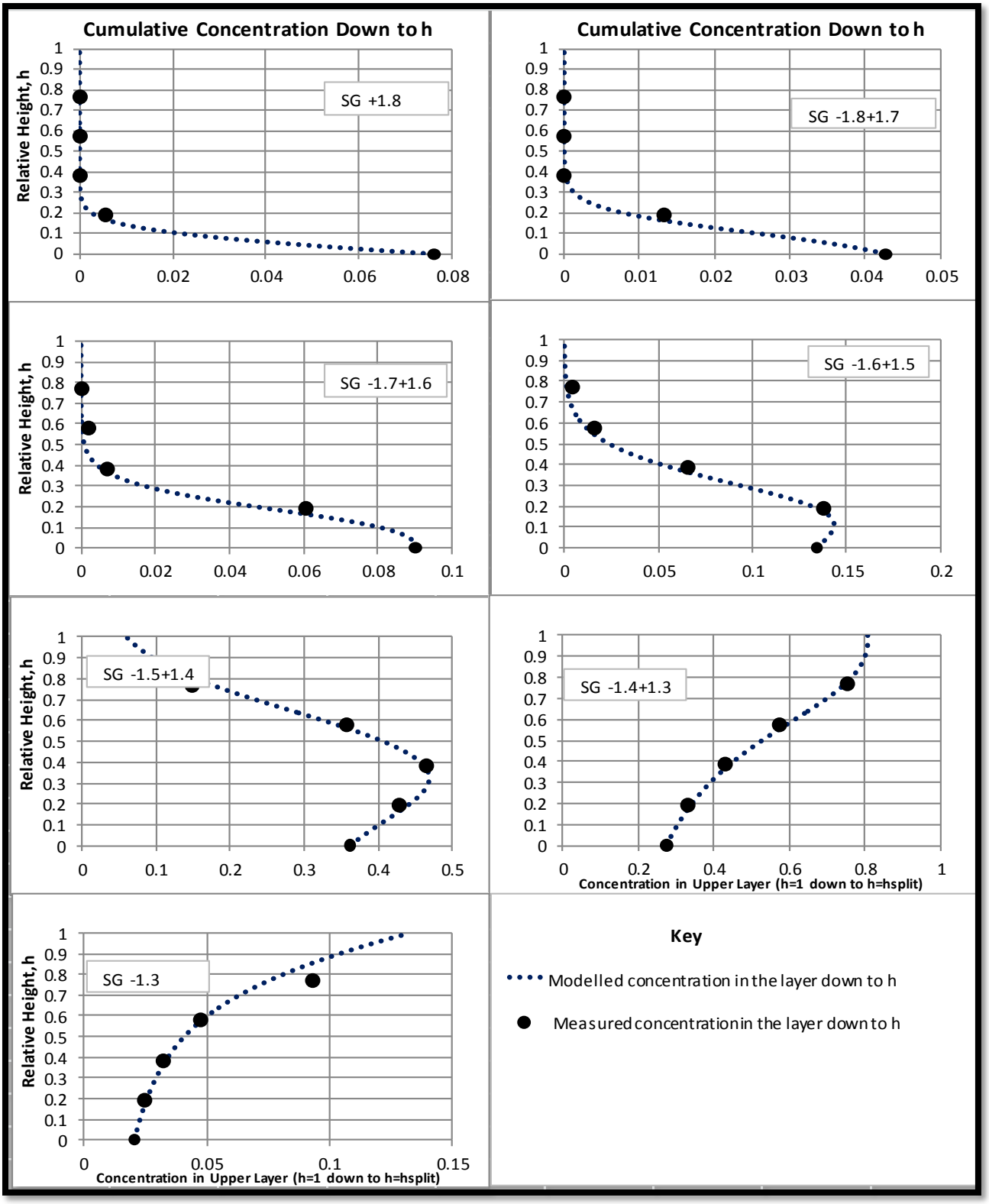

Figure 54: Cumulative concentration profile for sample A1B3 (-22.5mm+13.2mm)

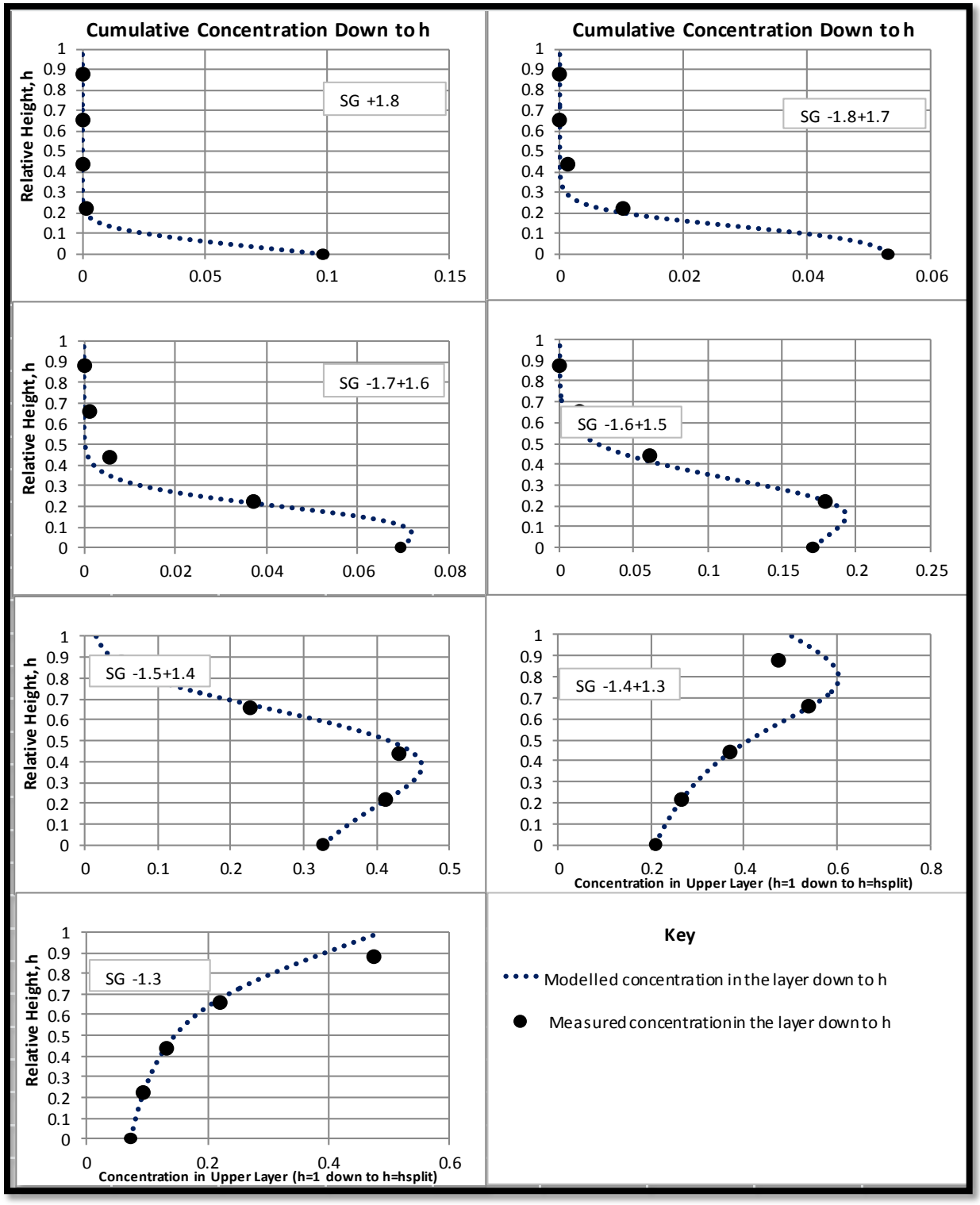

Figure 55: Cumulative concentration profile for sample A1B5 (-22.5mm+6.7mm)

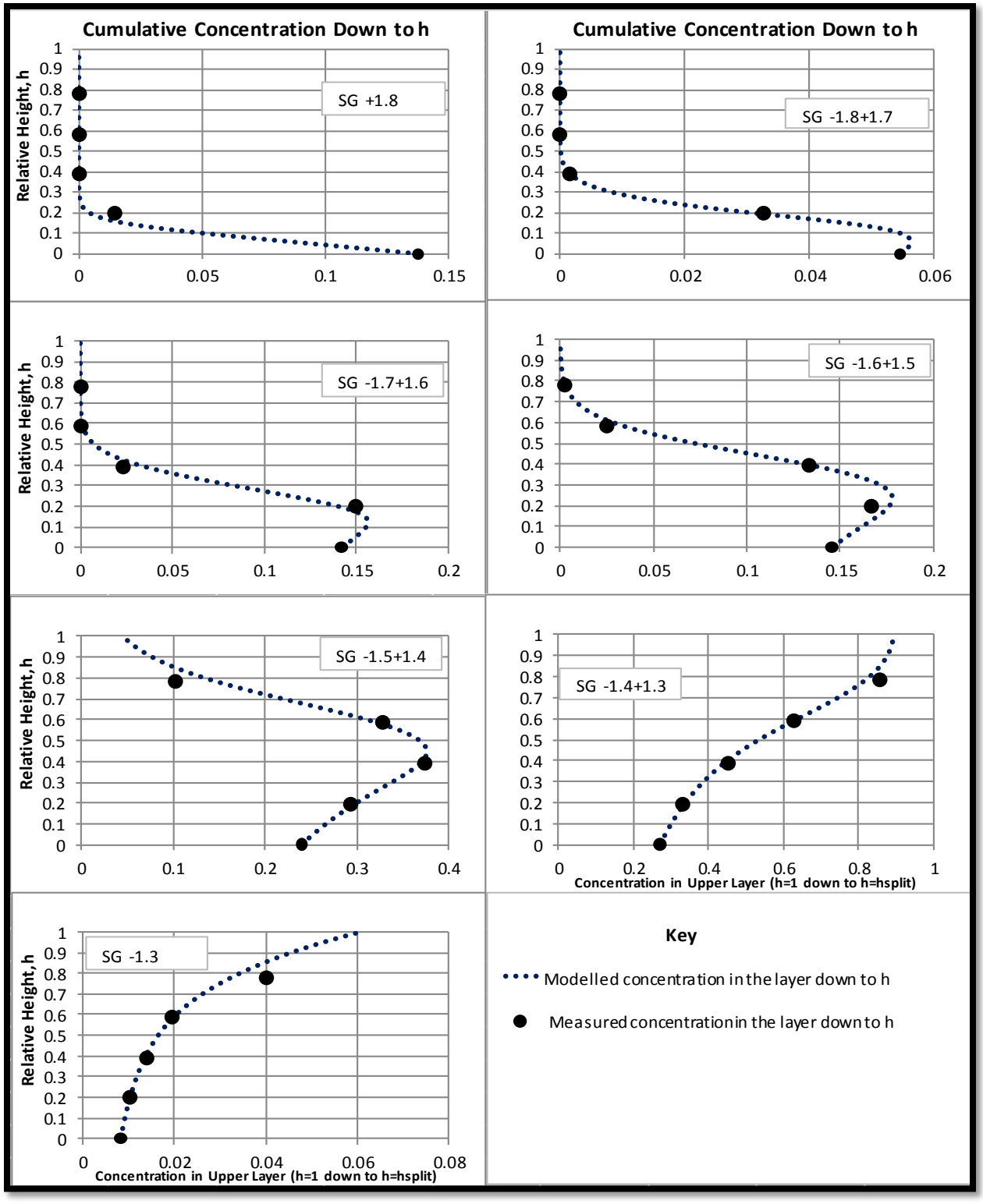

Figure 56: Cumulative concentration profile for sample A2B2 (-19mm+16mm)

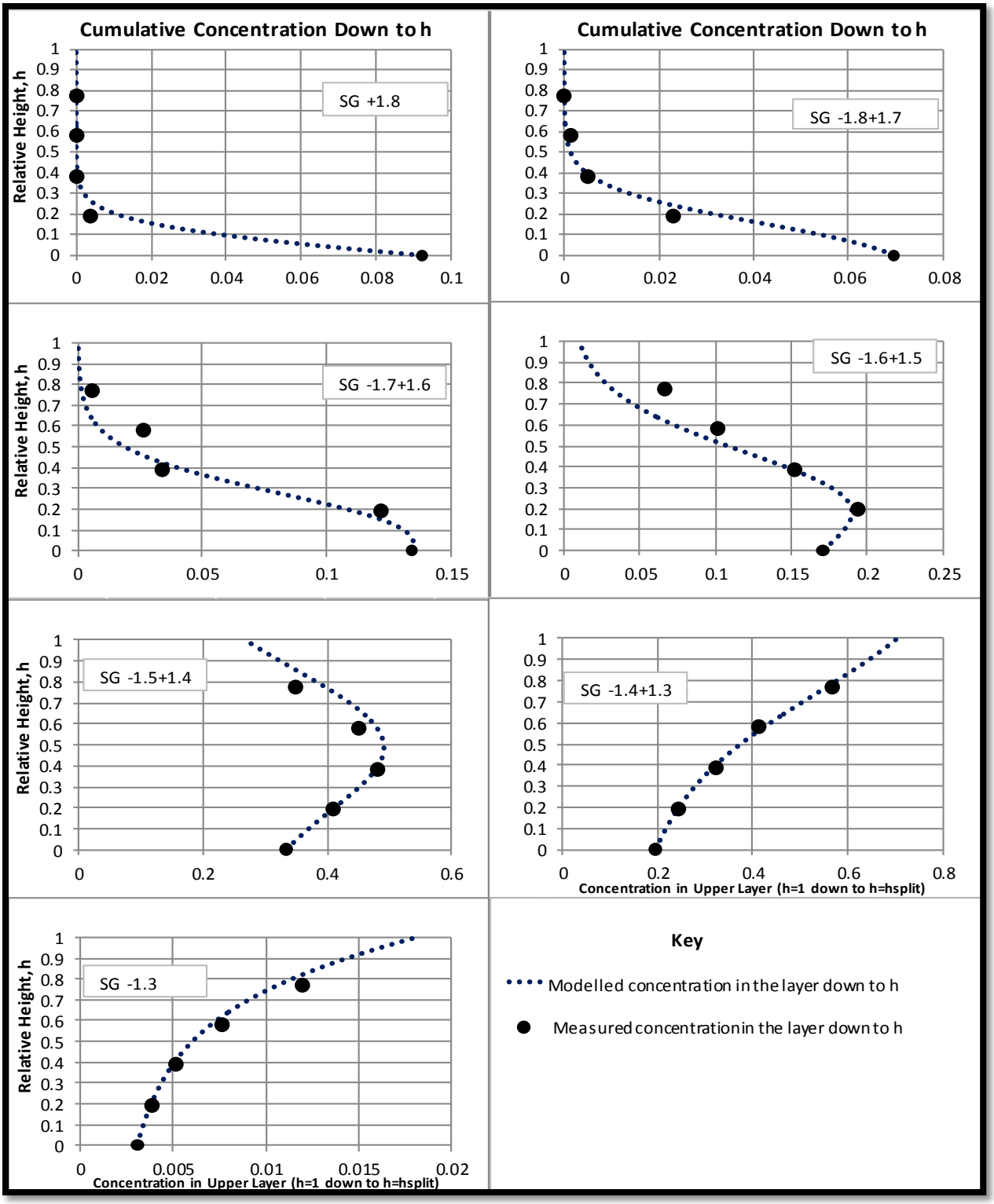

Figure 57: Cumulative concentration profile for sample A2B3 (-19mm+13.2mm)

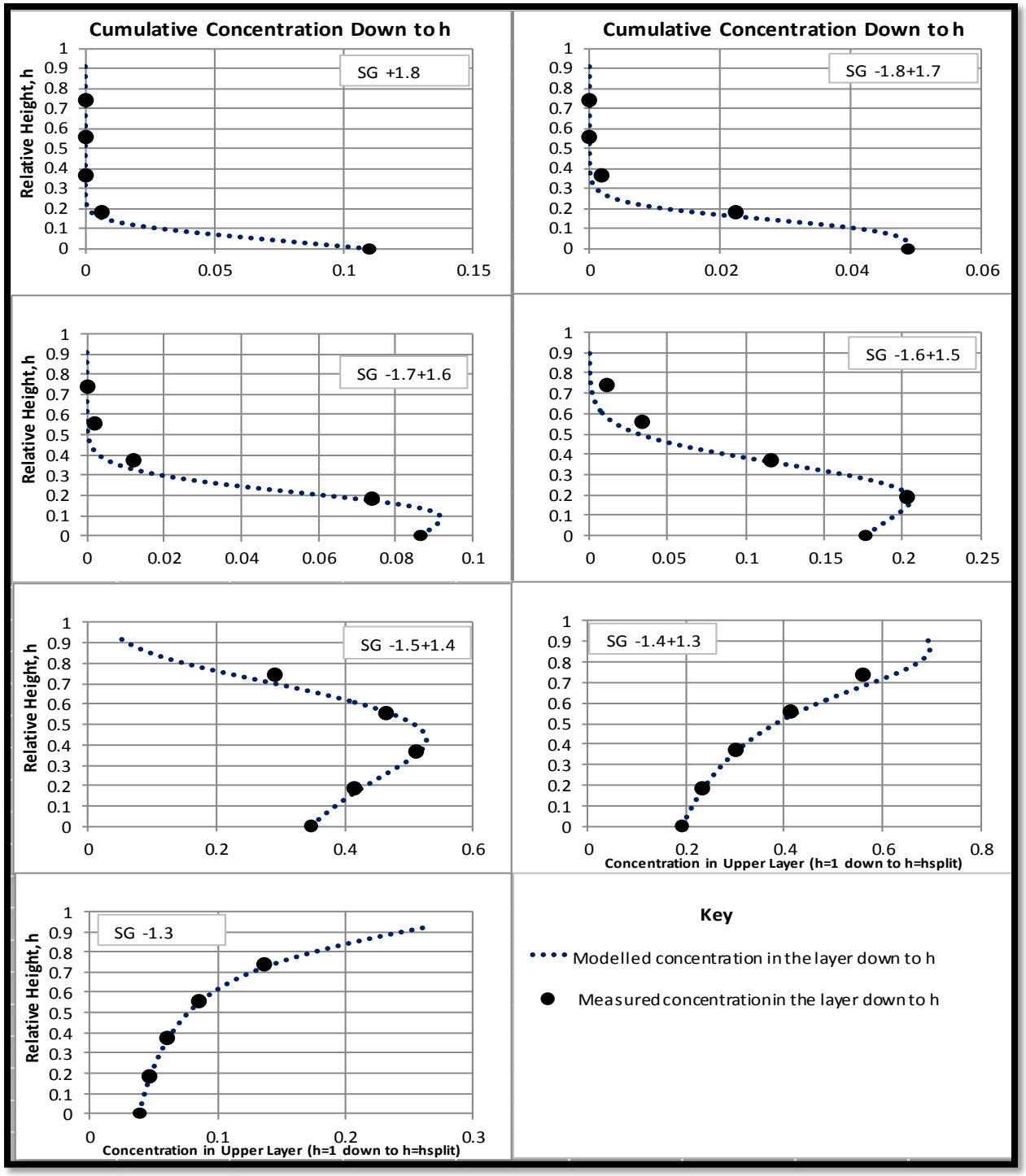

Figure 58: Cumulative concentration profile for sample A2B4 (-19mm+9.5mm)

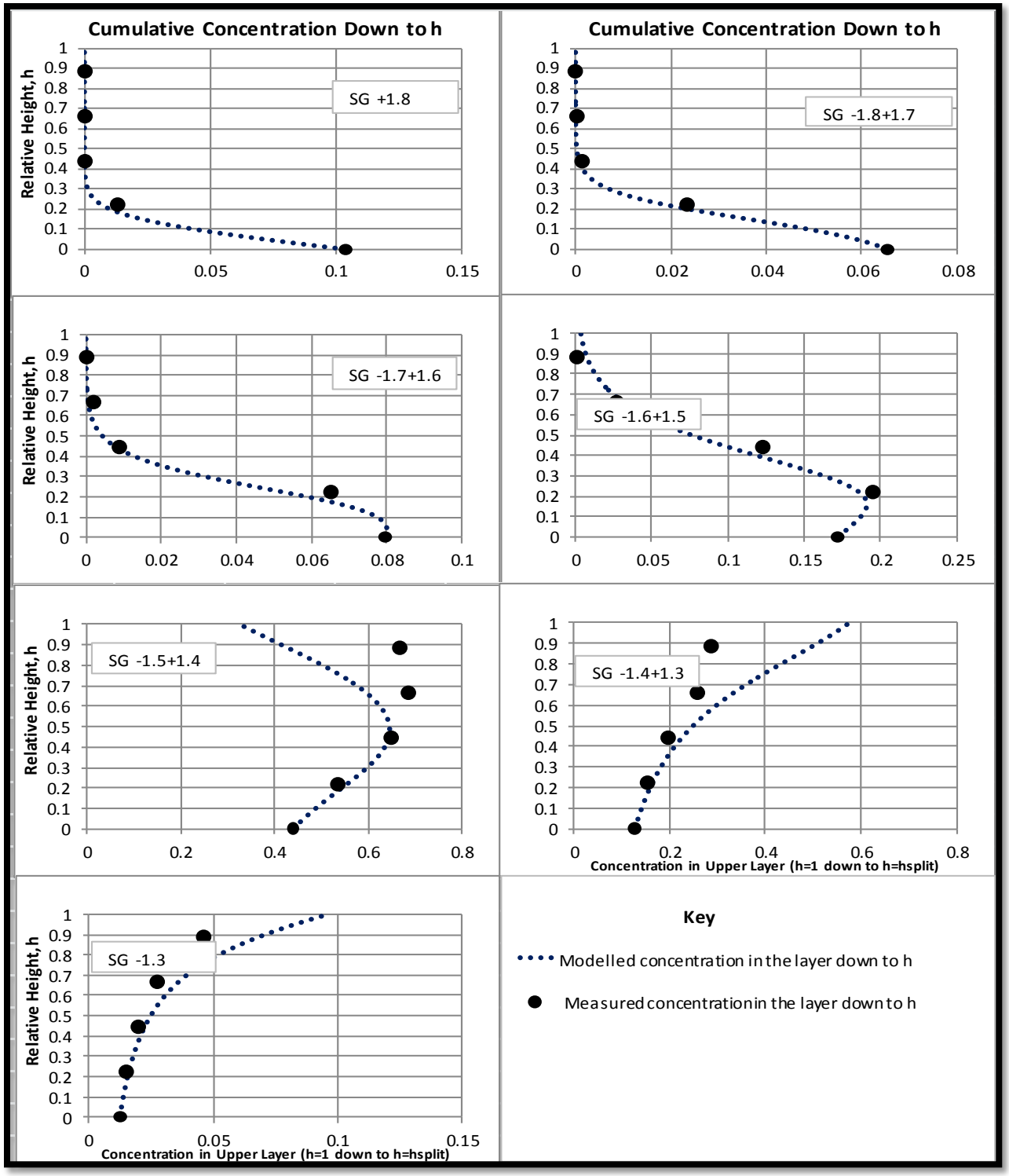

Figure 59: Cumulative concentration profile for sample A2B5 (-19mm+6.7mm)

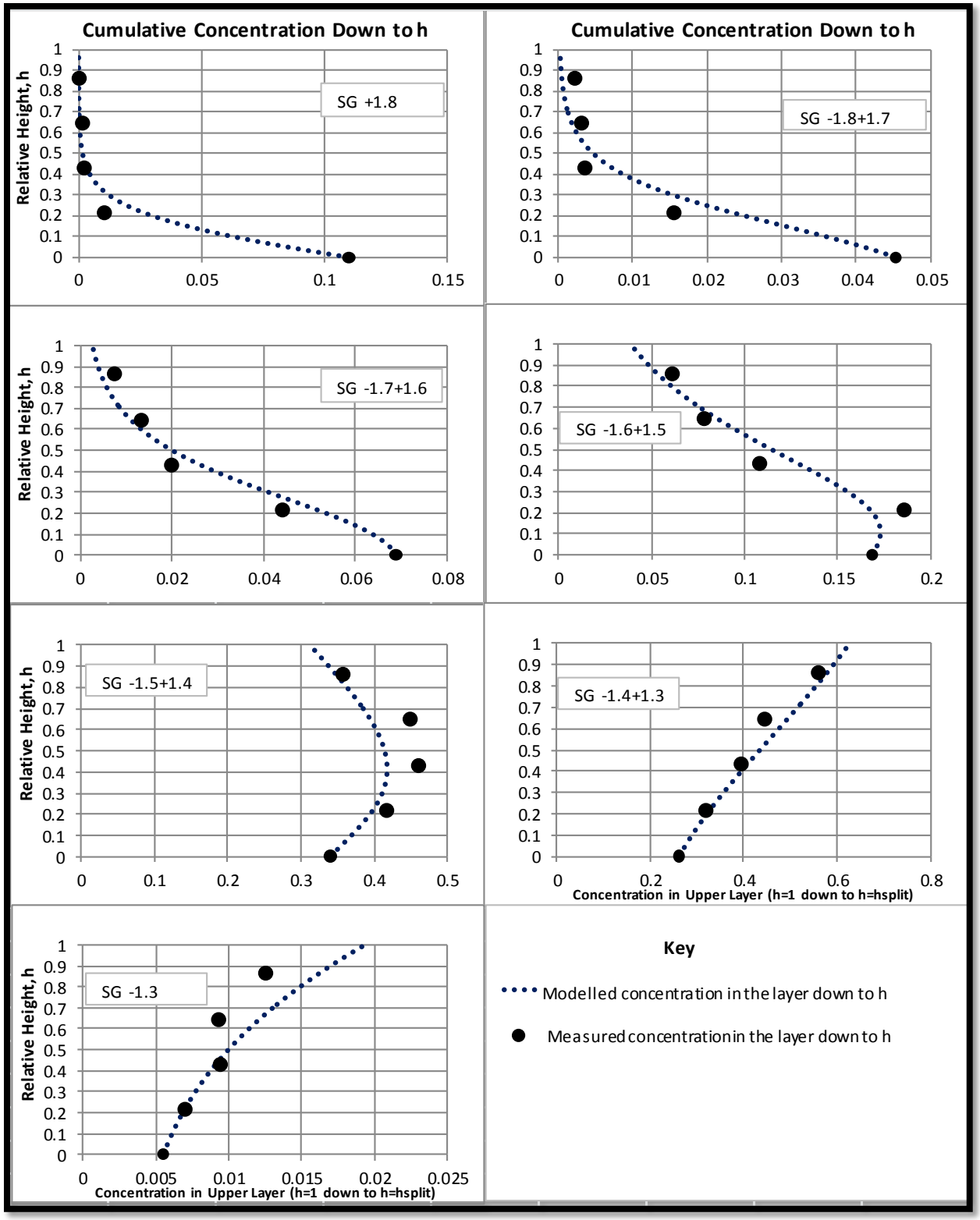

Figure 60: Cumulative concentration profile for sample A3B4 (-16mm+9.5mm)

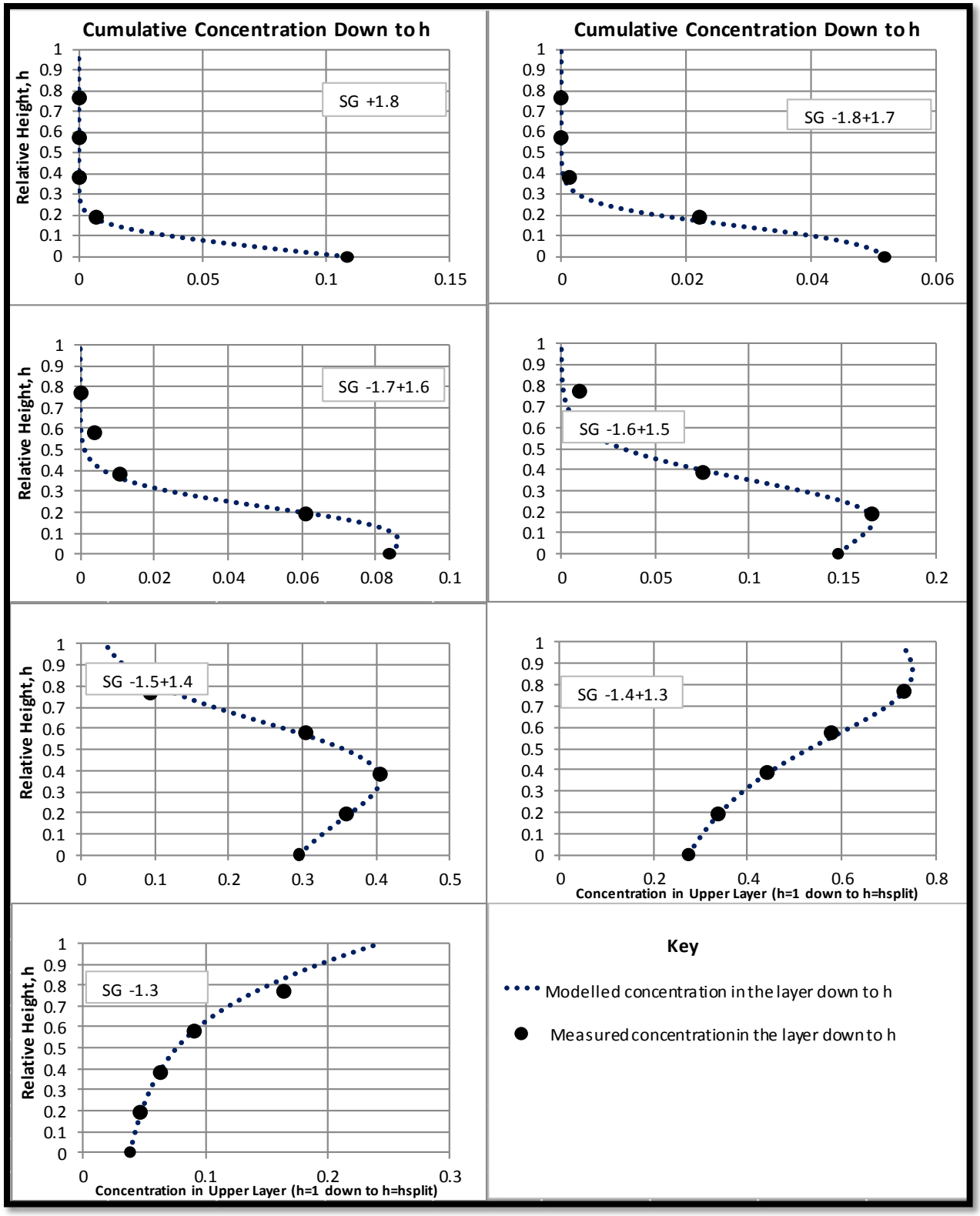

Figure 61: Cumulative concentration profile for sample A3B5 (-16mm+6.7mm)

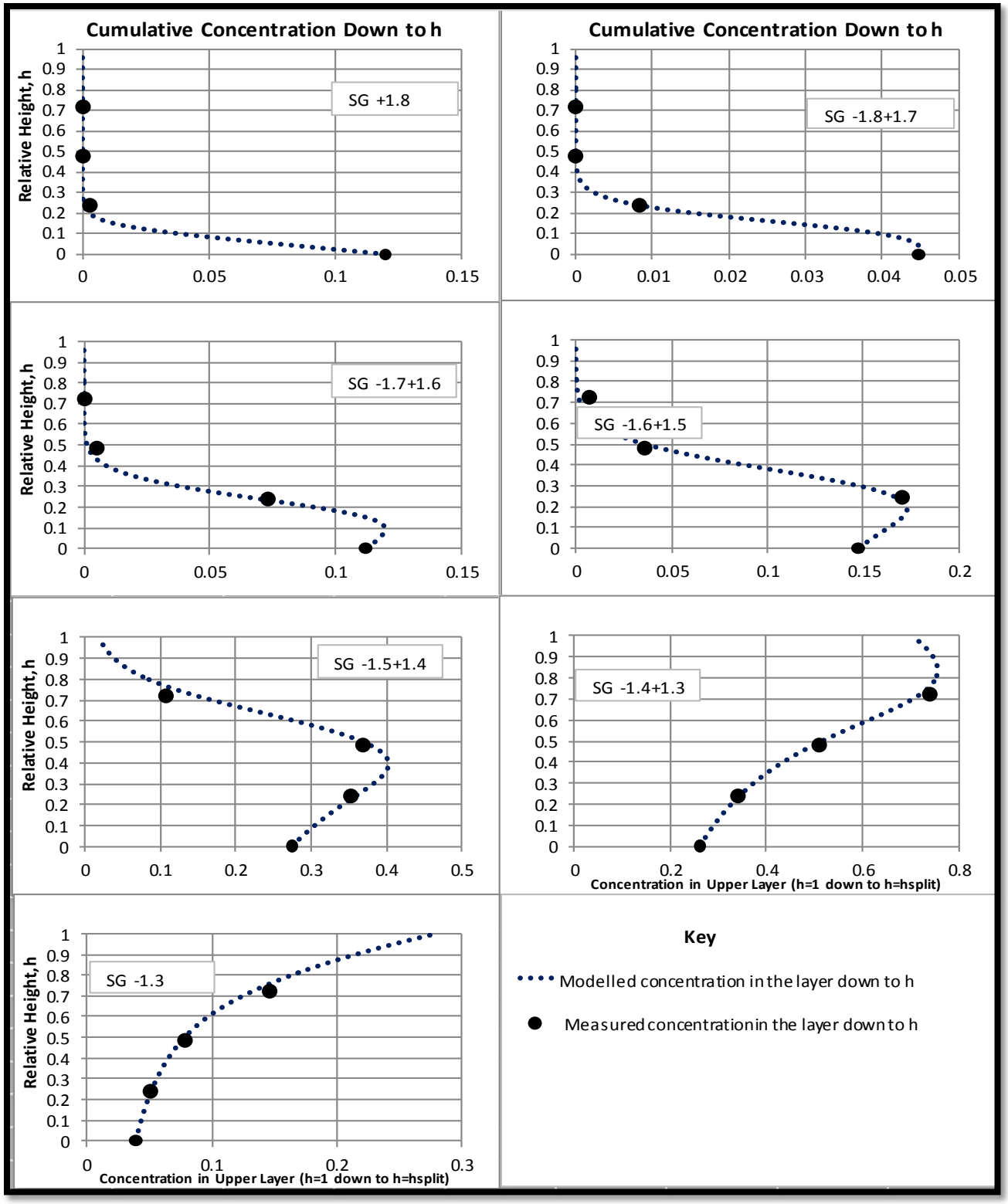

Figure 62: Cumulative concentration profile for sample A4B4 (-13.2mm+9.5mm)

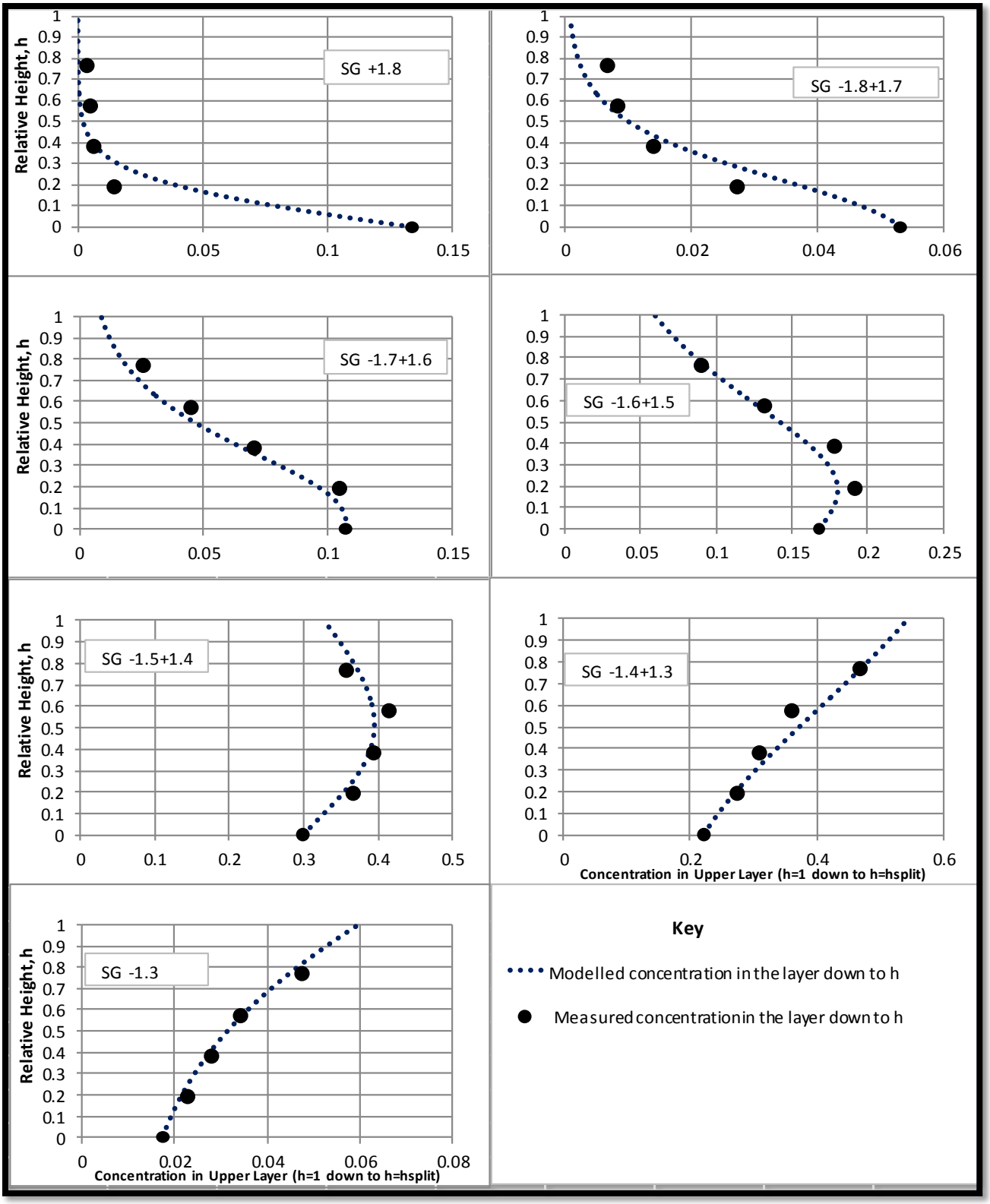

Figure 63: Cumulative concentration profile for sample A4B5 (-13.2mm+6.7mm)

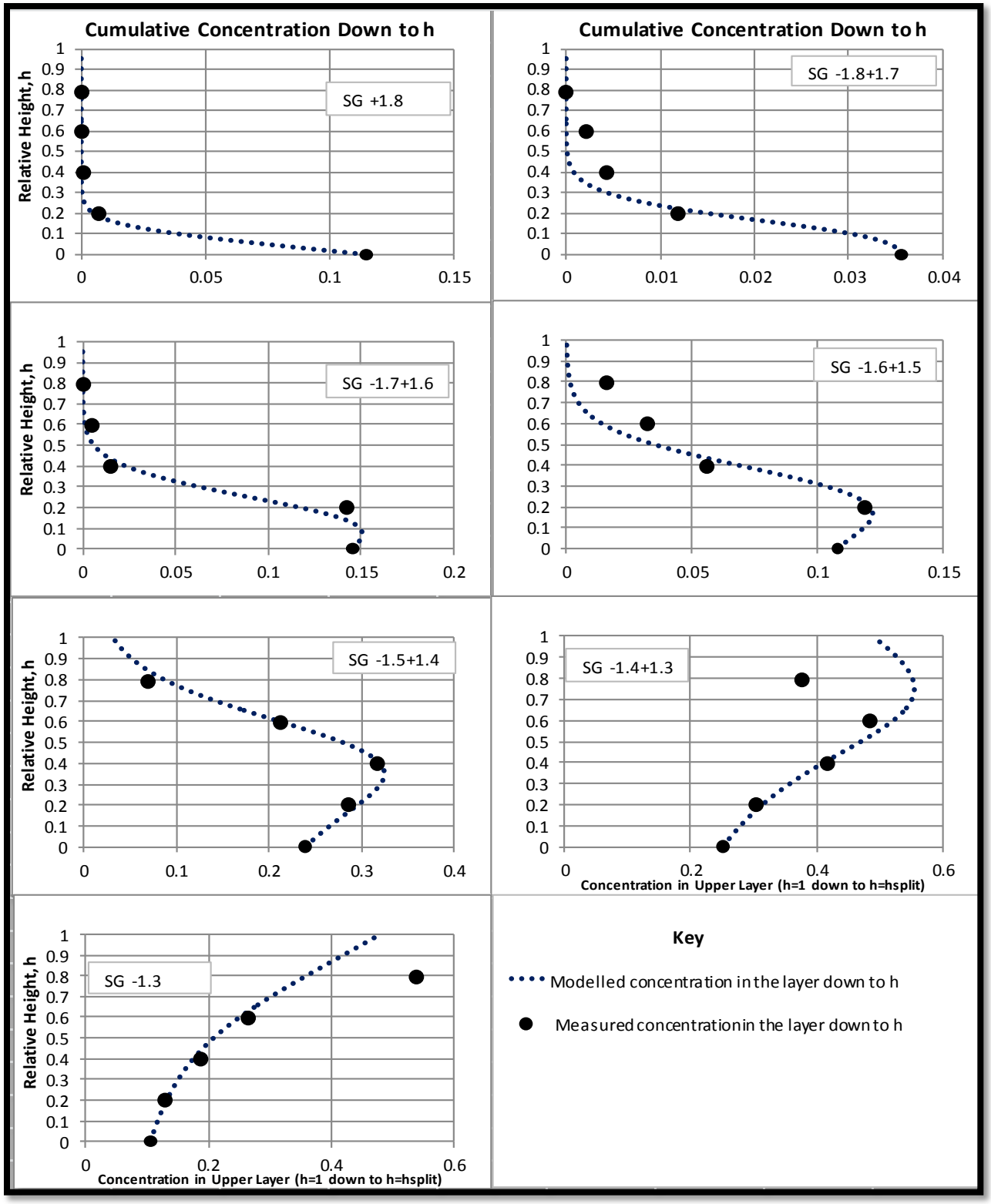

Figure 64: Cumulative concentration profile for sample A5B5 (-9.5mm+6.7mm)

Appendix B3: Cumulative recovery plots

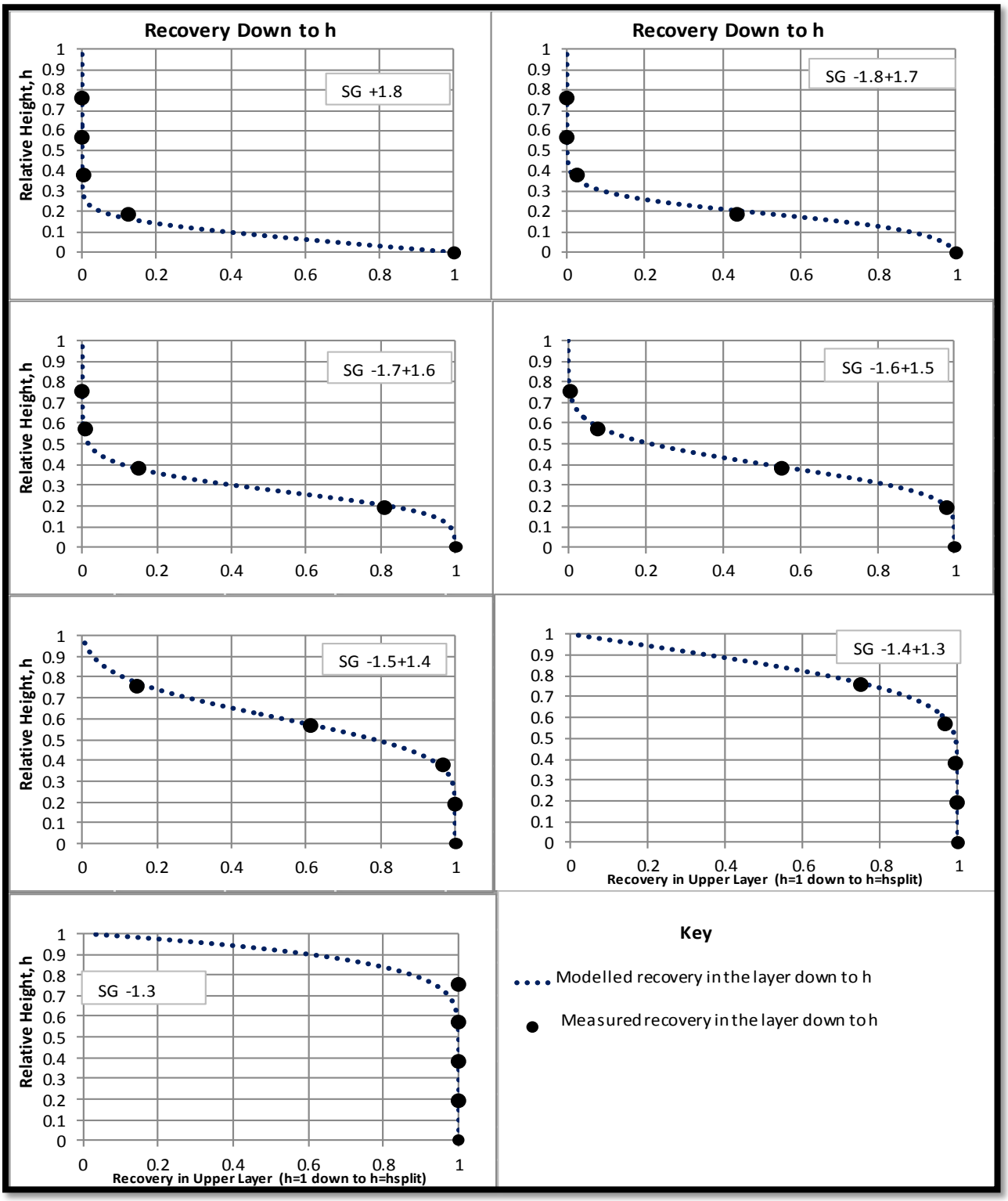

Figure 65: Cumulative recovery plots for sample A1B1 (-22.5mm+19mm)

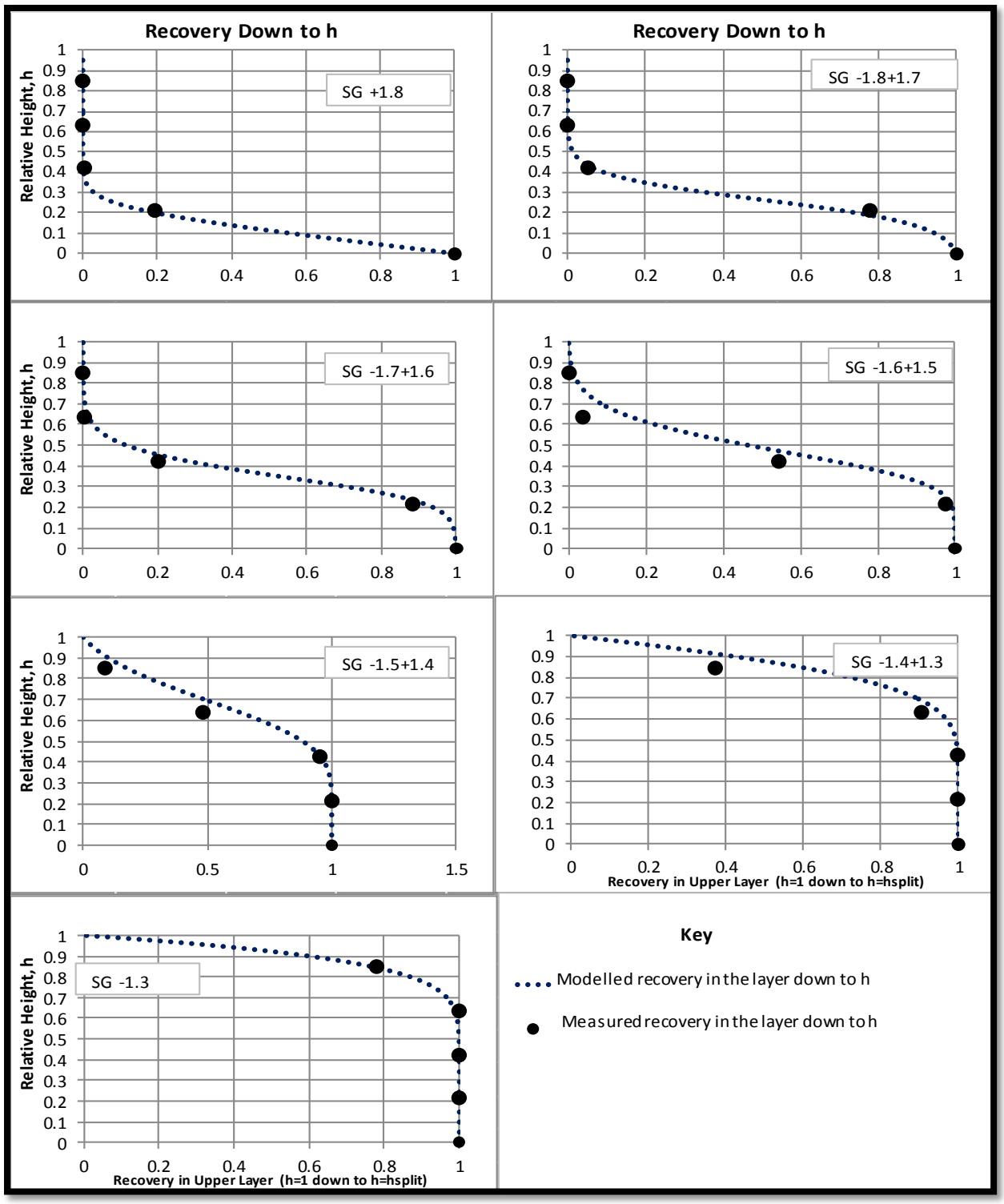

Figure 66: Cumulative recovery plots for sample A1B2 (-22.5mm+16mm)

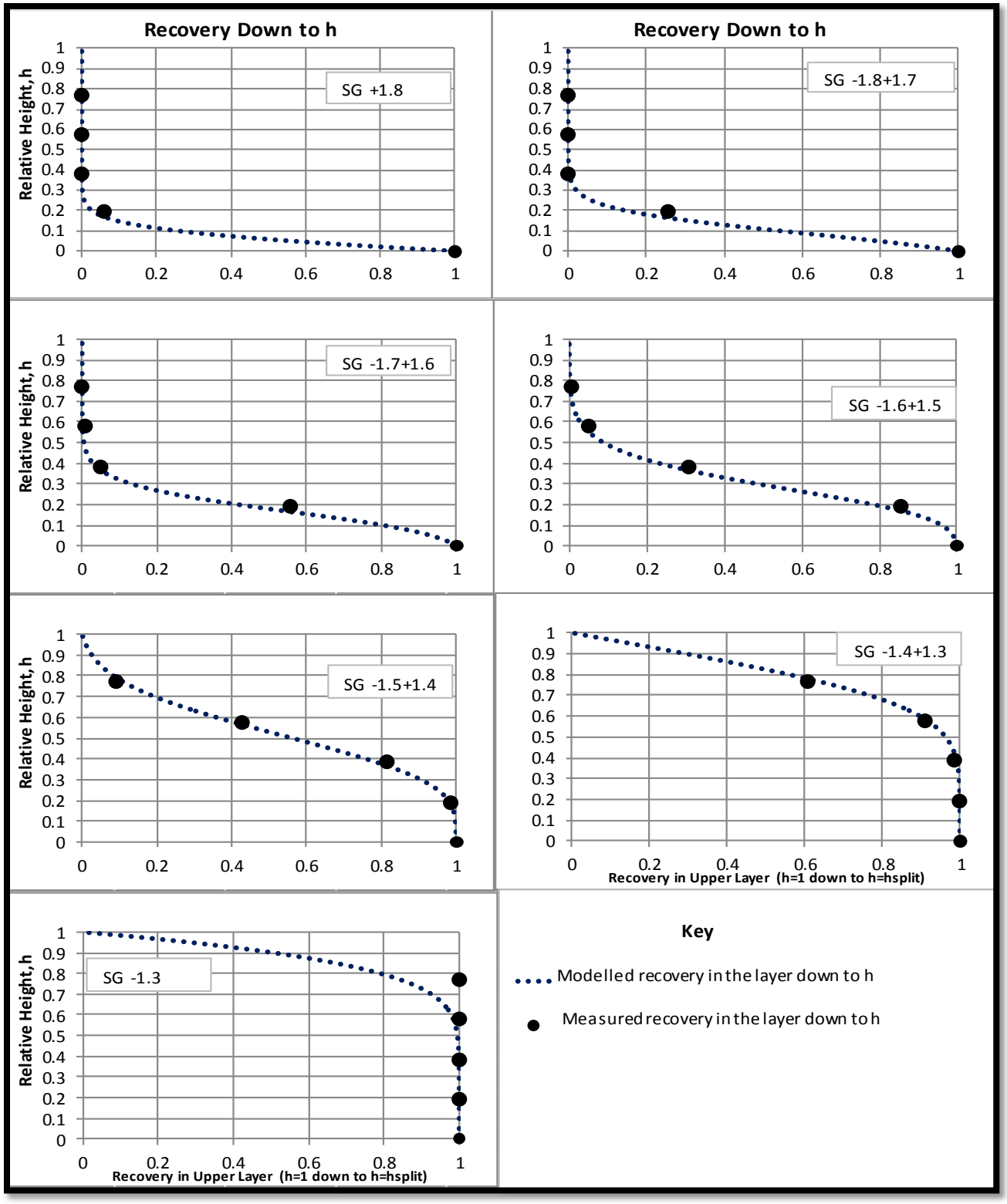

Figure 67: Cumulative recovery plots for sample A1B3 (-22.5mm+13.2mm)

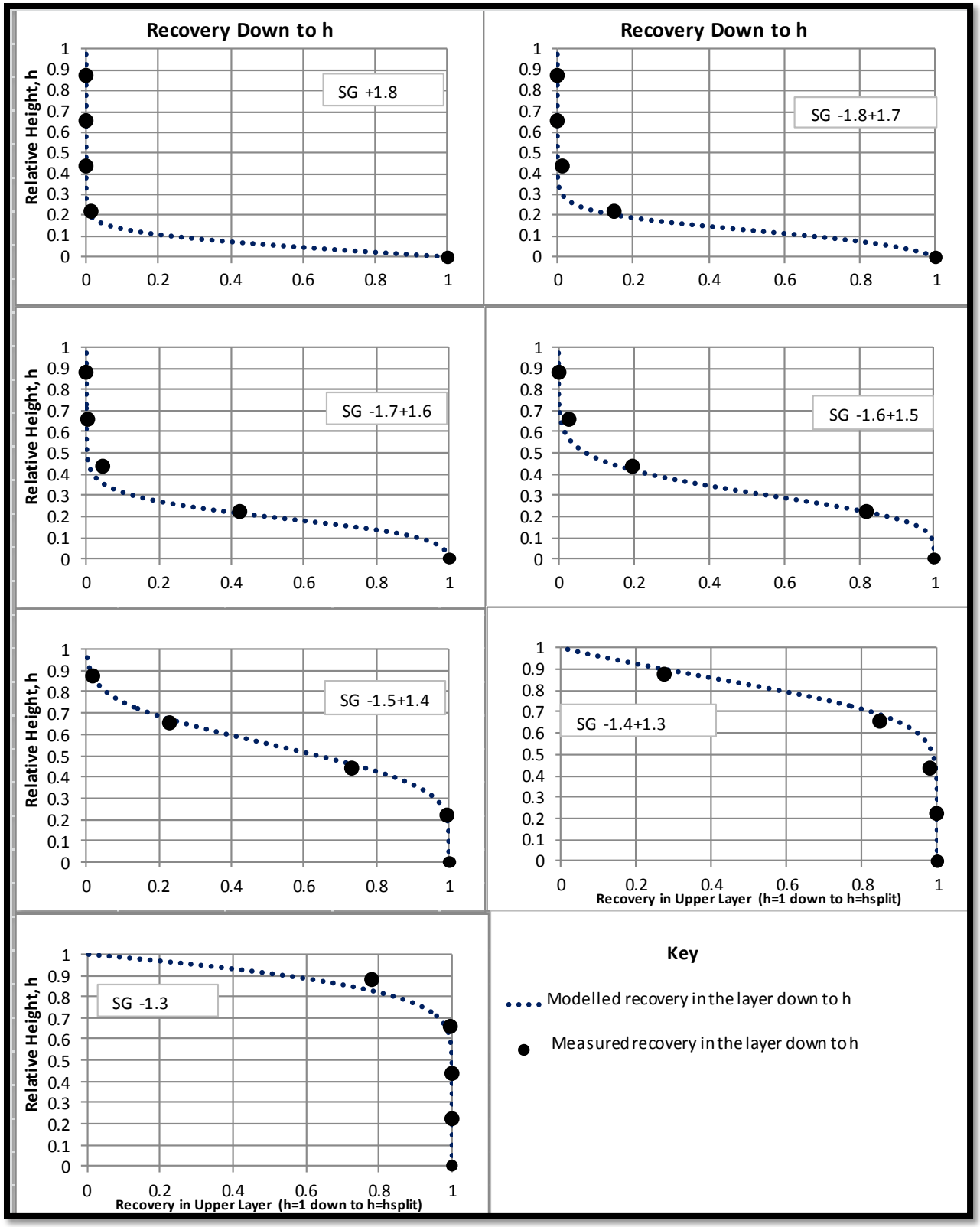

Figure 68: Cumulative recovery plots for sample A1B4 (-22.5mm+9.5mm)

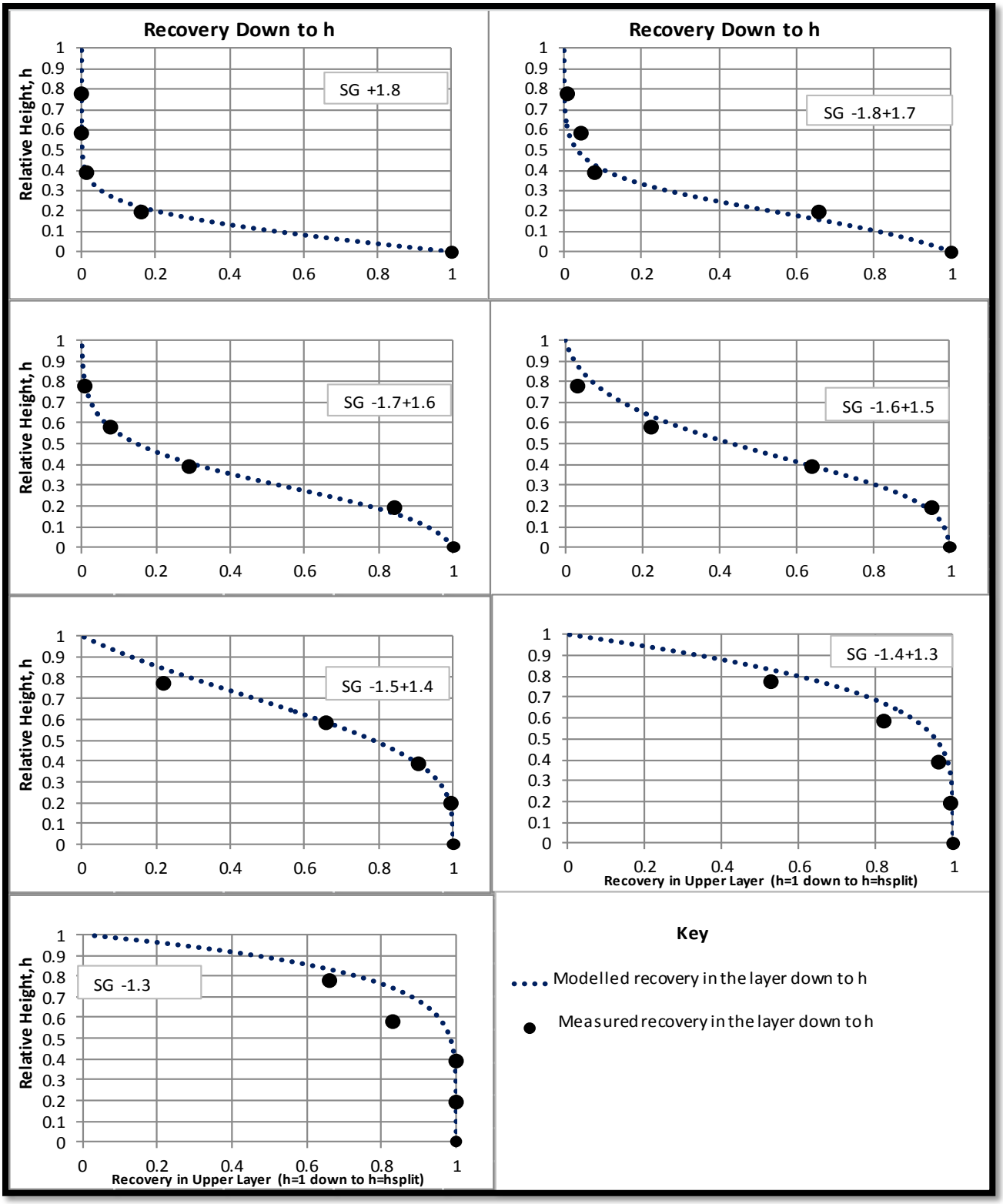

Figure 69: Cumulative recovery plots for sample A1B5 (-22.5mm+6.7mm)

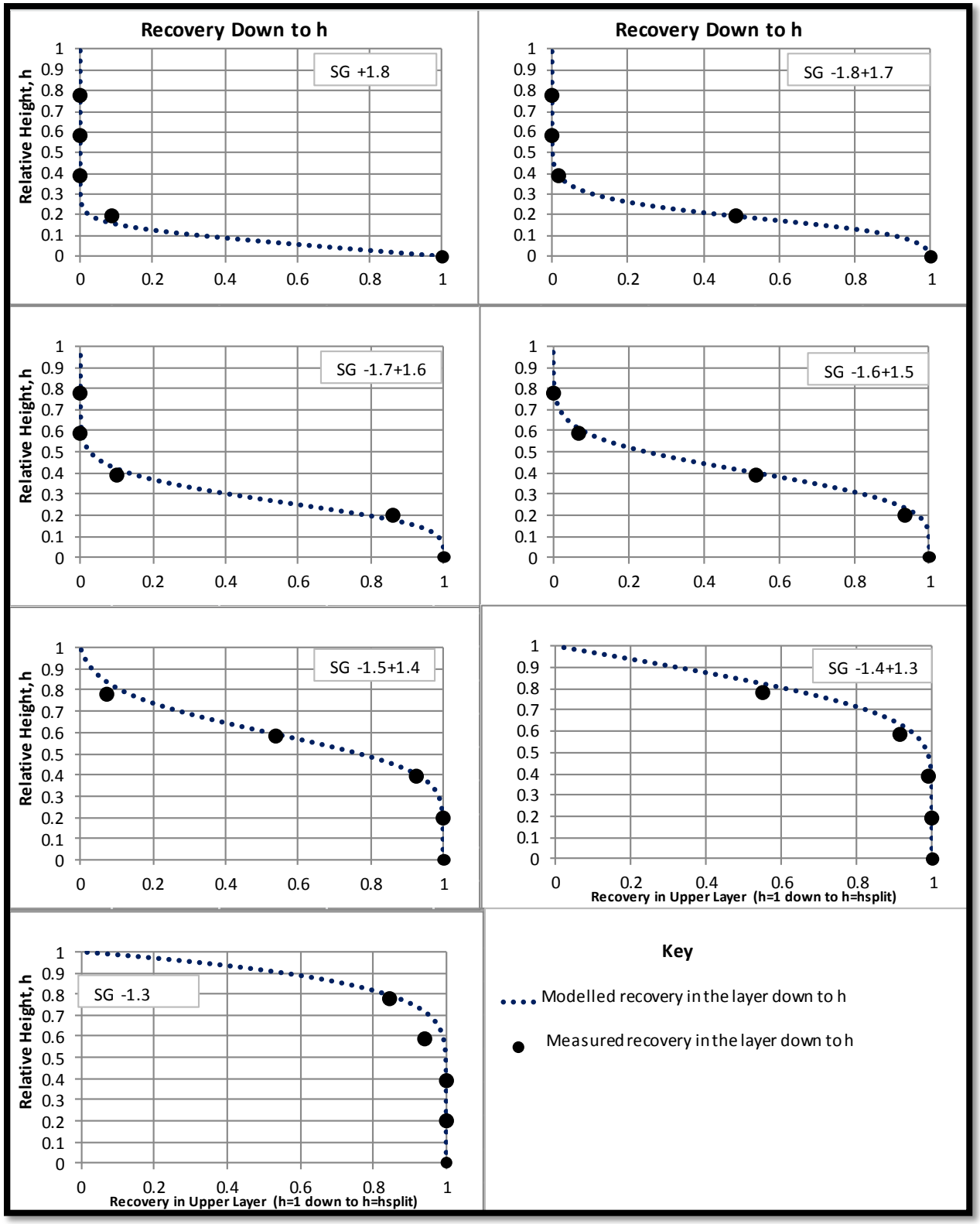

Figure 70: Cumulative recovery plots for sample A2B2 (-19mm+16mm)

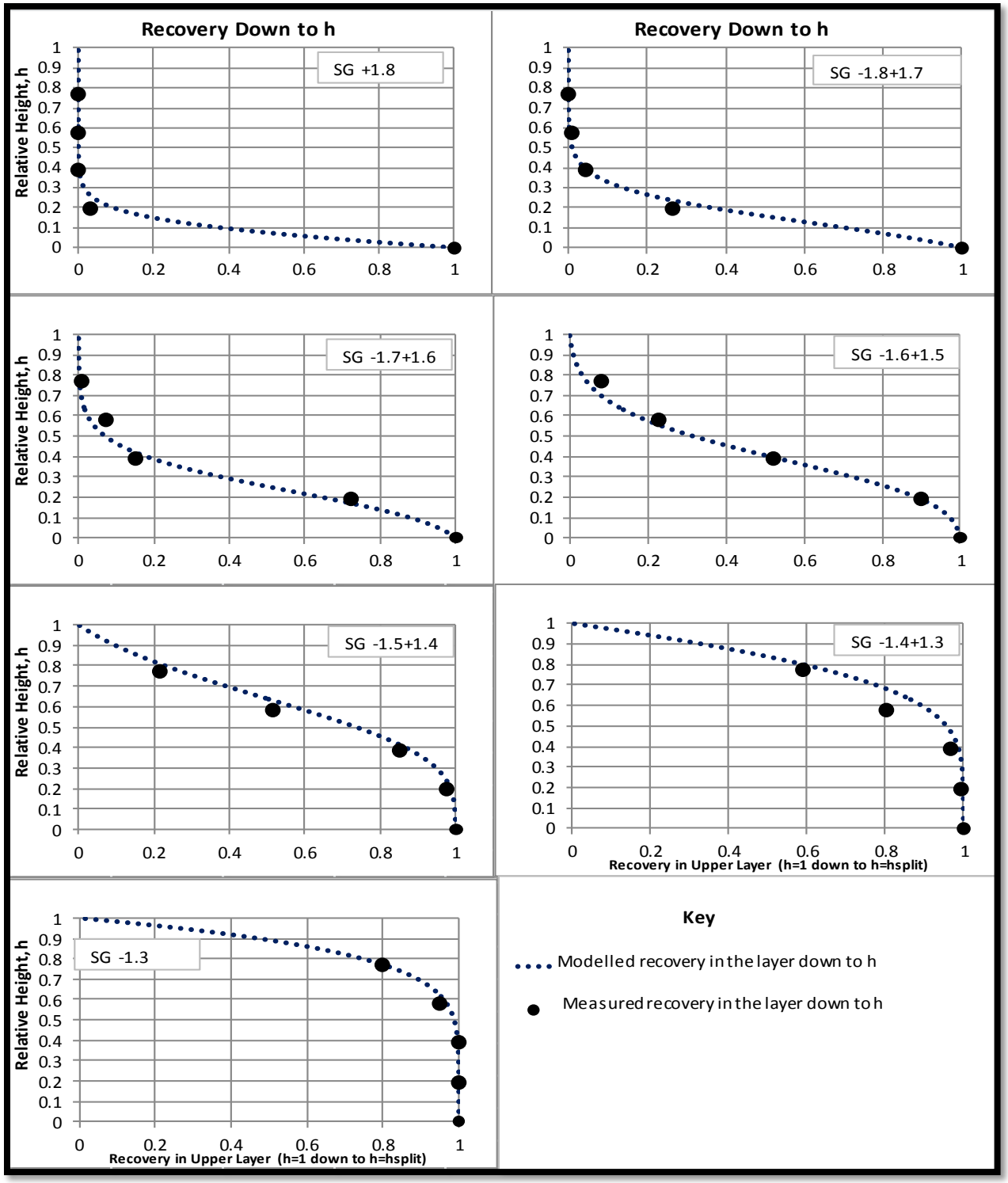

Figure 71: Cumulative recovery plots for sample A2B3 (-19mm+13.2mm)

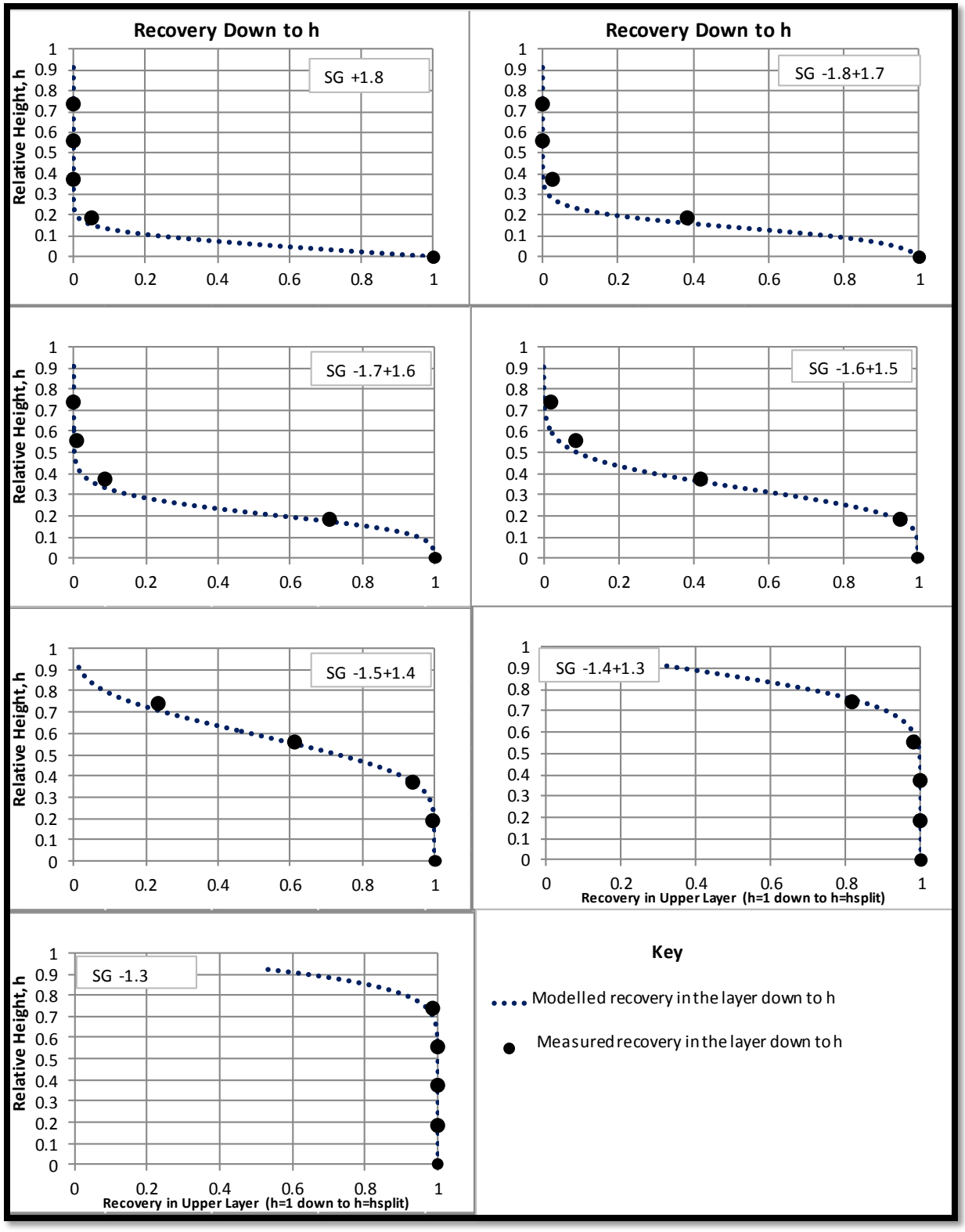

Figure 72: Cumulative recovery plot for sample A2B4 (-19mm+9.5mm)

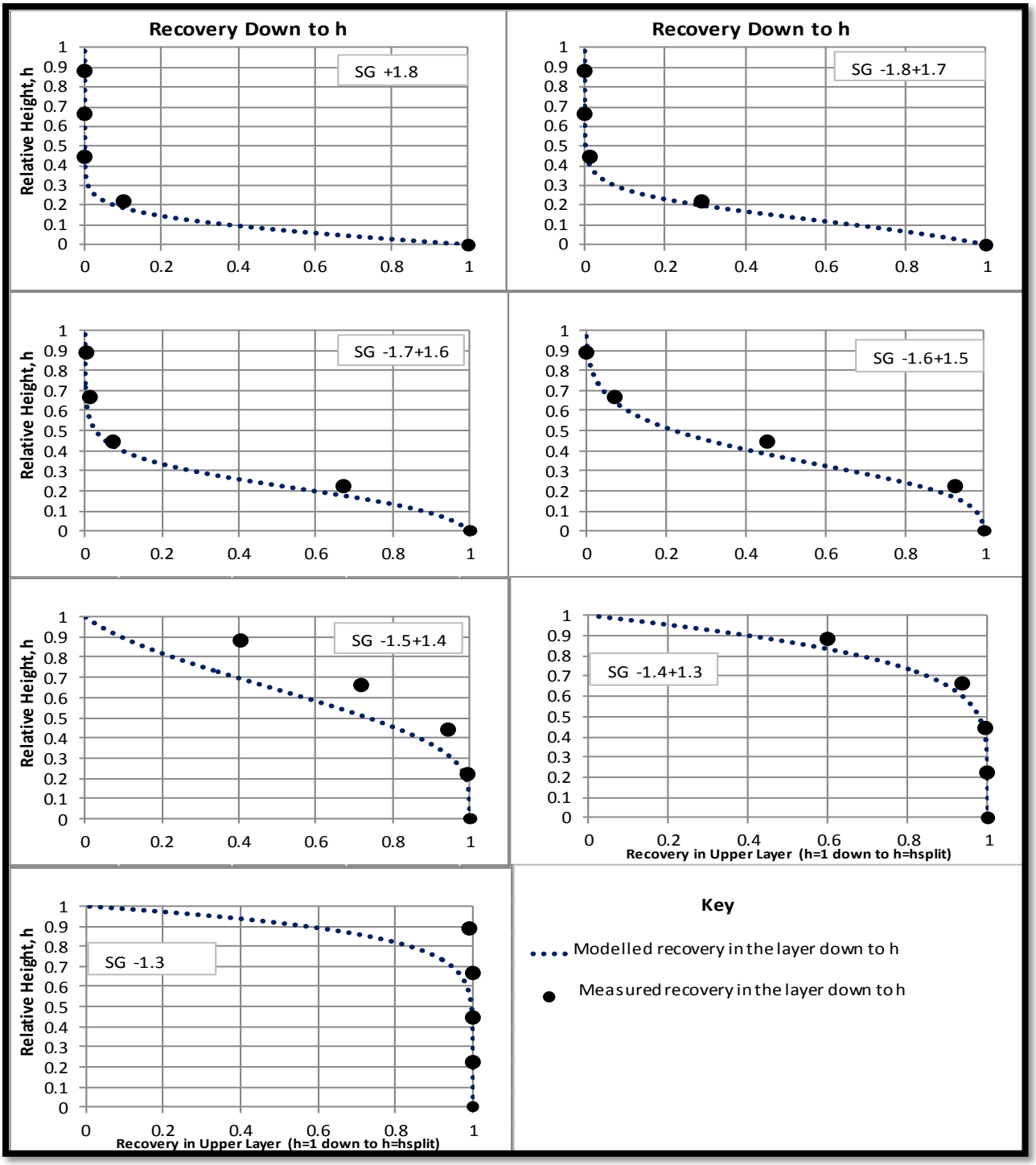

Figure 73: Cumulative recovery plots for sample A2B5 (-19mm+6.7mm)

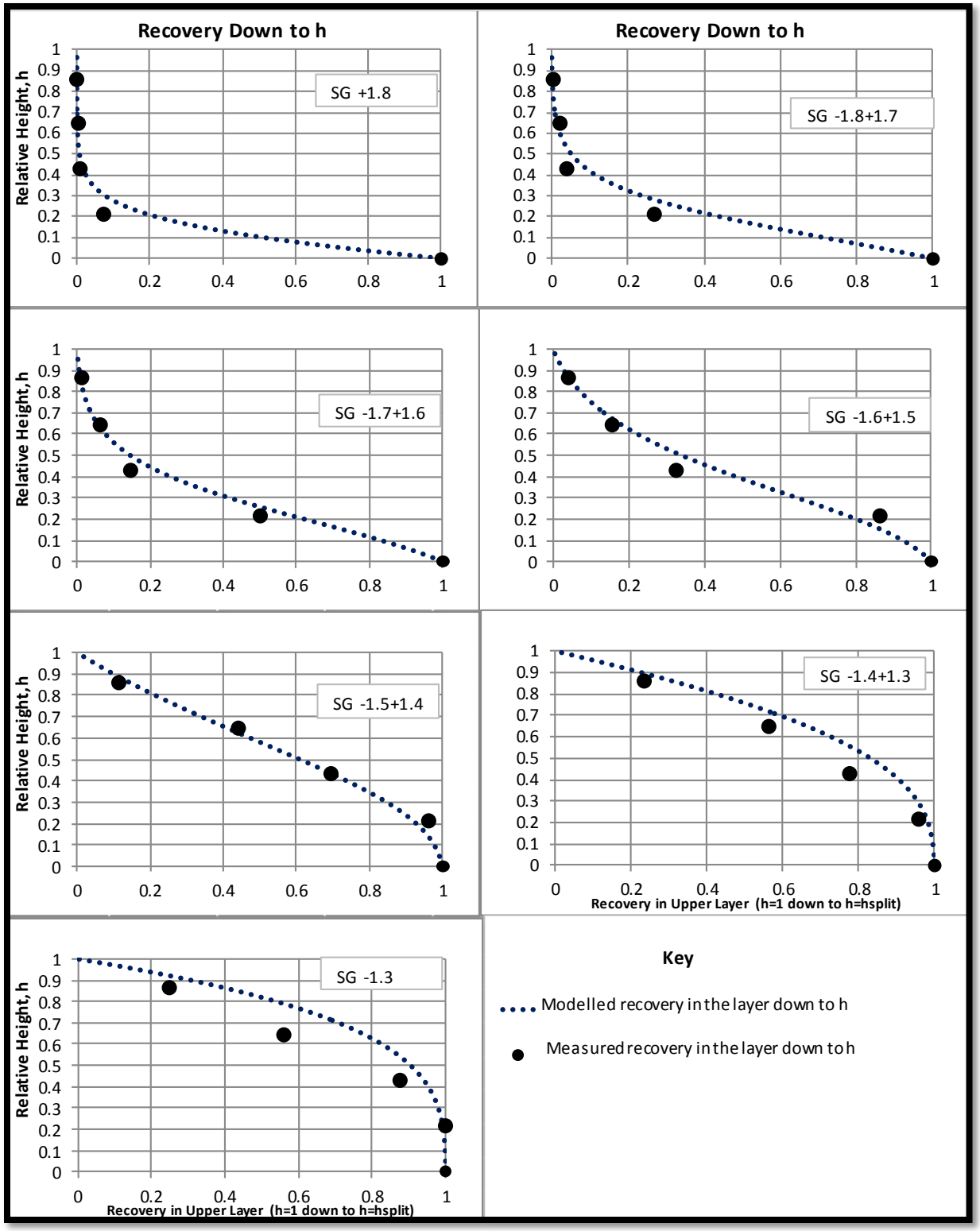

Figure 74: Cumulative recovery plots for sample A3B4 (-16mm+9.5mm)

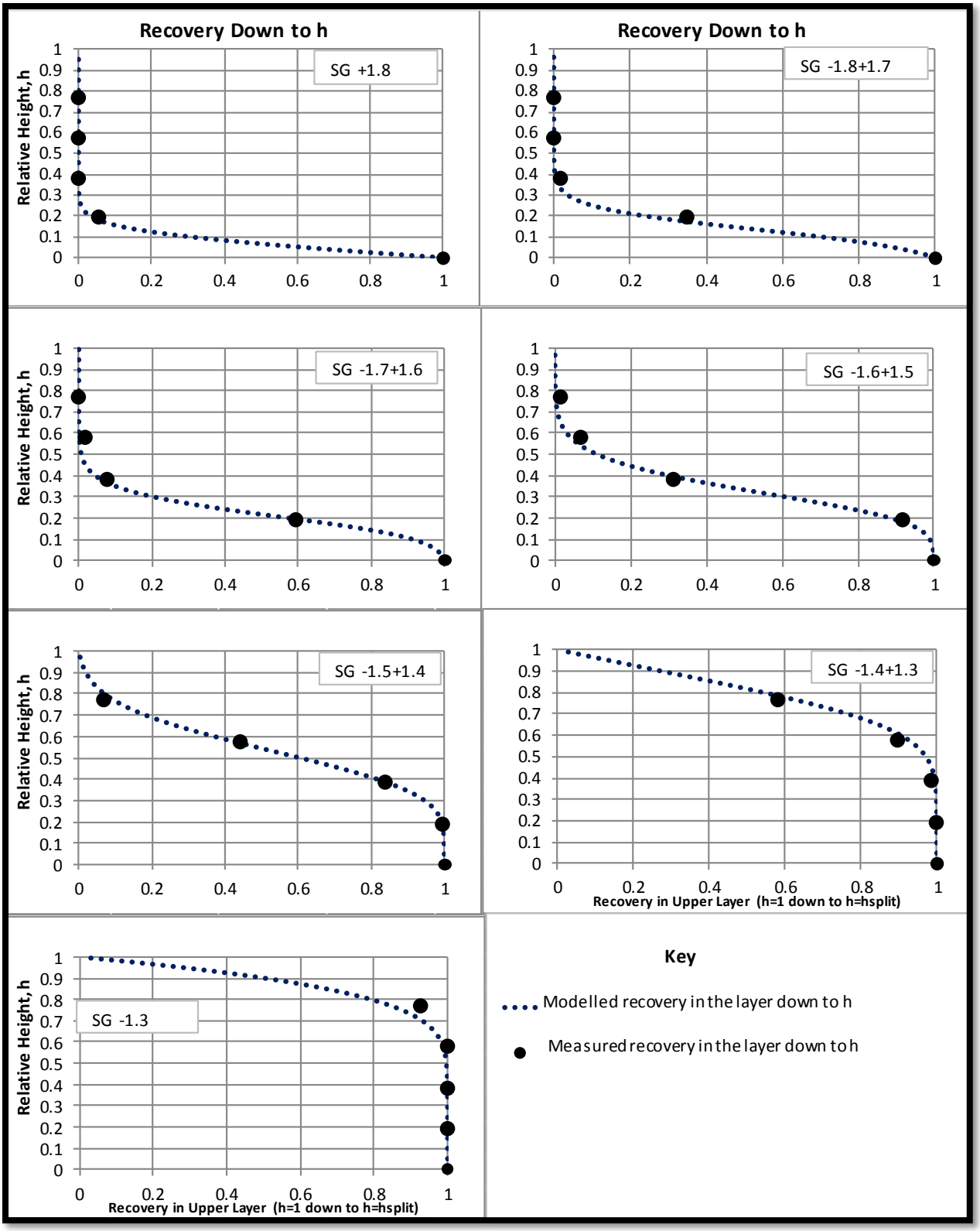

Figure 75: Cumulative recovery plots for sample A3B5 (-16mm+6.7mm)

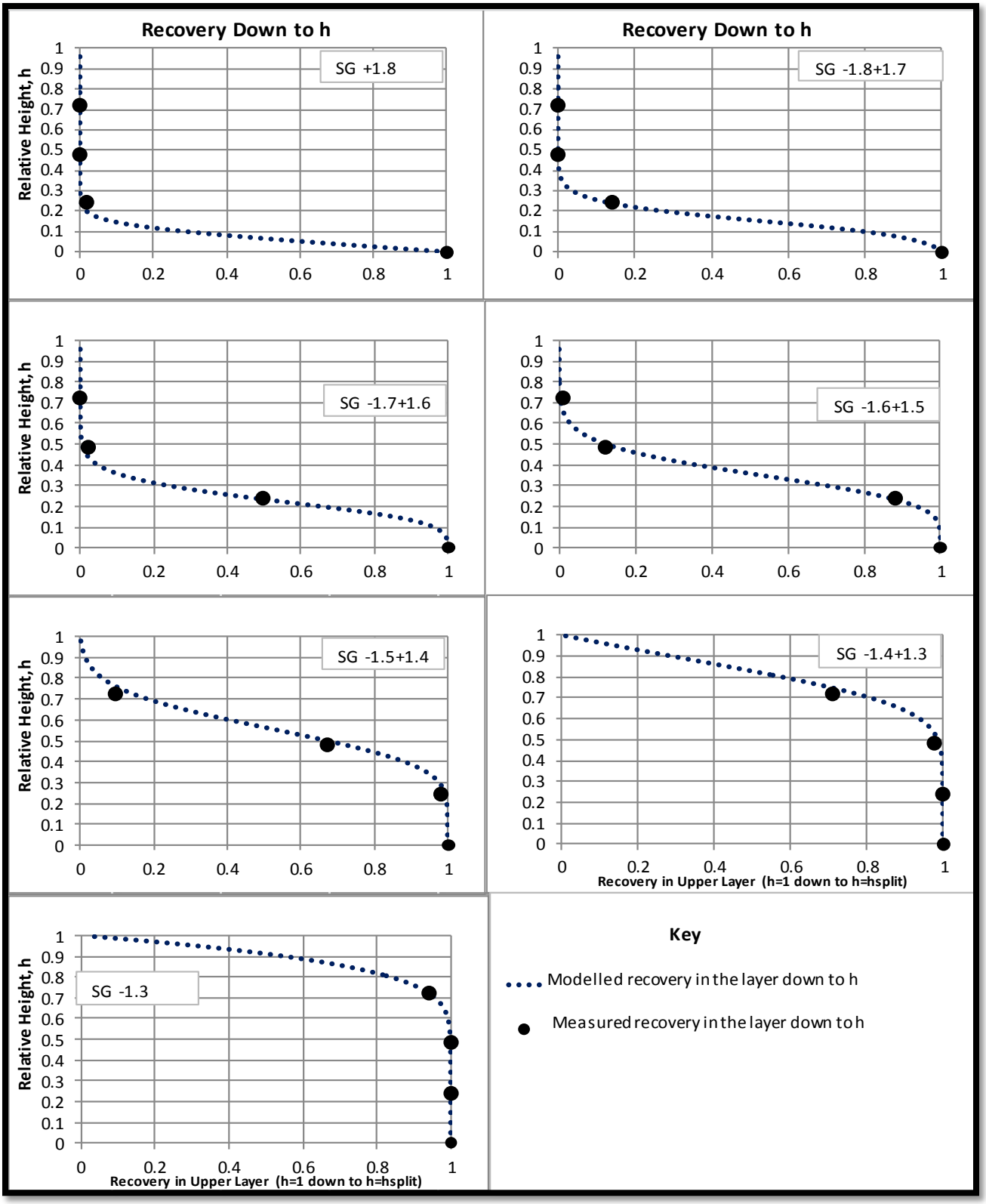

Figure 76: Cumulative recovery plots for sample A4B5 (-13.2mm-9.5mm)

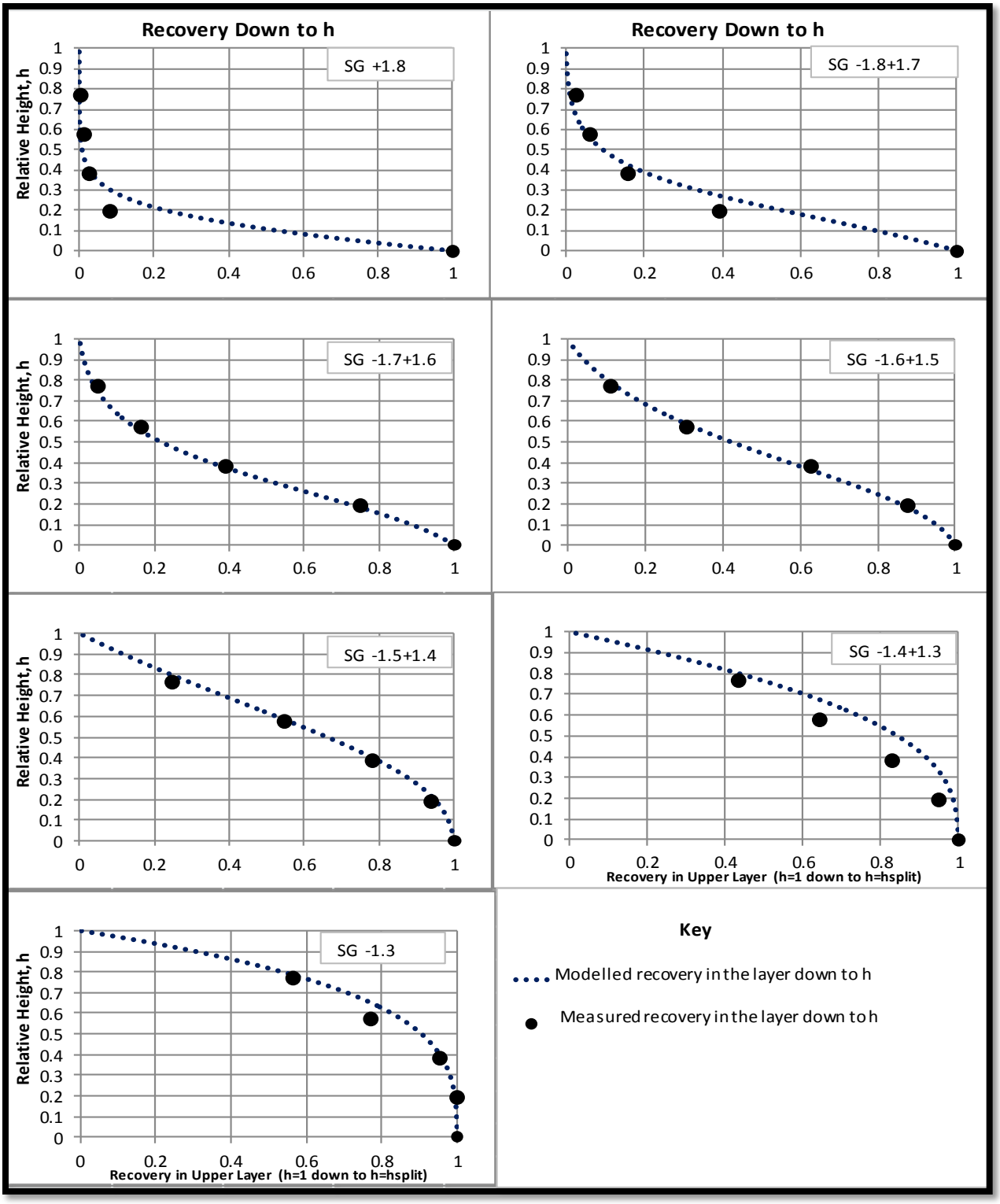

Figure 77: Cumulative recovery plots for A4B5 (-13.2mm+9.5mm)

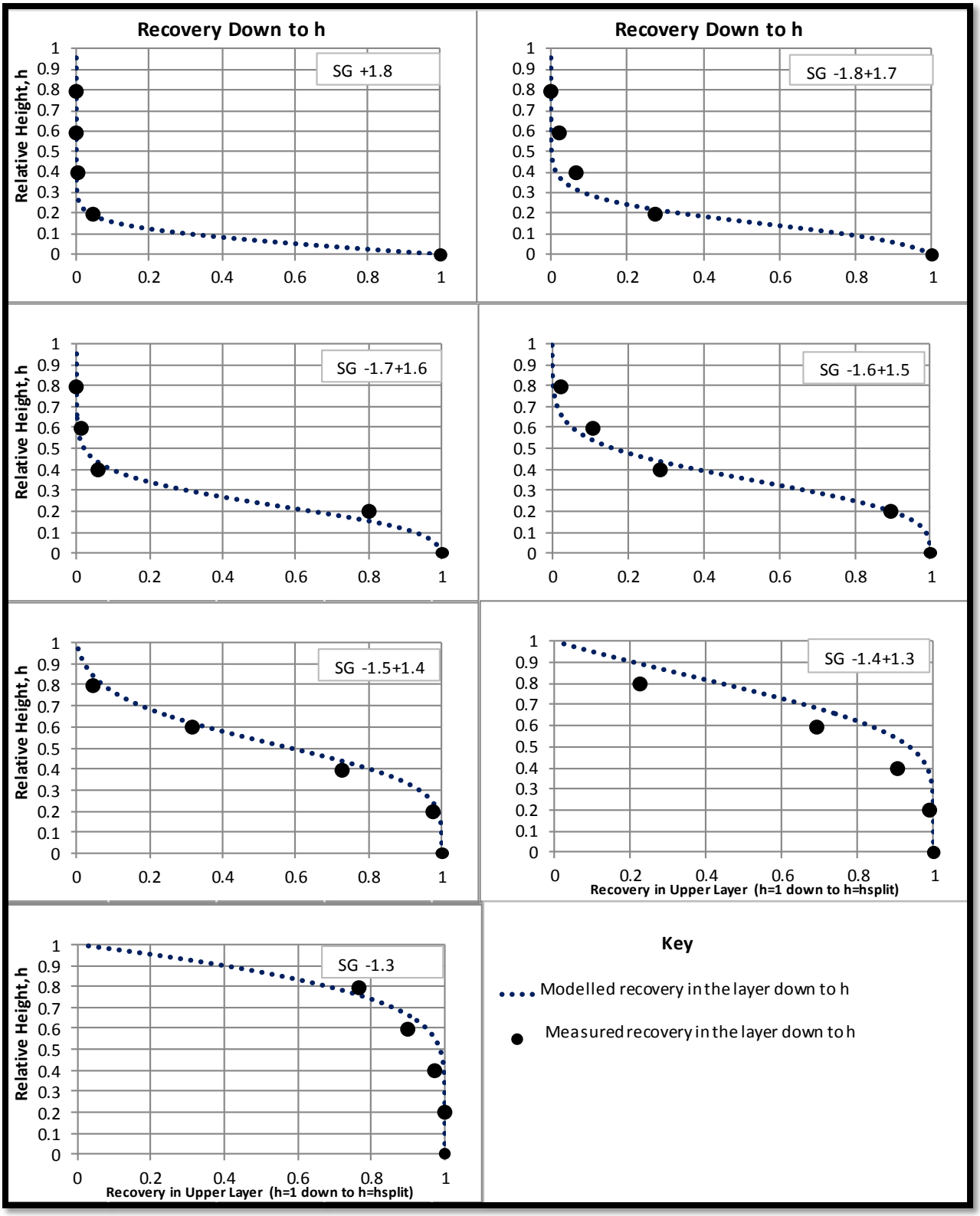

Figure 78: Cumulative recovery plots for sample A5B5 (-9.5mm+6.7mm)

Appendix B4: Influence of size effects on α

Table 27: Goodness of fit data for each data set ordered by Quality of fit and $\overline{SSD}$

Sample	Size Range (mm)		Drep (mm)	Rs	Alpha/Hbed	SSD	No. of Layers	$\overline{SSD}$	Quality of Fit
	top	*bottom*							
A1B1	22.5	19	20.7	1.18	0.905	0.0535	5	0.011	Good fit
A1B2	22.5	16	19.0	1.41	0.722	0.363	5	0.073	OK fit
A2B2	19	16	17.4	1.19	0.810	0.0905	5	0.018	Good fit
A1B3	22.5	13.2	17.2	1.70	0.690	0.127	5	0.025	OK fit
A2B3	19	13.2	15.8	1.44	0.425	0.165	5	0.033	OK fit -
A1B4	22.5	9.5	14.6	2.37	1.137	0.1405	5	0.028	Good fit
A2B4	19	9.5	13.4	2.00	0.797	0.085	5	0.017	OK fit
A3B3	16	9.5	12.3	1.68	0.235	0.418	5	0.084	poor fit
A1B5	22.5	6.7	12.3	3.36	0.495	0.229	5	0.046	poor fit
A2B5	19	6.7	11.3	2.84	0.638	1.1731	5	0.235	poor fit
A4B4	13.2	9.5	11.2	1.39	1.173	0.033	4	0.008	Good fit
A3B5	16	6.7	10.4	2.39	0.767	0.0512	5	0.010	Good fit
A4B5	13.2	6.7	9.40	1.97	0.186	0.2558	5	0.051	ok fit
A5B5	9.5	6.7	8.00	1.42	0.617	0.503	5	0.101	poor fit

Appendix C: Jig performance results

This presents all the relevant data pertaining to the EPM and the inefficiency.

Appenix C1: Effect of size and size range on EPM and I_c

Table 28: Effect cut size on EPM, -22.5mm+19mm

rho cut	EPM	Ic
1.72	0.075	0.0430
1.62	0.070	0.0432
1.56	0.065	0.0416
1.55	0.063	0.0403
1.5	0.050	0.0333
1.46	0.055	0.0376
1.41	0.045	0.0319
1.38	0.045	0.0326

Table 29: Effect of cut density on EPM, -22.5mm+16mm

rho cut	EPM	Ic
1.63	0.080	0.0490
1.55	0.060	0.0387
1.5	0.050	0.0333
1.45	0.055	0.0379
1.4	0.055	0.0392
1.36	0.050	0.0367

Table 30: Effect of cut density on EPM, -22.5mm+13.2mm

rho cut	EPM	Ic
1.66	0.085	0.0512
1.57	0.070	0.0445
1.55	0.063	0.0407
1.51	0.050	0.0331
1.47	0.055	0.0374
1.43	0.050	0.0349
1.39	0.040	0.0287
1.37	0.060	0.0437

Table 31: Effect of cut density on EPM, -22.5mm+9.5mm

rho cut	**EPM**	**Ic**
1.66	0.085	0.0512
1.58	0.075	0.0474
1.55	0.072	0.0464
1.53	0.07	0.0457
1.47	0.05	0.03401
1.42	0.045	0.0316
1.39	0.04	0.0287
1.35	0.04	0.0296

Table 32: Effect of cut density on EPM, -19mm+16mm

rho cut	EPM	Ic
1.63	0.08	0.0490
1.55	0.06	0.0387
1.5	0.05	0.0333
1.45	0.055	0.0379
1.4	0.055	0.0393
1.36	0.05	0.0368

Table 33: Effect of cut density on EPM, -19mm+13.2mm

rho cut	EPM	Ic
1.69	0.08	0.0473
1.62	0.08	0.0493
1.55	0.07	0.0451
1.5	0.085	0.0567
1.44	0.085	0.0590
1.4	0.07	0.05
1.36	0.055	0.0406

Table 34: Effect of cut density on EPM, -19mm+9.5mm

rho cut	EPM	Ic
1.61	0.085	0.052
1.55	0.063	0.0409
1.54	0.06	0.0389
1.48	0.055	0.0371
1.43	0.055	0.0384
1.39	0.05	0.0359
1.36	0.045	0.0330

Table 35: Effect of cut density on EPM, -19mm+9.5mm repeat

rho cut	EPM	Ic
1.7	0.09	0.0529
1.59	0.07	0.0447
1.55	0.059	0.0376
1.52	0.05	0.0328
1.49	0.05	0.0335
1.46	0.05	0.0342
1.42	0.045	0.0316
1.38	0.045	0.0326

Table 36: Effect of cut density on EPM, -19mm+6.7mm

rho cut	EPM	Ic
1.71	0.08	0.0467
1.64	0.075	0.0457
1.56	0.055	0.0352
1.55	0.0525	0.0338
1.52	0.045	0.0296
1.5	0.04	0.0267
1.48	0.04	0.0270

Table 37: Effect of cut density on EPM, -16mm+9.5mm

rho cut	EPM	Ic
1.68	0.09	0.0535
1.63	0.085	0.0521
1.55	0.074	0.0740
1.52	0.07	0.0462
1.48	0.07	0.0472
1.45	0.075	0.0517
1.4	0.1	0.0714
1.39	0.035	0.0251

Table 38: Effect of cut density on EPM, -16mm+6.7mm

rho cut	EPM	Ic
1.66	0.12	0.072
1.57	0.07	0.0445
1.55	0.063	0.0407
1.51	0.05	0.0331
1.47	0.05	0.0340
1.42	0.05	0.0352
1.39	0.045	0.0323
1.36	0.04	0.0294

Table 39: Effect of cut density on EPM, -13.2mm+9.5mm

rho cut	EPM	Ic
1.67	0.07	0.0419
1.61	0.07	0.0434
1.55	0.061	0.0392
1.51	0.055	0.0364
1.48	0.045	0.0304
1.42	0.05	0.0352
1.42	0.02	0.0142
1.36	0.05	0.0367

Table 40: Effect of cut density on EPM, -13.2mm+6.7mm

rho cut	EPM	Ic
1.72	0.15	0.08720
1.66	0.12	0.0722
1.58	0.12	0.0759
1.55	0.12	0.0789
1.52	0.12	0.0789
1.43	0.135	0.0944
1.37	0.125	0.0912
1.3	0.1	0.0769

Table 41: Effect of cut density on EPM, -9.5mm+6.7mm

rho cut	EPM	Ic
1.59	0.1	0.0628
1.55	0.089	0.0573
1.5	0.075	0.05
1.46	0.07	0.0479
1.39	0.065	0.0467
1.34	0.03	0.0223
1.32	0.02	0.0151